FINAL TECHNICAL REPORT

September 1994

INNOVATIVE PROCESSING OF COMPOSITES FOR ULTRA-HIGH TEMPERATURE APPLICATIONS

by

Reza Abbaschian
Department of Materials Science and Engineering
University of Florida
Gainesville, Florida

Sponsored by: The Advanced Research Projects Agency
Monitored by: The Office of Naval Research

ARPA Grant No. N00014-91-J-4075

BOOK III of IV

Executive Summary

The overall objective of this program was to provide a fundamental understanding of the processing science and technology necessary to fabricate ceramic-matrix, intermetallic-matrix, and metal-matrix composites with superior mechanical properties in high temperature and oxidizing environments. The composites are intended for use as structural materials for advanced aerospace applications at temperatures exceeding 1200°C (2200°F).

In order to accomplish the program objective, interactive research groups were established in three key areas of (a) Fiber Fabrication, (b) Coatings and Infiltration, and (c) Composite Fabrication. The objective of the fiber fabrication group was to develop new fibers which have superior strength and toughness at high temperatures and in oxidizing environments. The research effort focused on the development of two types of fibers: (1) glass-free mullite-based fibers, and (2) oxygen-free silicon carbide fibers. The coatings program had two primary objectives: (1) to control the characteristics of matrix/reinforcing phase interfaces (e.g., to control chemical reactions and bonding at a matrix/fiber interface) and (2) to develop coatings that will improve the oxidation resistance of metal-matrix and intermetallic-matrix composites. Coatings methods utilized included chemical vapor deposition, sol-gel processing, and solution coating with polymeric precursors to ceramics.

The composite fabrication group investigated various methods to incorporate reinforcing phases (i.e., fibers, whiskers, and particulates) into ceramic-, metal-, and intermetallic-matrices. Processing methods investigated included colloidal processing, chemical vapor infiltration, reactive hot-compaction and *in situ* coating, and microwave sintering. The objectives were not only to utilize innovative processing techniques, but also to develop and improved scientific understanding of processing-microstructure relationships in composites fabrication.

This annual report consists of seven sections compiled in four books as described below:

BOOK I

Section 1 Processing and Properties of Silicon Carbide Fibers
Principal Investigators: C.D. Batich
M.D. Sacks

Section 2 Processing of Mullite Composite Fibers
Principal Investigators: J.H. Simmons
M.D. Sacks
A.B. Brennan

Section 3 Chemical Vapor Deposition (CVD) and Chemical Vapor Infiltration (CVI)
Principal Investigator: T.J. Anderson

BOOK II

Section 1 — Processing and Properties of Intermetallic Matrix Composites
Principal Investigator: R. Abbaschian

Section 2 — Mechanical Alloying of $MoSi_2$
Principal Investigator: M.J. Kaufman

BOOK III

Section 1 — Processing of Ceramic Matrix Composites
Principal Investigator: M.D. Sacks

Section 2 — Processing of $BaO\text{-}Al_2O_3\text{-}2SiO_2$ Fibers
Principal Investigator: D.E. Clark

BOOK IV

Section 1 — Processing and Mechanical Property Characterization of Tape Cast, Multilayer, Alumina/Nickel Laminated Composites
Principal Investigator: J.J. Mecholsky

BOOK III

Section 1

Processing

of

Ceramic Matrix Composites

Principal Investigator: **M.D. Sacks**

Processing of Ceramic-Matrix Composites

PI: M.D. Sacks

Objectives

The overall objectives of this program were:

- To develop improved processing methods for enhancing densification, controlling shrinkage, and tailoring microstructure development in ceramic-matrix composites.
- To develop ceramic-matrix composites with properties (mechanical, chemical, and dielectric) suitable for high temperature structural applications.

These objectives were pursued through two general methods: (1) viscous, transient viscous, and pressure-assisted transient viscous sintering of ceramics and composites using submicron composite particles and (2) processing of ceramics and composites by liquid infiltration processing. Project results are summarized below.

Background and Research Approach

Ceramic-matrix composites with high relative density (low porosity) were fabricated by (i) sintering of submicron composite particles and (ii) reactive infiltration of metals. Background information on these approaches is provided below.

Powder compact densification is often hindered by the presence of "non-sinterable" inclusions (e.g., particles, whiskers). In particular, densification rates are severely impeded when the non-sinterable phase forms a connected network (i.e., when the concentration is large enough to form a percolation path). In conventional powder processing methods, randomly-mixed inclusions can form connected networks at relatively low volume fraction (see Fig. 1, left side). However, an effective method for avoiding the formation of percolation network is illustrated in the right side of Fig. 1. The non-sinterable particles B are coated with a layer of A, thereby completely isolating them from each other.

Previous studies have shown that non-sinterable inclusions have less effect on the densification rate when the matrix phase sinters by viscous flow. Thus, an especially effective method for enhancing densification rates is to utilize composite particles (as shown in Fig. 1, right side) in which the outer coating is an amorphous material. This approach not only allows fabrication of glass/ceramic composites at relatively low sintering temperatures, but also offers the possibility of developing novel microstructures in which a high concentration of crystalline phase is incorporated into a glassy matrix as isolated inclusions (Fig. 2, top right). Furthermore, the approach described above can also be applied to the fabrication of single-phase crystalline ceramics and crystalline ceramic-ceramic composites. This requires selection of appropriate core and coating materials that would react at elevated temperatures to eliminate the amorphous phase. An example is illustrated in Fig. 2 (bottom) in which the core is alumina and the coating is silica. If the size of the composite particles is selected properly, this combination should viscously sinter at relatively low temperature to

Figure 1

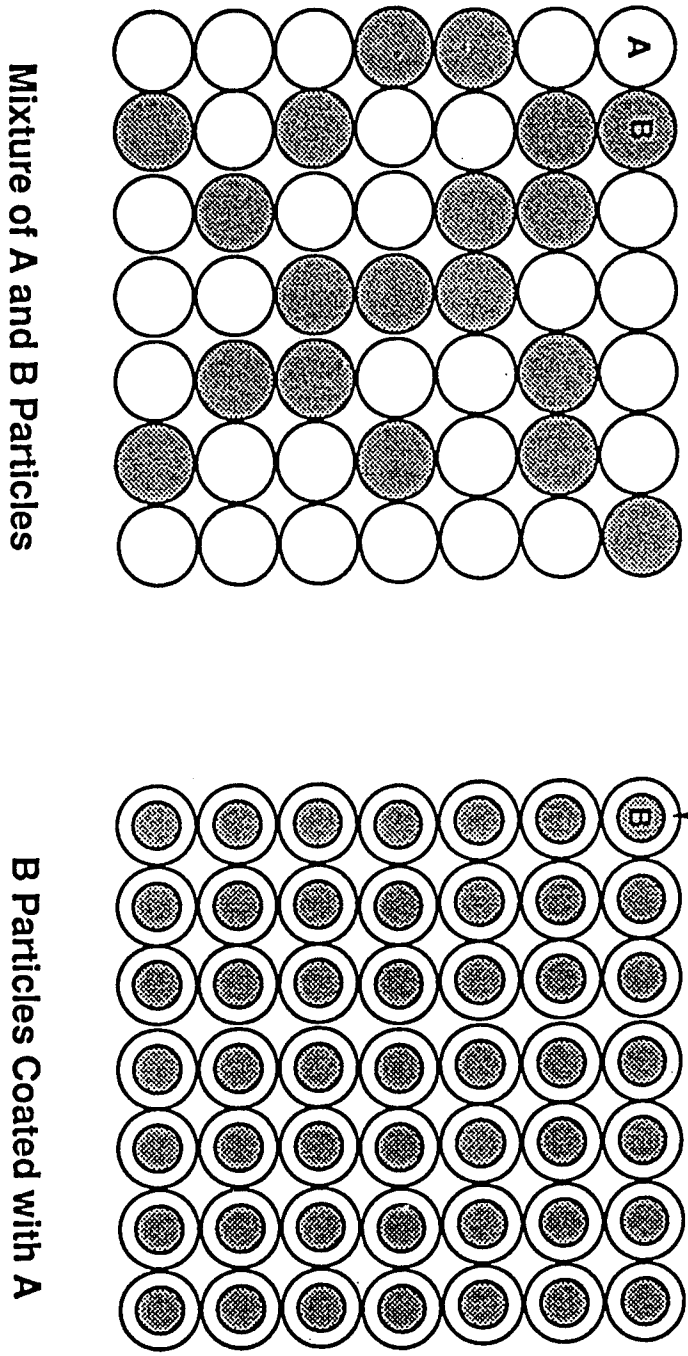

Figure 2

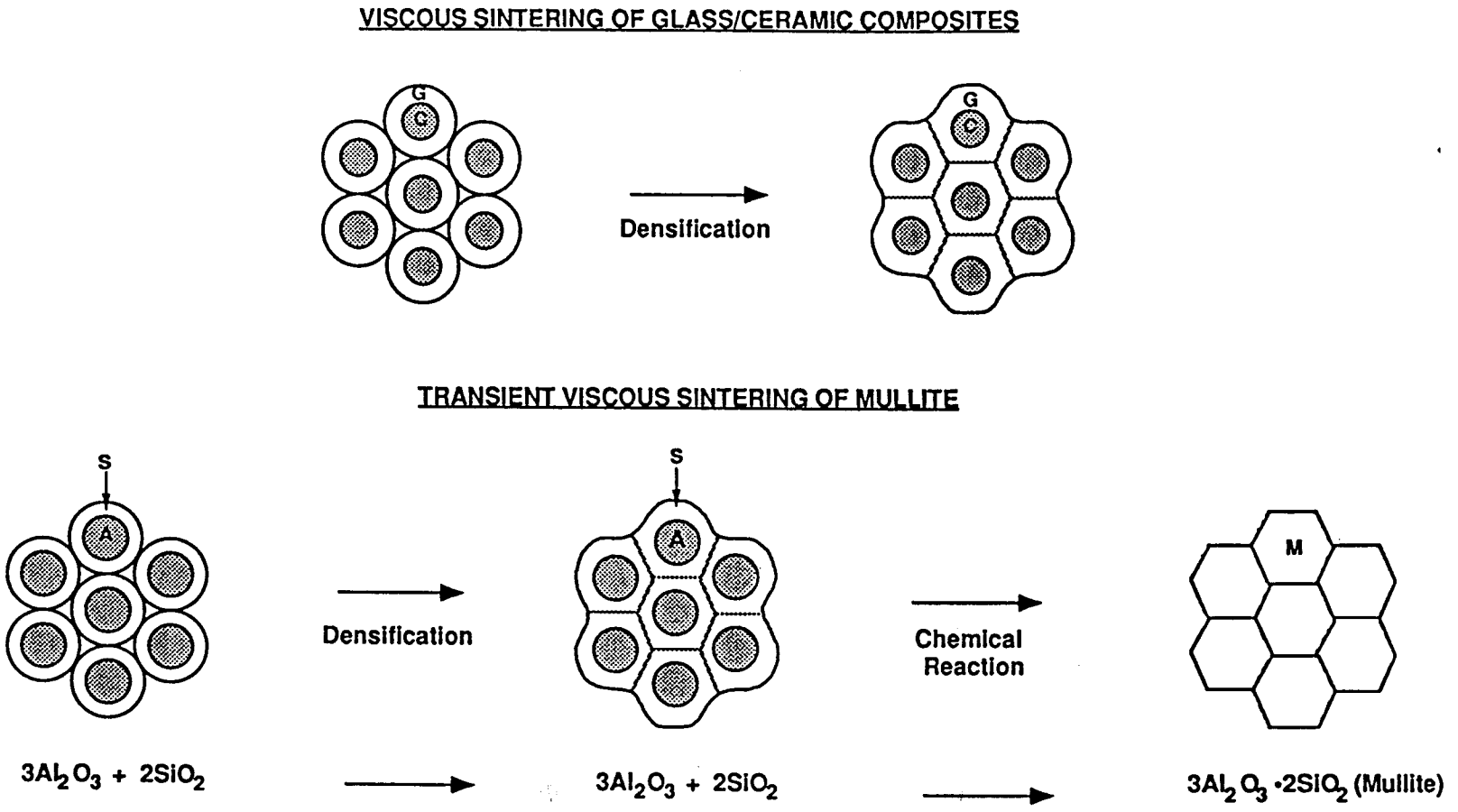
VISCOUS SINTERING OF GLASS/CERAMIC COMPOSITES
G
C
Densification
TRANSIENT VISCOUS SINTERING OF MULLITE
S
A
Densification
Chemical Reaction
M
3Al2O3 + 2SiO2
3Al2O3 + 2SiO2
3Al2O3 •2SiO2 (Mullite)

form an alumina/siliceous glass composite. At higher temperature, the core and coating would react to form mullite. This process is referred to as transient viscous sintering (TVS). This approach can also be used to fabricate other types of composites by mixing the silica-coated alumina particles with other silica-coated particles (i.e., with different crystalline core materials). In addition, by applying pressure during sintering, it should be possible to viscously densify fiber-reinforced composites. The approach illustrated in Fig. 2 depends upon the availability of coated particles in the appropriate size range (i.e., colloidal dimensions).

A completely different approach for producing high relative density (low porosity) ceramics and ceramic-matrix composites is to utilize reactive infiltration processing. For example, molten metal infiltration processing has been investigated extensively for low cost, near-net-shape manufacturing of SiC. Reaction-bonded SiC is typically fabricated by infiltrating molten silicon into a compacted body of SiC and carbon powders. The molten silicon rises through the porous compact by capillary action and reacts with the carbon to form "new" SiC which bonds the original SiC particles together. The resultant material is a two-phase composite of silicon carbide and silicon. If no carbon exists in the initial porous compact, the silicon infiltration process involves only the filling of the pore channels. The resulting material is referred to as siliconized silicon carbide. This material usually contains much more silicon as a second phase. However, the processing method is a relatively easy and cost effective method for fabricating large complex shapes. The major problem impeding the use of reaction-bonded or siliconized silicon carbide as a structural material for high temperature applications is the presence of a large amount of free silicon phase in the final product. It is the free silicon phase which degrades the mechanical properties (strength, hardness, creep resistance, etc.).

The primary objective of the research in infiltration processing was to improve mechanical properties and polishability of siliconized silicon carbide materials by increasing the SiC/Si ratio and reducing the size of silicon pockets in final microstructure (i.e., in addition to reducing the volume fraction of Si). The approach adopted in this study was to infiltrate extra silicon carbide or carbon into pore channels of the compact (preform) prior to the siliconization process. Both bulk and surface infiltration were investigated in order to modify bulk and surface properties of siliconized SiC composites. Infiltration involved filling the open pores of the porous SiC preform with the liquid precursor, solidifying the liquid "in situ" at a lower temperature, and then decomposing it into SiC or C at a higher temperature. In the case of the carbon precursor, carbon formed after the lower temperature decomposition step would subsequently react with molten silicon to form extra SiC during the siliconization process. A key issue for successful application of the liquid precursor infiltration approach is to select a suitable liquid precursor. The desired characteristics for an ideal liquid precursor are: (1) The liquid precursor should infiltrate rapidly into the porous solid preform. (2) After infiltration has been accomplished, the liquid precursor should be immobilized in the porous solid. Transport of the liquid precursor by capillary action should be avoided during subsequent heat treatment steps (e.g., drying, pyrolysis) because this will result in concentration gradients within the porous solid. Solvents and liquid precursor decomposition products should be removed by vapor transport mechanisms in order to produce a pyrolyzed product with good compositional uniformity. (3) A high yield of the desired solid phase (i.e., high specific volume) should be produced after the heat treatment steps for precursor decomposition and phase transformation. The number of infiltration cycles needed for a given process can be reduced if the yield per cycle can be increased. (4) Simple, low cost processing steps are desirable. For example, it would be desirable to accomplish infiltration at room temperature and at low pressures. Similarly, precursor decomposition and phase transformation would be less costly if heat treatment temperatures were low. (5) Low cost infiltrant materials are desirable.

Research Summary

Viscous, Transient Viscous, and Pressure-Assisted Transient Viscous Sintering of Ceramics and Composites Using Submicron Composites Particles

1. A process was developed for preparation of submicron composite particles. These particles consisted of inner cores of a crystalline material (e.g., alumina, silicon nitride, silicon carbide, zirconia) and an outer coating of amorphous silica. The volume ratio of amorphous silica/crystalline core could be readily varied over a wide range. The formation of dense, uniform coatings was demonstrated using a variety of techniques, including SEM, TEM, microelectrophoresis, X-ray Photoelectron Spectroscopy (XPS), etc. These particles were used to form a variety of bulk ceramics, glass/ceramic composites, and ceramic-ceramic composites using viscous sintering, transient viscous sintering (TVS), and pressure-assisted TVS.

2. Glass/ceramic composites (alumina/silica, silica/silicon nitride) were fabricated by viscous sintering using silica-coated composite particles. As discussed below (research summary item #3), the silica/alumina samples were transformed into mullite and mullite-based composites. The silica/silicon nitride composites have potential for applications which require low dielectric constant and good high temperature mechanical properties. Enhanced densification was demonstrated by directly comparing the sintering behavior for compacts prepared with the silica-coated silicon nitride particles vs. a mixture of silica particles and silicon nitride particles. (The green compact characteristics were similar to those schematically illustrated in Fig. 1.) The increased densification rate for the samples prepared with composite particles can be attributed to (1) viscous flow of the amorphous coating and (2) avoiding the formation of a percolation network of the "non-sinterable" phase. A fully dense ~60 vol% silica/40 vol% silicon nitride composite had an average dielectric constant value of ~5.0 over the frequency range 10^3-10^7 Hz and a loss tangent value of ~3 x 10^{-4} at 1 MHz. Composite powder compacts were also prepared with a controlled addition of ~10-12 vol% latex particles. By appropriate choice of sintering schedule, it was possible to produce a microstructure in which isolated, closed pores (~2 μm dia.) were dispersed in a dense silica/silicon nitride matrix. A ~60 vol% silica/40 vol% silicon nitride sample with ~11% porosity had an average dielectric constant value of ~4.3 over the frequency range 10^3-10^7 Hz and a loss tangent value of ~2 x 10^{-4} at 1 MHz. Results show that samples with closed, isolated 2 μm pores have essentially the same flexural strength as the samples without porosity. This indicates that the strength-limiting flaws are larger than 2 μm.

3. Mullite and mullite-based composites were fabricated by transient viscous sintering of amorphous silica-coated alumina particles. Compacts were sintered to near full density at relatively low temperatures (~1300°C) and subsequently heat treated at higher temperatures (~1500°C) in order to form mullite. The samples remained almost fully dense (i.e., almost zero porosity) after mullitization. By using a "seeding" technique to control nucleation of mullite, it was also possible to lower the mullitization temperatures (to ~1400°C) and develop microstructures with a fine, equiaxed grain structure. The temperature needed to accomplish densification and mullitization was not much higher than that used for samples prepared by sol-gel techniques. One of the advantages of the present method was that processing difficulties normally associated with "sol-gel" routes (i.e., large weight losses and shrinkages during drying and sintering) were less of a concern due to the use of (i) considerably larger particles and (ii) alpha alumina (i.e., instead of an alumina precursor).

A variety of mullite-based composites were prepared using the TVS technique. For example, mullite/alumina and mullite/siliceous glass composites were fabricated by simply changing the alumina/silica ratio of the composite particles. Samples could be densified at ~1300°C, while mullitization was carried out at higher temperatures. A dense composite with ~55 vol% Mullite/45 vol% silica had a dielectric constant value of ~4.9 and a loss tangent of ~7×10^{-4} at 1 MHz. Mullite/SiC_p composites were fabricated by sintering compacts prepared with mixtures of silica-coated particles, i.e., in which the core materials were alumina and silicon carbide particles. Densification and mullitization were accomplished at temperatures in the same range as those processed without the second phase. Mullite/SiC_w composites were prepared using silica-coated alumina particles and uncoated SiC whiskers. Samples with ≥96% relative density were obtained after sintering at 1500°C. A variety of evidence indicated that densification of the composite powders was largely controlled by viscous flow of the amorphous silica coating of the particles: (1) Samples with a wide range of alumina/silica weight ratios (i.e., 66/34 - 83/17) showed very similar densification behavior. (2) Samples prepared with coated second phase particles (i.e., silicon carbide) showed essentially the same densification behavior as samples prepared only with silica-coated alumina particles. (3) Samples containing ~15 vol% SiC whiskers showed relatively limited inhibition of densification, despite the fact that the whiskers were uncoated and their concentration exceeded the critical volume fraction for percolation. These samples densified at much lower temperatures compared to previous work on sintering of mullite/SiC whisker compacts.

4. Previous studies have shown that sialons and sialon-based composites have low dielectric constant, good oxidation resistance, and good high temperature mechanical properties. In this study, sialon-based composites were prepared by using mixtures of silica-coated alumina particles, silica-coated silicon nitride particles, and uncoated aluminum nitride particles. Samples were sintered under conditions to give almost fully crystalline samples that consisted primarily of one of the various sialon phases (J, β, or O). Dielectric constants in the range ~5.7-6.2 were observed for all samples.

5. Sintered glass/ceramic composites prepared from silica-coated particles can be deformed viscously at elevated temperatures to high strains. This was illustrated by compression stress-strain studies for dense composites prepared from silica-coated alumina particles. It was possible to deform samples to linear strains exceeding 80% without observing microcracking or cavitation. Samples were subsequently converted to dense, fine-grained mullite by further heat treatment. Based on these results, work was initiated to prepare fiber-reinforced composites by pressure-assisted TVS. Compression stess-strain behavior was studied for a silica-coated alumina powder compact reinforced with ~10 vol% Nicalon fibers. The sample was densified to ~97% at relatively temperature (1300°C) and pressure (~50 MPa).

6. Research was carried out to produce composite particles having multicomponent silicate glass coatings. The objective was to lower the sintering temperature by lowering the viscosity of the silicate glass coating on the crystalline core particles. The initial studies were directed toward preparation of silica coatings doped with boria. Borosilicate glass/alumina composite particles and borosilicate glass/silicon nitride particles have been produced with ~5-23 wt% B_2O_3/95-77 wt% SiO_2 coatings. Compacts prepared with these particles had sintering temperatures that were ~150-500°C lower than compacts prepared with 100% SiO_2-coated alumina particles.

Processing of SiC-Based Composites by Infiltration Processing

1. Two suitable liquids with relatively low viscosity (which is important in obtaining reasonable infiltration rates) and relatively moderate weight loss upon pyrolysis (which is important in ultimately obtaining a high yield of SiC) were developed for infiltration into porous SiC preforms. One was a ceramic precursor, 1,3,5-trimethyl-1,3,5-trivinylcyclotrisilazane, which was polymerized by heat treatment (120-150°C) in the presence of a proper initiator and subsequently pyrolyzed at elevated temperature (1000-1650°C) to produce a silicon carbide/silicon nitride mixture. With proper control over atmosphere and temperature, the polymer can be pyrolyzed to form only silicon carbide. The other liquid was a carbon precursor, an organic resin solution, which was heat treated in the range of 90-150°C and subsequently pyrolyzed above 650°C to form glassy carbon. The glassy carbon in the pores of the sintered preform was reacted with molten silicon to form "new" silicon carbide during the siliconization process.

2. The effect of liquid precursor infiltration on relative density and pore characteristics of the preforms was characterized by the Archimedes displacement method and mercury porosimetry measurements after each infiltration/polymerization/pyrolysis cycle. As the number of cycles increases (for both the ceramic and carbon precursors), the open porosity, median pore size, and apparent density decrease, while the bulk density increases.

3. The infiltration parameters, including infiltration time, pyrolysis temperature and number of infiltrations, were optimized for the carbon precursor. The infiltration time depends mainly on the sample thickness and the pore size distribution of the preform to be infiltrated. For the 3 mm thick porous SiC preforms used in this study, the first infiltration was nearly completed within a few minutes, while the second infiltration could be accomplished in less than 1 hour. The optimum pyrolysis temperature was 800°C. In order to achieve dense, bulk composites with maximum SiC/Si ratio, two infiltration/pyrolysis cycles were used.

4. After siliconization, both the apparent and bulk densities increase with increasing the number of infiltrations due to the increased SiC/Si ratio in the composites. Densities of siliconized SiC composites satisfy the "rule of mixtures" very well. Therefore, by measuring density values, the phase composition of the composite could be calculated. The phase composition of the final siliconized SiC composites can also be estimated from the open porosity of the SiC preform, weight gain after infiltration/pyrolysis process, and the additional weight loss of the precursor above the pyrolysis temperature (i.e., the weight loss during the siliconization process).

5. The carbon precursor infiltration was much more effective for increasing the SiC/Si ratio than the ceramic precursor. The SiC content of the siliconized composites was only increased 5-10 vol% after three or four successive infiltrations with the ceramic precursor. In contrast, the SiC content was increased ~14 and ~25 vol% after using only one and two carbon precursor infiltrations, respectively. The highest SiC contents achieved were in the range of ~91-93 vol%. In addition, lower pyrolysis temperatures (650-1000°C) were used for the carbon precursor compared to the ceramic precursor (1000-1650°C). For these reasons, the carbon precursor infiltration/pyrolysis process has better potential for commercial application.

6. Surface regions of porous SiC preforms were infiltrated with the carbon precursor to produce siliconized composites which had a dense surface layer of high SiC content (~95 vol%). The best results were obtained using three or four infiltration/pyrolysis cycles.

7. The mechanical properties, including flexural strength, Young's elastic modulus, Vickers hardness and fracture toughness, were increased by about 20-25% and 35-50% with one and two carbon precursor infiltrations, respectively. The average four-point flexural strength, Vickers hardness, elastic modulus, and fracture toughness for siliconized samples with two carbon precursor infiltrations were ~280 MPa, ~25 GPa, ~384 GPa, and ~4.0 $MPa \cdot m^{1/2}$, respectively. Also, the polishability of siliconized samples with carbon precursor infiltrations was improved significantly.

8. From the strength and fracture toughness data, the maximum flaw size was estimated to be ~150 μm which was independent of the number of carbon precursor infiltrations. It is believed that the large flaws originated from the bubbles incorporated in the original SiC preforms (which were supplied by an industrial collaborator). Therefore, efforts are currently being directed toward improving the initial forming process so that bubbles (and other large processing flaws) are eliminated.

9. Work was initiated using an Si-Mo alloy for reactive infiltration into carbon/SiC preforms in order to create $MoSi_2$/SiC composites. (Molybdenum disilicide has much better mechanical properties at high temperatures than silicon.) Investigations were directed toward determining the appropriate alloy composition and heat treatment conditions (temperature, time, and atmosphere) which would produce composites with minimal residual silicon.

Publications

1. M.D. Sacks, N. Bozkurt, and G.W. Scheiffele, "Fabrication of Mullite and Mullite-Matrix Composites by Transient Viscous Sintering of Composite Powders," J. Am. Ceram. Soc., 74 (10) 2428-2437 (1991).

2. M.D. Sacks, G.W. Scheiffele, N. Bozkurt, and R. Raghunathan, "Fabrication of Ceramics and Composites by Viscous and Transient Viscous Sintering of Composite Particles," pp. 437-455 in Ceramic Powder Science IV, Ceramic Transactions, Vol. 23, edited by S.-I. Hirano, G.L. Messing, and H. Hausner, American Ceramic Society, Westerville, OH, 1991.

3. M.D. Sacks, M.S. Randall, G.W. Scheiffele, and J.H. Simmons, "Processing of Silicate Glass/Silicon Nitride Composites with Controlled Microporosity," pp. 407-420 in Advanced Composite Materials, Ceramic Transactions, Vol. 19, edited by M.D. Sacks, American Ceramic Society, Westerville, OH, 1991.

4. M.D. Sacks, N. Bozkurt, and G.W. Scheiffele, "Transient Viscous Sintering of Mullite and Mullite-Matrix Composites," pp. 111-123 in Advanced Composite Materials, Ceramic Transactions, Vol. 19, edited by M.D. Sacks, American Ceramic Society, Westerville, OH, 1991.

5. M.D. Sacks, G.W. Scheiffele, N. Bozkurt, R. Raghunathan, and A.E. Bagwell, "Processing of Composite Powders: Fabrication of Ceramics and Composites by Viscous Sintering and Transient Viscous Sintering," Chapter 50 in Chemical Processing of Advanced Materials, edited by L.L. Hench, J. West, and D.R. Ulrich, Wiley, NY, 1992.

6. K. Wang, "Processing of Improved Siliconized Silicon Carbide by Liquid Infiltration Methods," M.S. Thesis, University of Florida, 1992.

7. A.E. Bagwell, "Fabrication and Characterization of SiALONS and SiALON-Based Composites Prepared by a Novel Processing Technique," M.S. Thesis, University of Florida, 1992.

8. M.D. Sacks, R. Raghunathan, I.Y. Park, and G.W. Scheiffele, "Processing and Properties of Glass/Ceramic Composites with Low Dielectric Constant Prepared from Microcomposite Particles," pp. 243-259 in Materials in Microelectronic and Optoelectronic Packaging, Ceramic Transactions, Vol. 33, edited by H.C. Ling, K. Niwa, and V.N. Shukla, American Ceramic Society, Westerville, OH, 1993.

A copy of reference 8 is attached.

PROCESSING AND PROPERTIES OF GLASS/CERAMIC COMPOSITES WITH LOW DIELECTRIC CONSTANT PREPARED FROM MICROCOMPOSITE PARTICLES

M.D. Sacks, R. Raghunathan, I.Y. Park, and G.W. Scheiffele, Department of Materials Science and Engineering, University of Florida, Gainesville, FL 32611

ABSTRACT

Glass/ceramic composites with low dielectric constant and low loss tangent were fabricated using microcomposite particles which consisted of inner cores of a crystalline phase (α-Si_3N_4 or α-Al_2O_3) and outer coatings of a glassy phase (SiO_2 or B_2O_3-SiO_2). Powder compacts prepared with microcomposite particles (SiO_2/Si_3N_4) showed enhanced densification compared to conventionally-processed compacts prepared with a mixture of glass and crystalline particles (SiO_2 + Si_3N_4). The sintering temperatures required for densification of compacts prepared with microcomposite particles decreased significantly as the concentration of B_2O_3 in the siliceous coating increased. This was attributed to the decreased viscosity of the coating as the B_2O_3 content increased. SiO_2/Si_3N_4 composites with ~9-10 vol% closed, isolated, spheroidal pores (~2 μm dia.) were prepared by using a mixture of microcomposite particles and polystyrene particles. The incorporation of microporosity resulted in a lower dielectric constant (~4.4 at 1 MHz) compared to a fully dense sample (~4.9 at 1 MHz) with the same SiO_2/Si_3N_4 volume ratio (~60/40). The samples had the same loss tangent (2 x 10^{-4}) and average flexural strength (183 MPa) values. SEM observations of fracture surfaces suggested that the strength values for these samples could be increased by reducing the concentration of large processing-related flaws (e.g., powder agglomerates).

INTRODUCTION

The ceramic materials used in microelectronics packaging applications must have (i) excellent electrical properties (low dielectric constant, low loss tangent, high resistivity), (ii) good thermal properties (e.g., coefficient of thermal expansion, CTE, match with chip and/or metallizing materials), (iii) resistance to corrosion (e.g., due to moisture), and (iv) adequate mechanical properties (strength, fracture toughness) to withstand stresses imposed during fabrication and handling of the package. In recent years, many investigations have been directed toward the development of ceramic materials with lower dielectric constant (in order to

increase signal propagation speed) and co-firing compatibility with lower resistivity metals such as copper, silver, etc. (in order to produce packages with higher circuit density). In particular, glass/ceramic compositions have been utilized to achieve both lower dielectric constant and lower sintering temperatures.[1-14] This includes (i) "glass-ceramic" materials in which glass powder compacts are sintered to high relative density (low porosity) and can be subsequently crystallized to nearly glass-free materials and (ii) "glass + ceramic" composites in which powder compacts prepared with mixtures of glass and crystalline ceramic particles are sintered to high relative density. The crystalline components usually have higher dielectric constant than the glassy phases, but they also improve mechanical and thermal properties of the material. A difficulty in processing "glass + ceramic" composites is that powder compact densification rates usually decrease as the volume fraction of crystalline ceramic particles increases.[14,15] Composite densification may be severely impeded when the concentration of "non-sinterable" inclusions is sufficient to form a connected particulate network (i.e., percolation path). Thus, it may be necessary to (i) limit the amount of crystalline phase in the powder mixture and/or (ii) modify the glass composition so that the melt viscosity is lower at the sintering temperature. These approaches have been effective in producing hermetic composites with high relative density, but they impose compositional constraints which limit the range of physical properties that can be achieved.

Another approach for producing "glass + ceramic" composites is based on the processing of glass/ceramic microcomposite particles.[14,16] These particles consist of crystalline cores and outer coatings of amorphous SiO_2. As schematically illustrated in Fig. 1, the controlled spatial distribution of the two phases prevents the formation of a connected network of the non-sinterable

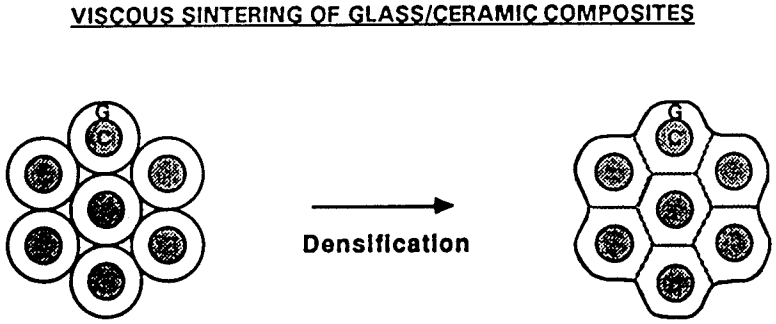

FIG. 1. Schematic illustration of viscous sintering of glass (G)/crystalline ceramic (C) composites using powder compacts prepared with microcomposite particles. The particles have an outer layer of glassy phase and a core of crystalline phase.

crystalline particles in the powder compact. Furthermore, the distribution of the amorphous phase facilitates densification via the viscous flow mechanism. Thus, lower sintering temperatures can be achieved and composites with higher volume fraction of crystalline phase can be produced. In some systems, it is also possible to react the glass and ceramic phases (after densification) to produce a fully crystalline material. The latter process is known as transient viscous sintering (TVS).[16,17]

The present study focuses on the development of glass + ceramic composites using microcomposite particles which consist of (i) crystalline Si_3N_4 or Al_2O_3 cores and (ii) amorphous SiO_2 or borosilicate coatings. A technique for introducing controlled microporosity into the samples is also utilized in order to produce composites with lower dielectric constant.[14]

EXPERIMENTAL

Microcomposite Particles

The preparation of silica-coated microcomposite particles has been described previously.[17] SiO_2 coatings were deposited on core particles using tetraethyl orthosilicate (TEOS)▲ as the starting material. The core particles used in this study were α-Al_2O_3♦ and α-Si_3N_4.◄ The as-received powders were first fractionated using gravitational and centrifugal fluid classification techniques[18] in order to remove hard agglomerates. The fractionated Al_2O_3 and Si_3N_4 powders had median Stokes' diameters in the range ~0.2-0.35 μm, as determined by a centrifugal photosedimentation technique.† The microcomposite particles were prepared by mixing core particle/ethanol suspensions with TEOS/ethanol solutions. SiO_2 was precipitated onto the core particles by adding ammoniated water to the suspension. The final SiO_2/core particle ratio in the microcomposite particles can be varied by adjusting the concentrations of the components in the initial coating suspension.[17] In this study, the composite particles were prepared with approximately 40 vol% crystalline phase and 60 vol% SiO_2.* After precipitation, the suspension of coated particles was filtered and the collected

---

▲ Fisher Scientific, Fair Lawn, NJ.
♦ AKP-50, Sumitomo Chemical America, New York, NY.
◄ SN-E-10, Ube Industries (America), Inc., New York, NY.
† Model CAPA-700, Horiba Instruments, Inc., Irvine, CA.

* This composition is approximate because it is calculated from the ratio of TEOS/crystalline core particles used in the coating suspensions. However, the precipitation of SiO_2 onto the core particles does not occur with 100% yield, i.e., some siliceous species remain in solution. Thus, the crystalline phase concentration in the composite particle may be slightly higher than the calculated value.

powder was washed with deionized water and subsequently dried. Figures 2A and 2B show transmission electron micrographs (TEM)▼ for typical SiO_2/Si_3N_4 and SiO_2/Al_2O_3 composite particles, respectively. It is evident that the SiO_2 coatings are uniformly deposited onto the core particles. X-ray photoelectron spectroscopy§ was used to confirm that the external layer of the particles was SiO_2.[19] X-ray diffraction¶ and high resolution transmission electron microscopy‡ showed that the SiO_2 coatings were amorphous.[19]

Microcomposite particles with borosilicate coatings were formed in the same manner as described above except that precipitation was carried out using mixtures of tributyl borate (TBB)▸ and TEOS. The ratio of B_2O_3/SiO_2 in the coating was altered by varying the TBB/TEOS ratio in the starting solution. Borosilicate/Si_3N_4 particles with ~23 wt% B_2O_3 in the silicate phase and borosilicate/Al_2O_3 particles with ~10 and ~17 wt% B_2O_3 in the silicate phase were prepared.* Since the amount of core particles was kept constant during the coating experiments, the silicate coating/core particle ratio varied with the amount of B_2O_3 added. The volume ratio was ~65/35 for the borosilicate/Si_3N_4 particles, while the ratios were ~62/38 and ~64/36 for the borosilicate/Al_2O_3 particles with ~10 and ~17 wt% B_2O_3, respectively, in the silicate phase.** Figures 2C and 2D show TEM micrographs of borosilicate-coated Al_2O_3 particles.

Green Compact Preparation and Sintering

SiO_2/Si_3N_4 composites were prepared using both silica-coated microcomposite particles and a mixture of SiO_2 and Si_3N_4 particles. In the latter case, the SiO_2 powder was prepared by solution-precipitation using TEOS as the precursor and the Si_3N_4 was the same fractionated powder used in preparation of the silica-coated microcomposite particles. These powders were mixed in aqueous suspension in a ratio of ~60 vol% SiO_2/~40 vol% Si_3N_4 (i.e., the same ratio as

---

▼ Model 200CX, Japan Electron Optics Co. Ltd., Tokyo, Japan.
§ Model XSAM800, Kratos Analytical, Manchester, United Kingdom
¶ Model APD 3720, Philips Electronic Instruments Co., Mt. Vernon, NY.
‡ Model 4000-FX, Japan Electron Optics Co. Ltd., Tokyo, Japan.
▸ Johnson Matthey Alfa Products, Danvers, MA.

* The B_2O_3 concentrations in the silicate phases were determined by inductively coupled plasma (ICP) spectroscopic analysis (Plasma II Model 5800, Perkin Elmer Corp., Norwalk, CT).

** The silicate coating/core particle ratios are approximations calculated from the ratios of components in the coating solutions and estimated true densities of the borosilicate phase.

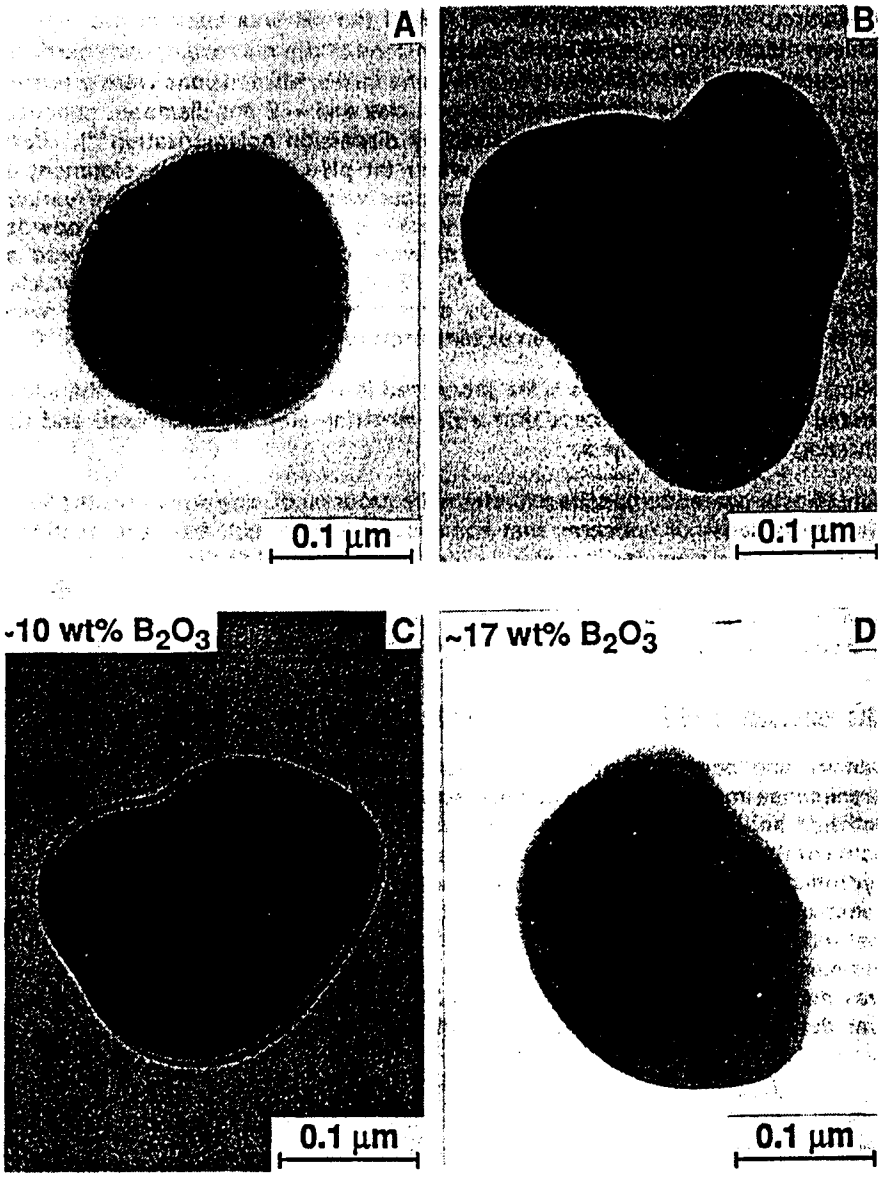

FIG. 2. TEM micrographs of microcomposite particles: (A) SiO_2/Si_3N_4, (B) SiO_2/Al_2O_3, (C) borosilicate (~ 10 wt% B_2O_3)/Al_2O_3, and (D) borosilicate (~ 17 wt% B_2O_3)/Al_2O_3.

in the microcomposite particles). The suspension was subjected to ultrasonication to break down agglomerates and the pH was adjusted (to ~9) to achieve electrostatic stabilization. Suspensions of the microcomposite particles were prepared in the same manner. In some cases, suspensions were prepared with mixtures of the microcomposite particles and ~2 μm diameter, spherical polystyrene (PS) particles (synthesized by dispersion polymerization[20]). Both types of particles dispersed well in water (at pH ≈ 9) due to development of negative surface charges. Green compacts were prepared from the various suspensions by slip casting into preforms set upon plaster blocks. The powder compacts (disks and rectangular bars) were oven-dried and pre-sintered at temperatures in the range 600-800°C. Samples prepared with PS particles developed ~2 μm spheroidal voids after this treatment. Compacts were subsequently sintered in nitrogen at temperatures in the range 1150-1300°C.

Silica-coated Al_2O_3 particles were processed in the same manner as the silica-coated Si_3N_4 particles except that a pre-sintering step was not used and the sintering atmosphere was air.

Borosilicate-coated composite particles were processed using ethanol as the liquid medium because of concerns that some B_2O_3 might leach from the coating if particles were suspended in water for an extended period of time. Particles were mixed with polymeric dispersants and ultrasonicated to break down agglomerates. Suspensions were slip cast and the resulting powder compacts were oven-dried and subsequently sintered in air at temperatures in the range 600-1200°C.

Characterization of Glass/Ceramic Composites

Density and open porosity of sintered compacts were determined using the Archimedes immersion method. Microstructure observations were made on both polished and fracture surfaces using scanning electron microscopy (SEM).▲▲ Some of the polished samples were etched with a dilute (~0.5 - 2 wt%) aqueous hydrofluoric acid solution. Measurements of dielectric properties (dielectric constant and loss tangent) were made at 1 MHz using a non-contacting electrode method.◆◆ Average strength was determined by four-point bending tests on 8-10 samples having dimensions of ~25 mm x ~5 mm x ~2 mm. Vickers hardness was measured using a 500 g load and 20 s dwell time.◀◀ Fracture toughness was determined by the indentation method of Anstis et al.[21]

▲▲ Model JSM-6400, Japan Electron Optics Co., Ltd., Tokyo, Japan.

◆◆ HP 4192 Impedance Analyzer and HP 16451B Dielectric Test Fixture, Hewlett-Packard Co., Palo Alto, CA.

◀◀ Micromet 3, Buehler, Ltd., Lake Bluff, IL.

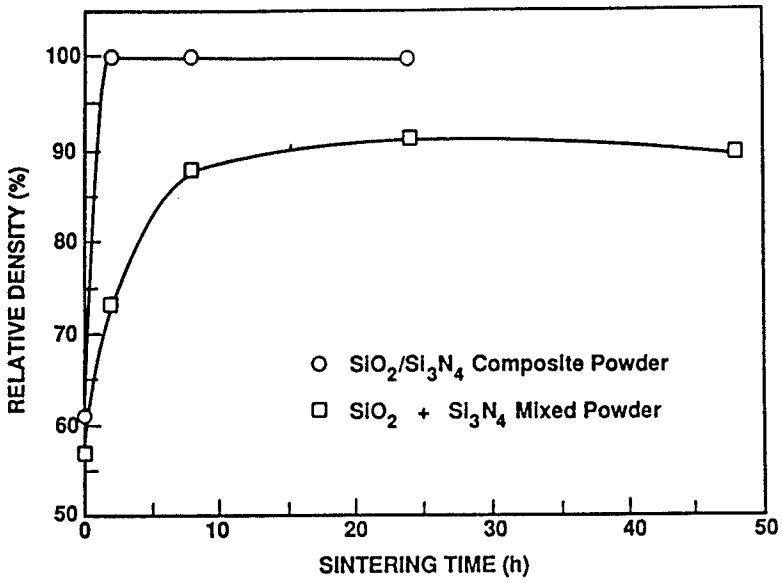

FIG. 3. Plots of relative density vs. sintering time at 1300°C for two types of ~60 vol% SiO_2/~40 vol% Si_3N_4 powder compacts. Compacts were prepared from (i) a mixture of SiO_2 particles and Si_3N_4 particles and (ii) amorphous silica-coated Si_3N_4 particles.

RESULTS AND DISCUSSION

Silica/Silicon Nitride Composites

Densification behavior was directly compared for powder compacts prepared with the silica-coated Si_3N_4 composite particles and the mixture of SiO_2 particles and Si_3N_4 particles.* Figure 3 shows plots of relative density vs. sintering time for ~60 vol% SiO_2/~40 vol% Si_3N_4 samples. The sample prepared with the microcomposite particles reached nearly 100% relative density after heat treatment for 2 h at 1300°C. In contrast, the sample prepared with the powder

* An effort was made to maintain similar particle sizes and green compact densities for the two types of samples so that the spatial distribution of the phases (SiO_2 and Si_3N_4) was the key variable influencing densification behavior. The composite particles were slightly larger (median Stokes' diameter of ~0.3 μm compared to a value of ~0.25 μm for the particle mixture), while the green compact prepared with them had slightly higher packing density (~61% vs. ~57%).

mixture reached only ~73% relative density under the same sintering conditions. Even with prolonged sintering times, the maximum relative density achieved was only ~90%. This result suggests that densification was inhibited due to the formation of a rigid network of "non-sinterable" Si_3N_4 particles. The Si_3N_4 concentration (~40 vol%) significantly exceeds the percolation threshold value for a random mixture of particles.[22] Si_3N_4 particle-particle contacts were evident in the polished microstructure of the sintered (1300°C, 2 h) powder mixture sample (Fig. 4A). In contrast, the Si_3N_4 particles were dispersed well in the SiO_2 matrix of the corresponding sample prepared with the microcomposite particles (Fig. 4B). Microstructure observations also showed that the sample was essentially pore-free.

Green compacts prepared with a mixture of ~88 vol% silica-coated Si_3N_4 particles and ~12 vol% PS particles were sintered at 1300°C (0.4-0.5 h). This resulted in shrinkage and elimination of the fine interparticle pores associated with the packing of the microcomposite particles. In contrast, the larger (~2 μm) spheroidal voids created by pyrolysis of the PS particles underwent relatively little shrinkage at this temperature. However, as densification of the SiO_2/Si_3N_4 matrix occurred, the spheroidal voids were closed off from the sample surface. Figure 5A shows a fracture surface of the sintered sample which illustrates that pores are closed and mostly isolated. A higher magnification micrograph of a polished and etched surface (Fig. 5B) shows that SiO_2/Si_3N_4 matrix is almost fully dense and that the Si_3N_4 particles are well-dispersed in the silliceous glass phase.

Table I lists dielectric properties for the ~60 vol% SiO_2/~40 vol% Si_3N_4 samples that were prepared with the microcomposite particles. A fully dense sample (sintered at 1300°C for 2 h) had a dielectric constant of 4.9 and a loss tangent of 2×10^{-4} (at 1 MHz). As expected, the incorporation of ~10% closed pores resulted in lower dielectric constant (4.4 at 1 MHz). The loss tangent was unchanged (2×10^{-4}).

Table I also lists mechanical properties for the SiO_2/Si_3N_4 composites with and without closed porosity. The fully dense sample had an average flexural strength of 183 MPa, average Vickers hardness of 8.7 GPa, and average fracture toughness of 2.3 MPa•$m^{1/2}$. These properties are significantly better than values reported for silicate glasses[10,23,24] and are comparable to values reported for various silicate glass/crystalline ceramic composites and crystallized glass-ceramics (e.g., cordierite) with low dielectric constant.[3-13] The incorporation of ~9% closed porosity in the SiO_2/Si_3N_4 composites resulted in a lower average hardness (6.5 GPa), but the average flexural strength remained the same (183 MPa).* The latter result indicates that the closed, spheroidal pores are not the

---

* The fracture toughness could not be determined on the porous sample because the cracks generated during indentation were not well-defined.

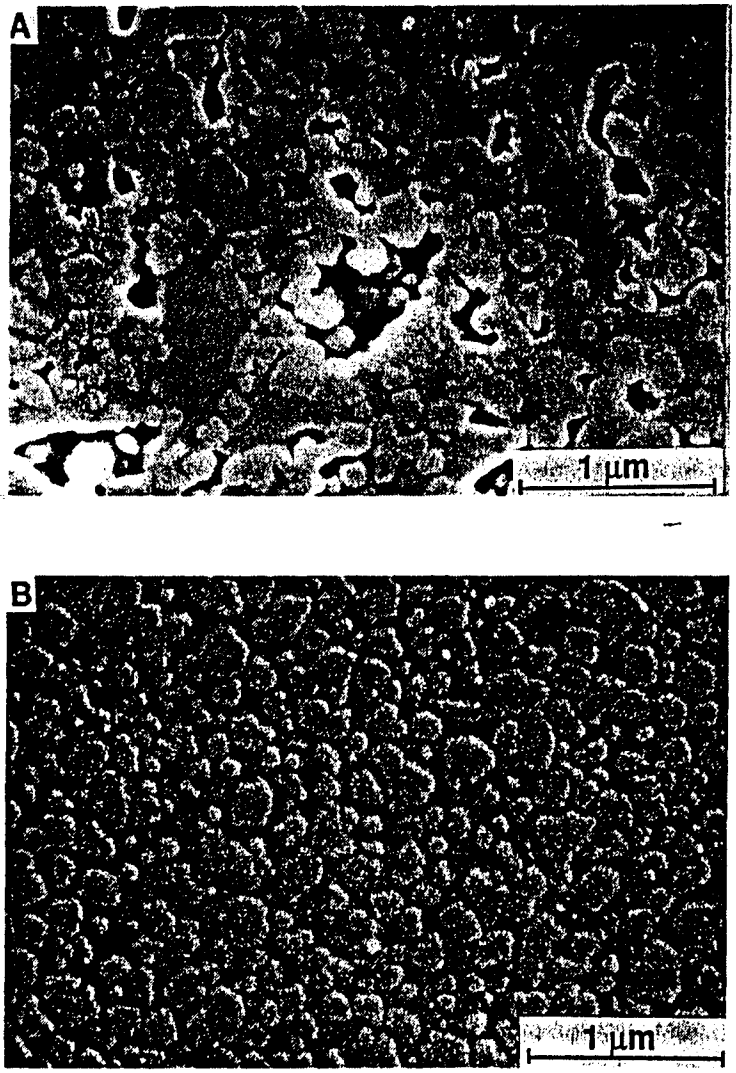

FIG. 4. SEM micrographs of polished and etched SiO_2/Si_3N_4 samples (sintered at 1300°C, 2h) that were prepared from the (A) mixture of two types of particles and (B) microcomposite particles.

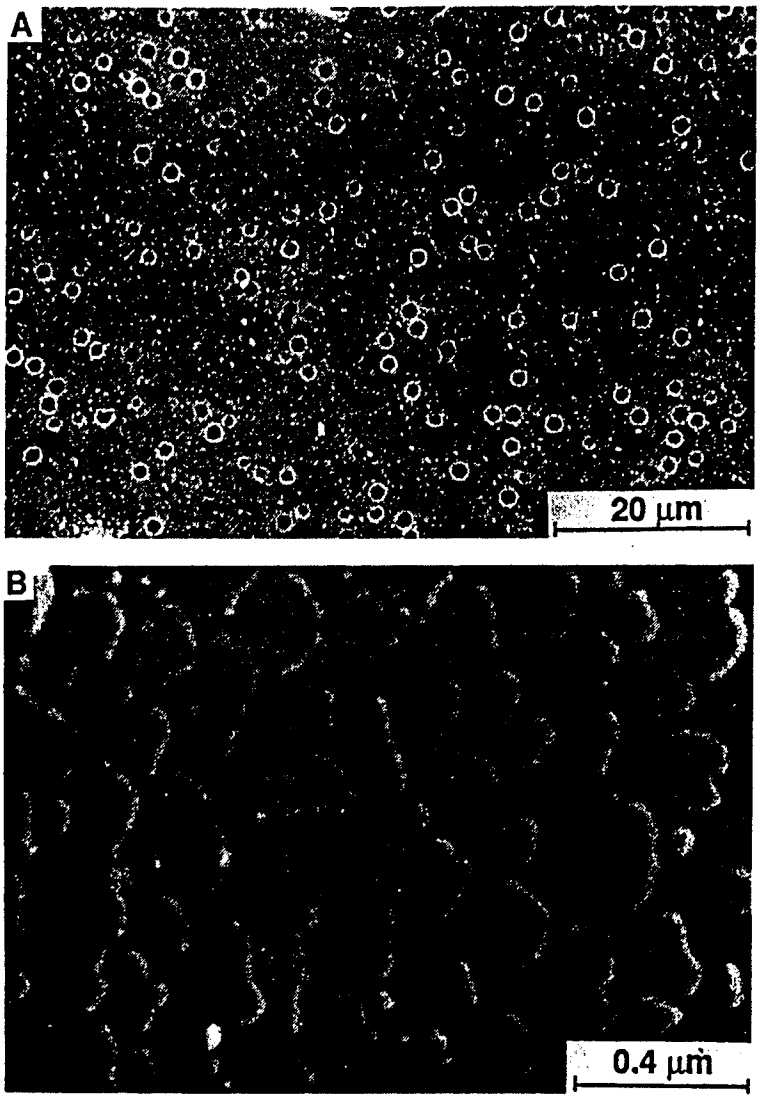

FIG. 5. SEM micrographs of SiO_2/Si_3N_4 sample (sintered at 1300°C, 2 h) prepared from a mixture of microcomposite particles and PS particles. (A) Lower magnification micrograph of a fracture surface shows the closed, spheroidal pores. (B) Higher magnification micrograph of a polished and etched surface shows the dense matrix in which the Si_3N_4 particles are dispersed in the siliceous glass phase.

Table I. Properties of 60 vol% Silica/40 vol% Silicon Nitride Samples

	Zero Porosity	Microporous*
Flexural Strength (MPa)	183 (±33)	183 (±43)
Vickers Hardness (GPa)	8.7 (±0.2)	6.5 (±0.1)
Fracture Toughness (MPa•$m^{1/2}$)	2.3 (±0.2)	
Dielectric Constant (at 1 MHz)	4.9	4.4
Loss Tangent (at 1 MHz)	2×10^{-4}	2×10^{-4}

* The samples used in the mechanical and dielectric property measurements had ~9% and ~10% closed porosity, respectively.

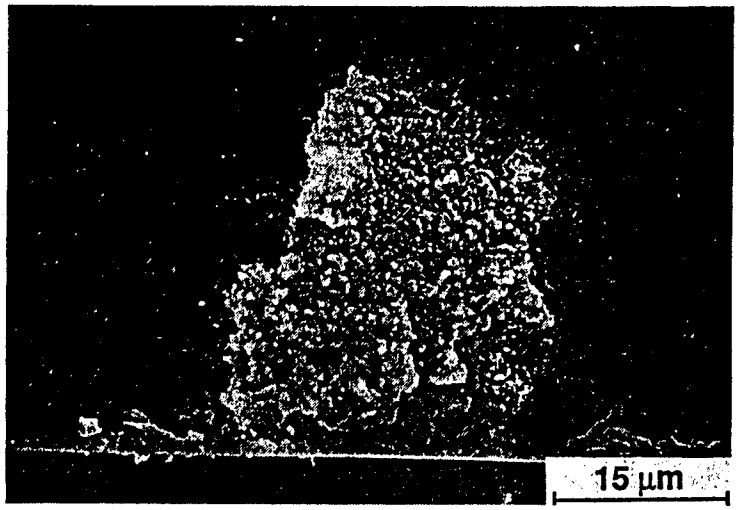

FIG. 6. SEM micrograph of a fracture surface of a SiO_2/Si_3N_4 sample (sintered at 1300°C, 2 h) showing a large processing defect (powder agglomerate).

strength-limiting flaws in the SiO_2/Si_3N_4 composites. Preliminary observations of fracture surfaces suggests that the strength may be limited by uncontrolled processing defects, e.g., powder agglomerates which were not broken down during processing. Figure 6 shows an example of a sintered powder agglomerate which apparently initiated fracture in one of the pore-free samples.

Borosilicate/Alumina and Borosilicate/Silicon Nitride Composites

Figure 7A shows a plot of open porosity vs. sintering temperature for compacts prepared with coated Al_2O_3 particles containing 0, ~10, and ~17 wt% B_2O_3 additions to the siliceous phase. The sintering temperatures decreased dramatically as the B_2O_3 content increased. The sample with ~17 wt% B_2O_3 in the siliceous coating reached nearly zero open porosity at only 950°C, i.e., ~350°C lower than the sample with no B_2O_3 addition. The enhanced densification is attributed to the much lower viscosity of the borosilicate glass. It was noted in the experimental section that the Al_2O_3/silicate glass ratio in these samples decreased slightly with increasing amount of B_2O_3 addition. In conventional sintering of glass/ceramic particle mixtures, a decrease in the crystalline phase content would be expected to increase the densification rate. In the present study, however, the change in Al_2O_3 content should have minimal effect on the densification kinetics because the process is dominated by viscous flow of the amorphous siliceous coating. This was confirmed by the observation that the densification behavior for the sample prepared with no B_2O_3 (~59 vol% SiO_2/~41 vol% Al_2O_3) was virtually the same as obtained in a previous study[17] in which the silica-coated composite particles had much higher Al_2O_3 contents, i.e., ~52-73 vol%.

Figure 7B shows a plot of open porosity vs. sintering temperature for the compacts prepared with the ~60 vol% SiO_2/~40 vol% Si_3N_4 composite particles and ~65 vol% borosilicate/~35 vol% Si_3N_4 particles. Due to the high B_2O_3 content (~23 wt%) in the silicate coating, the latter sample reaches nearly zero open porosity at only ~750°C, i.e., ~500°C lower than the sample prepared with no B_2O_3. Again, this is attributed to the low viscosity of the silicate glass phase. (The difference in crystalline phase content should have minimal effect on the densification rate because sintering is dominated by viscous flow of the amorphous phase.) Figure 8 shows an SEM micrograph of a polished and etched surface of a sintered (800°C) borosilicate/Si_3N_4 sample. The sample shows no porosity and the fine silicon nitride particles are dispersed in the borosilicate glass matrix. The dielectric constant and loss tangent for this sample were 4.4 and 1×10^{-4}, respectively, at 1 MHz.

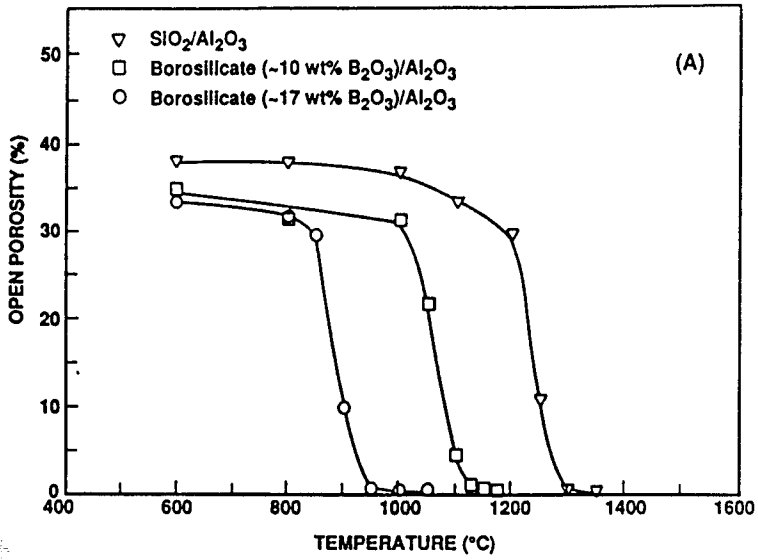

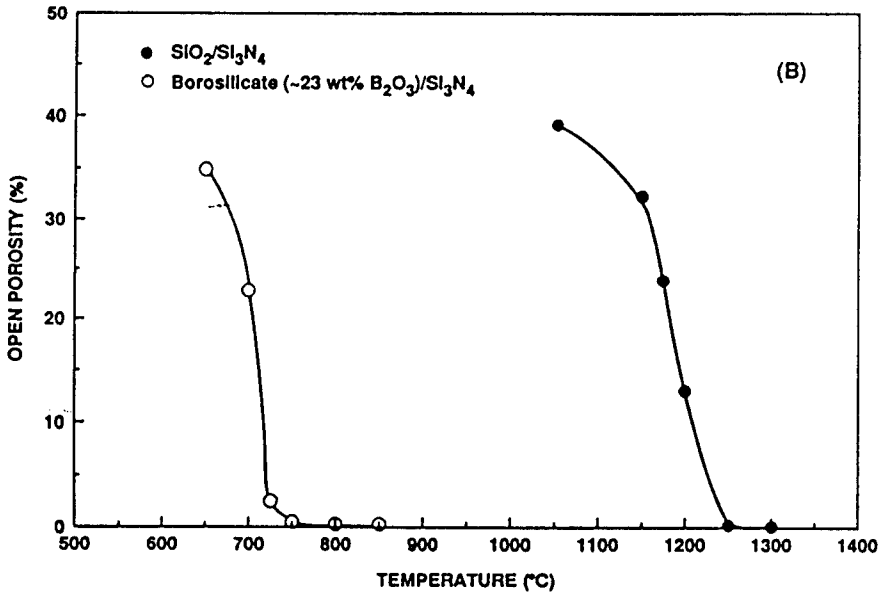

FIG. 7. Plots of open porosity vs. sintering temperature for compacts prepared with (A) silica-coated Al_2O_3 particles and borosilicate-coated Al_2O_3 particles and (B) silica-coated Si_3N_4 particles and borosilicate-coated Si_3N_4 particles.

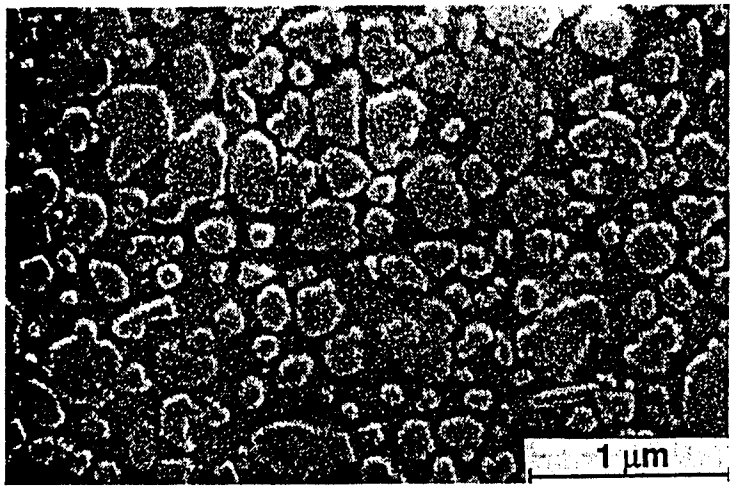

FIG. 8. SEM micrograph of a polished borosilicate/Si_3N_4 sample (sintered at 800°C, 2 h).

CONCLUSION

A novel process was developed in which bulk glass/ceramic composites were fabricated using microcomposite particles consisting of inner cores of a crystalline phase (Al_2O_3 or Si_3N_4) and outer coatings of a glassy phase (SiO_2 or B_2O_3-SiO_2). Powder compacts prepared with these microcomposite particles showed enhanced densification. This was demonstrated by directly comparing the sintering behavior of compacts prepared with silica-coated Si_3N_4 composite particles vs. a mixture of SiO_2 + Si_3N_4 particles; a composite powder compact with ~60 vol% SiO_2/~40 vol% Si_3N_4 reached almost full density within 2 hours at 1300°C, while a mixed powder compact had only ~90% relative density after 48 h at 1300°C. The increased densification rate for the former sample was attributed to two factors: (i) densification occurred by viscous flow of the amorphous coating of the microcomposite particles and (ii) the formation of a connected network of the non-sinterable inclusions was avoided by encapsulating the crystalline particles with the siliceous phase.

Samples with ~60 vol% SiO_2/~40 vol% Si_3N_4 and ~9-10 vol% closed, isolated, spheroidal pores (~2 μm dia.) were prepared by using a mixture of microcomposite particles and polystyrene particles. The incorporation of microporosity resulted in a lower dielectric constant (~4.4 at 1 MHz) compared to a fully dense sample (~4.9 at 1 MHz) with the same SiO_2/Si_3N_4 ratio. Both samples had low

loss tangent values ($\sim 2 \times 10^{-4}$). The average flexural strengths were also the same (183 MPa), but the porous sample had lower Vickers hardness (8.7 vs. 6.5 GPa). The mechanical and dielectric properties for these composites are similar to or better than reported values for many other glass + ceramic and glass-ceramic systems of interest for microelectronics packaging applications.[1-13] It may be possible to incorporate a larger amount of closed pores into the samples (and thereby lower the dielectric constant even further) by optimization of the powder characteristics and processing conditions (e.g., the size distributions for the microcomposite particles and the PS particles, sintering conditions, etc.). It may also be possible to obtain higher strength levels in these samples by reducing the concentration of large processing-related flaws (e.g., powder agglomerates).

Glass/ceramic composites were also prepared using borosilicate-coated microcomposite particles. Powder compact sintering temperatures decreased significantly as the concentration of B_2O_3 in the siliceous coating increased. This was attributed to the decreased viscosity of the coating as the B_2O_3 content increased. A sample with ~ 23 wt% B_2O_3 in the coating and an overall borosilicate glass/Si_3N_4 volume ratio of $\sim 65/35$ was sintered to almost full density at only $\sim 800^{\circ}C$. The sample had dielectric constant and loss tangent values of 4.4 and 1×10^{-4}, respectively, at 1 MHz.

In summary, silica-coated and borosilicate-coated microcomposite particles were used to fabricate bulk glass/ceramic composites with good dielectric and mechanical properties. It should be possible to produce other bulk composites with a much broader range of properties (dielectric, mechanical, thermal, etc.) by preparing microcomposite particles with different chemical compositions of the core and coating phases.

ACKNOWLEDGMENT

Experimental contributions from M.M. Amini, C.S. Khadilkar, Y.J. Lin, D. Parker, and A. Ulicny are gratefully acknowledged. This work was supported by the Defense Advanced Research Projects Agency (MDA972-88-J-1006 and N0014-91-J-4075); National Science Foundation, Division of Materials Research, Ceramics and Electronic Materials Program (DMR-8451916); Florida High Technology and Industry Council; and IBM Corp.

REFERENCES

1. A.H. Kumar, P.W. McMillan, and R.R. Tummala, "Glass-Ceramic Structures and Sintered Multilayer Substrates Thereof with Circuit Patterns of Gold, Silver, and Copper," U.S. Pat. No. 4 301 324, 1981.
2. N. Kamehana, K. Niwa, and K. Murakawa, "Packaging Material for High Speed Computers," pp. 388-392 in IEEE 33rd Electronics Components Conference Proceedings, IEEE, Washington, DC, 1983.

3. Y. Shimada, K. Utsumi, M. Suzuki, H. Takamizawa, M. Nitta, and T. Witari, "Low Firing Temperature Multilayer Glass-Ceramic Substrate," IEEE Trans. Components, Hybrids, Manufacturing Technol., 6 [4] 382-388 (1983).

4. S. Nishigaki, S. Yano, J. Fukuta, M. Fukuya, and T. Fuwa, "A New Multilayered, Low-Temperature-Fireable Ceramic Substrate," pp. 225-234 in Proceedings of the 1986 International Symp. on Microelectronics, ISHM, Reston, VA, 1985.

5. K. Kondo, M. Okuyama, and Y. Shibata, "Low Firing Temperature Ceramic Materials for Multilayer Ceramic Substrates," pp. 77-87 in Advances in Ceramics, Vol. 19. Edited by J.B. Blum and W.R. Cannon. American Ceramic Society, Westerville, OH, 1986.

6. K. Kawakami, M. Takabatake, T. Minowa, J. Chiba, and M. Sasaki, "A Low-Temperature Cofired Multilayer Ceramic Substrate," ibid., pp. 95-102.

7. Y. Shimada, Y. Yamashita, Y. Shiozawa, M. Suzuki, and H. Takamizawa, "Low Dielectric Constant Multilayer Glass-Ceramic Substrate with Ag-Pd Wiring for VLSI Package," pp. 398-405 in IEEE 37th Electronics Components Conference Proceedings, IEEE, Washington, DC, 1987.

8. H. Emura, K. Onituka, and H. Maruyama, "Multilayered Ceramic Substrates with Low Dielectric Constants," pp. 375-385 in Advances in Ceramics, Vol. 26. Edited by M.F. Yan, K. Niwa, H.M. O'Bryan, Jr., and W.S. Young. American Ceramic Society, Westerville, OH, 1987.

9. R.R. Tummala, "Ceramics and Glass-Ceramic Packaging in the 1990s," J. Am. Ceram. Soc., 74 [5] 895-908 (1991).

10. K. Kata, Y. Shimada, and H. Takamizawa, "Low Dielectric Constant New Materials for Multilayer Ceramic Substrate," IEEE Trans. Components, Hybrids, Manuf. Technol., 13 [2] 448-453 (1990).

11. J.-Y. Hsu, N-C. Wu, and S-C. Yu, "Characterization of Material for Low-Temperature Sintered Multilayer Ceramic Substrates," J. Am. Ceram. Soc., 72 [10] 1861-1867 (1989).

12. R.N. Master, L.W. Herron, and R.R. Tummala, "Cosintering Process for Glass-Ceramic/Copper Multilayer Ceramic Substrate," IEEE Trans. Components, Hybrids, Manuf. Technol., 14 [4] 780-783 (1991).

13. G. Partridge, C. Elyard, and H.D. Keatman, "Glass Ceramic Materials for Use in Substrate and Packaging Applications," Glass Technol., 30 [6] 215-219 (1989).

14. M.D. Sacks, M.S. Randall, G.W. Scheiffele, R. Raghunathan, and J.H. Simmons, "Processing of Silicate Glass/Silicon Nitride Composites with Controlled Microporosity," pp. 407-420 in Ceramics Transactions, Vol. 19. Edited by M.D. Sacks. American Ceramic Society, Inc., Westerville, OH, 1991.

15. M.N. Rahaman and L. De Jonghe, "Effect of Rigid Inclusions on the Sintering of Glass Powder Compacts," J. Am. Ceram. Soc., 70 [12] C-348 - C-351 (1987).

16. M.D. Sacks, G.W. Scheiffele, N. Bozkurt, and R. Raghunathan, "Fabrication of Ceramics and Composites by Viscous and Transient Viscous Sintering of Composite Particles," pp. 437-455 in Ceramics Transactions, Vol. 22. Edited

by S.-I. Hirano, G.L. Messing, and H. Hausner. American Ceramic Society, Inc., Westerville, OH, 1991.

17. M.D. Sacks, N. Bozkurt, and G.W. Scheiffele, "Fabrication of Mullite and Mullite-Matrix Composites by Transient Viscous Sintering of Composite Powders," J. Am. Ceram. Soc., 74 [10] 2428-2437 (1991).
18. H.-W. Lee "Suspension Processing and Pressureless Sintering of Silicon Carbide Whisker-Reinforced Alumina-Matrix Composites," Ph.D. Dissertation, University of Florida, 1990.
19. M.D. Sacks, G.W. Scheiffele, N. Bozkurt, R. Raghunathan, and Y.J. Lin, unpublished work.
20. Y.Y. Lu, M.S. El-Aasser, and J.W. Vanderhoff, "Dispersion Polymerization of Styrene in Ethanol: Monomer Partitioning Behavior and Locus of Polymerization," J. Polymer Sci., Part B: Polymer Physics, 26, 1187-1203 (1988).
21. Anstis, G.R., Chantikul, P., Lawn, B.R., and Marshall, D.B., "A Critical Evaluation of Indentation Techniques for Measuring Fracture Toughness: I, Direct Crack Measurements", J. Am. Ceram. Soc., 64 [9] 533-38 (1981).
22. R. Zallen. The Physics of Amorphous Solids. Wiley, New York, 1983.
23. L.A. Ketron, "Fiber Optics: The Ultimate Communications Media," Am. Ceram. Soc. Bull., 66 [11] 1571-1578 (1987).
24. L.E. Sanchez and D. Ngo, "Electrical Characterization of Matched Impedance Cofired, High Speed, Microelectronic Packages Made From Low Dielectric Constant, Boron-Doped, Sol-Gel Silica," Int. J. Hybrid Microelectronics, 12 [2] 95-100 (1989).

BOOK III

Section 2

Processing

of

$BaO\text{-}Al_2O_3\text{-}2SiO_2$ Fibers

Principal Investigator: **D.E. Clark**

PROCESSING OF $BaO \cdot Al_2O_3 \cdot 2SiO_2$ - A HIGH-TEMPERATURE MATRIX MATERIAL

D.E. Clark, D.C. Folz, Z. Fathi and A.D. Cozzi
Department of Materials Science and Engineering
University of Florida
Gainesville, FL 32611-2066

ABSTRACT

Microwave processing was investigated as a processing alternative to thermal heating for fabrication of a high temperature matrix -- $BaO \cdot Al_2O_3 \cdot 2SiO_2$. The processing route chosen in this investigation involves the synthesis of a gel-derived barium aluminosilicate glass followed by densification, nucleation and crystallization stages in the presence of an alternating electric field. Furthermore, microwave energy was used to 1) densify gel-derived silica glass for production of ultra-high optical quality glass, 2) crystallize lithium disilicate glass, and 3) interdiffuse potassium for sodium ions in a sodium aluminosilicate glass. The crystallization kinetics of the celsian phase from $BaO \cdot Al_2O_3 \cdot 2SiO_2$ glass was examined. The Celsian phase is desirable as a composite matrix material because of its potentially high use temperature ($>1500^\circ$ C) and its low coefficient of thermal expansion ($2.2 \times 10^{-6}/^\circ$ C). The parent glass ($BaO \cdot Al_2O_3 \cdot 2SiO_2$) was prepared by the sol-gel process. A second composition of $(Sr_{0.15},Ba_{0.85})O \cdot Al_2O_3 \cdot 2SiO_2$ also has been produced using sol-gel techniques in order to evaluate the effect of strontium on the formation of the monoclinic celsian phase. Several different seed materials also were investigated to determine their potential for promoting formation of the monoclinic phase. Stabilization of the gel was performed in a Deltec conventional furnace while densification and crystallization were performed in a Raytheon QMP 2101B-6 microwave oven operating at 2.45 GHz as well as in the conventional furnace.

INTRODUCTION

There is increasing evidence of unusual effects brought about by microwave energy. These effects include enhanced reaction kinetics and enhanced crystallization and diffusion rates. The overall objective of this study was to investigate microwave processing as an alternative method for fabricating a high-temperature matrix -- $BaO \cdot Al_2O_3 \cdot 2SiO_2$. The processing route chosen to accomplish this goal addresses the use of microwave energy to

study the densification, nucleation and crystallization of $BaO \cdot Al_2O_3 \cdot 2SiO_2$ glass. The goal of the proposed effort was achieved through the study of each of these processing steps in the presence of an alternating electric field. The following report consists of four major sections, each of which summarizes the work that was performed in these areas of interest. The densification study (Section I) was carried out using gel-derived silica. The crystallization study in the presence of microwaves (Section II) was performed on a lithium disilicate glass. The materials selected for the microwave-driven diffusion study (Section III) were a series of sodium aluminosilicate glasses. The results of these studies provided the rational and the scientific basis necessary for accomplishing the overall objective of the proposed effort -- to fabricate a barium aluminosilicate high temperature matrix using mcirowave energy(Section IV).

Why Microwave Energy?

Microwave energy is a unique energy source and offers an alternative processing method by which shorter processing times often are achieved. A better understanding of microwave/materials interaction and equipment design is a key factor to scale-up of this technology for industrial applications. With the exception of food processing and several other applications (eg., rubber curing), microwave processing of materials still is in an early stage of industrial implementation. The proposed effort addresses the fabrication of a new material using microwave energy and the fundamentals behind microwave/materials interactions.

Why Barium Aluminosilicates?

Barium aluminosilicate glass-ceramics are being investigated as matrix materials in high-temperature ceramic composites for structural applications. There are several reasons for choosing $BaO \cdot Al_2O_3 \cdot 2SiO_2$ as a matrix material. The potential maximum use temperature in air is $>1500^\circ$ C, higher than the lithium aluminosilicates and the calcium aluminosilicates and comparable to the upper use temperature of mullite, which is in the range of 1600° C as determined from the phase diagram. Another appealing characteristic is its resistance to thermal shock, due primarily to its low coefficient of thermal expansion ($\alpha = 2.29 \times 10^{-6}/^\circ$ C from RT to 1000° C). This low thermal expansion (lower than SiC at $\alpha = 4.3\text{-}5.6 \times 10^{-6}/^\circ$ C from RT to 1000° C [1]) would put the matrix in compression during

cool down and could increase the strength of the composite. Other advantages include good resistance to oxidation as well as formability (net shaping) prior to crystallization.

Celsian, the monoclinic phase, is stable at temperatures $<1590^{\circ}$ C and is the crystalline phase of interest. However, hexacelsian, the high-temperature, hexagonal phase, often is the primary phase that nucleates even at low temperatures. The hexagonal phase is undesirable because of its higher coefficient of thermal expansion ($\alpha = 8 \times 10^{-6}/^{\circ}$ C) and because it transforms at 300 $^{\circ}$ C to the orthorhombic phase, accompanied by a 3 percent volume change. Hot pressed composites of celsian with 20 volume percent of SiC fiber reinforcement produced samples with > 90 percent of the calculated density and ultimate flexural strengths above 500 MPa[2]. No physical testing results at high temperatures have been reported for this system. Bahat examined the heterogeneous nucleation of $BaO \cdot Al_2O_3 \cdot 2SiO_2$ with several nucleating agents [3]. He reported that hexacelsian still was the primary phase to crystallize. Bahat continued work in the $BaO \cdot Al_2O_3 \cdot 2SiO_2$ system with a kinetic study of the hexacelsian-celsian phase transformation [4]. He found that the complete transformation often took days. Seeding the hexacelsian with 5 percent celsian reduced the transformation time to a few hours.

Glass-ceramics are pore-free, fine-grained, polycrystalline ceramics produced by controlled crystallization of glass. The small crystallites apparently provide a barrier to the propagation of cracks initiated at the surface. This phenomenon can make glass-ceramics significantly tougher than the glasses from which they were formed. In general, glass-ceramics possess low coefficients of thermal expansion, high elastic moduli and have strengths considerably higher than the parent glasses from which they are derived.

Ceraming, the process by which glasses are transformed into glass-ceramics, can be achieved by two means. The traditional process consists of conventional melting of the raw materials followed by rapid cooling to the glassy state, bypassing the formation of any crystalline phases. The glass then is subjected to controlled heat-treatment to bring about nucleation and crystallization of the desired phase(s). When a reinforcing phase such as SiC is added, the process becomes more complicated. Due to the high melting temperature of the raw materials, the glass must first be fritted so that a second phase can be added before forming, densifying and crystallizing the end product.

Many researchers have used the traditional method with hot pressing or hot isostatic pressing for nucleation, crystallization and densification in the production of celsian [2,5]. The melting of $BaO \cdot Al_2O_3 \cdot 2SiO_2$ glass requires temperatures in excess of 2100° C. Thus, sophisticated furnaces are required for processing. The major problems associated with this technique are (a) contamination from the molybdenum electrode in amounts up to 1 wt%, (b) uncontrolled heterogeneous nucleation influenced by the impurities and the walls of the container, and (c) crystallization of the therdynamically unstable hexagonal phase.

Other research groups have pursued a low-temperature sol-gel method for the formation of the parent glass [6-8]. Although the parent glass is synthesized readily by the sol-gel process, only hexacelsian has been crystallized to date. In the traditional processing method, substitution of strontium for barium has produced direct crystallization of the celsian phase [9].

Microwave heating is fundamentally different from conventional processing. Depending on the microwave absorption of the material, heat generation can be volumetric and within the material rather than originating from external heating sources. Consequently, the thermal profiles generated within a ceramic article when subjected to microwaves are quite different from those generated by infrared heating. Microwave processing makes it possible to achieve uniform heating in both small and large shapes. Furthermore, the thermal stresses accompanying the conventional processing methods appear to be of a lesser magnitude when the samples are processed in the presence of a microwave electric field. Although the fundamentals behind material/microwave interactions are not completely understood, a wide range of ceramic materials have been processed with microwave energy. The potential benefits brought about by the use a microwave electric field may include reduction in manufacturing costs due to energy savings and shorter processing times, improved product yield, improved or unique microstructures and synthesis of new materials.

The power absorbed by a material is described by the equation

(1)

$$P_{abs} = 2\pi f \epsilon_0 \epsilon''_{eff} |E^2| V$$

where

P_{abs}	=	power absorbed,
f	=	frequency,
ϵ_0	=	permittivity of free space,
ϵ''_{eff}	=	effective dielectric loss factor,
$\|E\|$	=	internal electric field strength, and
V	=	volume of material.

The resulting temperature rise brought about by this absorption is

(2)

$$P_{abs} = 2\pi f \epsilon_0 \epsilon''_{eff} |E|^2 V$$

where

ΔT	=	temperature rise,
Δt	=	time of exposure,
ρ	=	density of material, and
C_p	=	specific heat.

The kinetics of bulk crystallization involve a combination of nucleation and growth, both of which require energy to be added to the system. In addition to thermal energy, microwave radiation also adds energy of an electrical and magnetic nature. Therefore, microwave processing is a good candidate for investigating crystallization kinetics.

Since crystallization is a diffusion-controlled process, any enhancement in the diffusion would result in increased crystallization kinetics. The microwave heat treatments described here (Section II) have been shown to enhance crystallization at lower temperatures and produce more uniform microstructures. This observation is significant in light of the results found in reference 8 where the author reported increased porosity in samples, possibly due to Ostwald ripening of the early nucleating crystallites.

It is difficult to heat celsian with stand alone (microwave heating only) due to its low dielectric loss. However, we have demonstrated that other low loss materials (such as Al_2O_3) can be heated with a combination of microwaves and conventional methods. This

combination, referred to as microwave hybrid heating (MHH), results in more volumetric heating of the material and translates into more uniform microstructures throughout the sample. In the case of celsian, we expect more uniform crystallization with MHH than with conventional heating. Further, the addition of a strong microwave absorbing reinforcement phase (such as SiC) may provide the same results using stand-alone microwaves.

PROJECT GOALS

The goals of this investigation were to 1) produce a high-temperature ($>1500\ ^\circ C$) matrix with a coefficient of thermal expansion similar to or lower than a suitable reinforcement phase and chemically and physically compatible with reinforcement preferred agents, and 2) understand microwave/materials interactions.

PROJECT OBJECTIVES (JULY 1, 1993 - JUNE 30, 1994)

1. Evaluate $BaO \cdot Al_2O_3 \cdot 2SiO_2$ as a potential matrix material.
2. Investigate sol-gel as an alternative processing route to traditional glass-ceramic processing.
3. Investigate the use of microwave energy for processing glass-ceramics.
4. Study the effect of microwaves on densification.
5. Study the effect of microwaves on crystallization.
6. Study the effect of microwaves on diffusion.

EXPERIMENTAL AND RESULTS

The experimental section is subdivided into four sections, each of which summarizes the results obtained in densification, crystallization, diffusion using microwave energy and the fabrication of a barium aluminosilicate high temperature matrix.

Section I. Densification

Dense, foam free, transparent gel-derived silica was produced using microwave energy (1600W). A processing schedule using microwave energy for 14 hours yielded a dense silica glass with high transmission (>93%) and a UV cut-off similar to that of fully dense gel-derived silica glass processed conventionally under chlorination. The dehydration process has not been completed under the processing conditions described in this study. More work is needed in order to improve on the dehydration process of samples irradiated with microwave energy.

Since large quantities of water ($OH+H_2O$) are bound to the structure of porous gel-derived silica, special care is required to remove the water (dehydration process) and densify these materials. The ultimate goal is to fabricate ultrahigh optical quality, gel-derived silica glass [13,14]. Generally, water is removed through condensation reactions[15]. When heated to adequate temperatures, water disassociates from the porous structure and evaporates through the open channels of the gel. However, viscous sintering and pore closure often commence before the dehydration process is completed. This results in water entrapment inside the already closed pores and complete water removal is not achieved. The water trapped inside the gels often results in foaming of the samples in the final stage of sintering. Water removal can be accelerated by heat treating the gel samples in controlled atmospheres. Thus, in most cases, the production of fully dense silica with low water concentration (less than 1000 ppm) is achieved by long heat treatments under chlorination [16].

Recently, microwave energy was investigated as an alternative means by which porous silica gels could be heated [17,18]. This processing method offers promise for the production of dense gel-derived silica glass. Furthermore, microwave processing has two unique features when compared to conventional heating (IR heat + convection): 1) internal and uniform (volumetric) heating, and 2) possible coupling with O-H and Si-OH dipoles. This characteristic volumetric heating reduces thermal gradients across the samples and lessens their tendency to crack during processing. Furthermore, volumetric heating

promotes fast heating rates that cannot be achieved under normal conventional processing conditions [16].

Microwave heating is intrinsically different from conventional heating. The ability of electromagnetic radiation (in the MW frequency range) to polarize molecules and the inability of these dipoles to keep up with the rapid reversal of the electric (polarizing) field results in heat generation. There are no known publications about the dielectric behavior of porous silica gels in the microwave frequency range and over the temperature range of interest in this study. Upon microwave irradiation, some of the existing dipoles such as, $-H^+$ and $-OH^-$, may couple with the oscillating electric field. Although this mechanism is speculative, the authors feel that microwave coupling with the $-H^+$ and $-OH^-$ groups may promote the condensation reaction responsible for water removal. The work presented in this section was designed to examine the critical factors of dehydration and densification of porous silica gels in the presence of microwave energy.

The samples used for this study were produced at the University of Florida, Advanced Materials Research Center (AMRC). The type VI porous silica gels were TMOS-derived with an average pore radius of 30Å. The preparation and characterization of the gel-silica monoliths have been reported previously by Araujo, LaTorre and Hench et al[19].

Microwave hybrid heating techniques were used to produce dense, crack free, transparent, gel-derived silica glass. These techniques often are used to heat many low-microwave-absorbing ceramic materials, such as silica or alumina. The samples were placed in a SALI insulating chamber lined with a microwave susceptor (SiC) which, in turn, assisted in heating the samples. The SALI insulation cavity (Zircar Products Inc.) has a density of 2.5 gm/cc and consists of 80% alumina and 20% silica. Changing the thickness of the SiC lining allowed the samples to be processed at similar temperatures, but under different incident microwave powers. This type of heating is referred to as microwave hybrid heating or dual heating since heat generation in the samples is caused by microwave energy and radiant heat from the susceptor [20,21]. The insulating/suscepting chamber is illustrated in Figure 1(a). The processing times required to achieve densification were reduced significantly as compared to conventional processing techniques. However, UV transmission

analysis revealed water trapped inside the optically transparent silica glass. The dehydration process was incomplete.

A new MHH chamber was designed to improve the dehydration process of the gel-derived silica samples. This was achieved by reducing the amount of SiC lining on the walls of the insulating cavity. By altering the amount of susceptor in the cavity, the samples were processed at the desired temperatures under more microwave incident power than previously reported. Another MHH chamber was investigated in this study. This susceptor/thermal insulation arrangement is referred to as the "picket fence", Figure 1(b).

A micropycnometer (Quantachrome, Inc.) with nitrogen gas was utilized for bulk density measurements. An average of three measurements for each sample was taken as the sample's bulk density and the standard deviation was less than 0.01.

Ultraviolet(UV)-Visible(VIS)-Near Infrared(NIR) transmission [14,19,20] is used widely to evaluate the water content of glasses. Water in glasses results in an absorption over the 2600nm-3200nm wavelength range. A Perkin Elmer UV-VIS-NIR Spectrophotometer with wavelength range from 185.5nm to 3200nm was used to determine the water content of the microwave processed samples.

Water removal is accelerated and densification and sintering are enhanced with increasing temperatures. The dehydration process may be optimized if the samples were heated to temperatures just below those of densification, basically heat treating the samples prior to the onset of sintering. Since the densification process is accompanied by shrinkage, evaluating the temperature at which shrinkage starts could indicate the temperature range over which there is a compromise between densification and water removal.

A series of glass samples were heat treated in the microwave oven at various temperatures (950° C-1200° C) with a 15 minutes soak time. The samples were taken out of the oven and quenched in air. This was followed by dimensional measurements. The results of the gel's diametral shrinkage following the various thermal treatments are illustrated in Figure 2. The silica-gel sintering and/or densification appears to be accelerated in the 1100-1200° C temperature range. The temperature at which shrinkage

starts appears to be approximately 1050° C. The thermal treatments used in this study were based on this information.

Figure 3 shows the UV-VIS-NIR transmission spectra of typical microwave-processed, gel-derived silica glass samples. The spectra of some microwave-processed samples are contrasted with that of a fully dense glass conventionally heat treated using chlorination. The microwave-processed samples were subjected to different heating schedules. The spectra of a sample processed according to the MHH processing schedule using an 800W microwave energy source over 7 hours is contrasted with those of samples processed with MHH under 1600W incident power for 3.5, 7 and 14 hours, respectively. The samples processed for 14 hours under 1600W power exhibited low water content and high transmission (>93%); furthermore, their UV cut-off was similar to that of the fully dense sample produced conventionally. Table 1 shows the processing time, densification temperatures, and the density of typical gel-silica-derived glasses subjected to different thermal treatments. As illustrated in Table I, the total processing time is much shorter for gel-silica samples processed in the presence of microwave energy. The densification temperature of the gel-derived silica samples processed with 1600 W microwave energy was lower than that of the samples processed conventionally or with microwave energy using 800W incident power.

Figure 4 shows a comparison of samples processed in air at various temperatures in both microwave and conventional ovens. Microwave energy appears to be an efficient method for producing dense silica glass. Since gel dehydration was not completed under the processing conditions described in this study, more work is needed to optimize the microwave heating schedule in order to produce dense silica glass containing less than 1000ppm of water.

Section II. Crystallization of $Li_2O \cdot 2SiO_2$ Glass

The $Li_2O \cdot 2SiO_2$ system was chosen as the lead-in material for $BaO \cdot Al_2O_3 \cdot 2SiO_2$ for several reasons. The $Li_2O \cdot 2SiO_2$ is a simple material that crystallizes readily and its crystallization kinetics are well documented.

Rods of lithium disilicate were nucleated at 450° C for 3 hours in a conventional furnace. The bars then were cut into discs and crystals were grown over a range of temperatures using both microwave and conventional heating. X-ray diffraction analysis was performed on the samples to determine the crystalline phases present. Peak intensities were compared to determine the relative percent crystallinity due to differing heat treatments. The effect of the heat-treatment parameters using both microwave and conventional heating on the extent of crystallization were investigated.

Glass samples were prepared from TiO_2-free silica and reagent grade Li_2CO_3. A batch of SiO_2 + 33.3 mol% Li_2O was melted at 1350° C for 72 hours in a covered platinum crucible. The glass was cast as rods (75 mm long and 13 mm in diameter) and annealed at 300° C for 12 hours. Nucleation was performed at 450° C for 4 hours on all of the rods simultaneously to ensure consistency. Discs 4 mm thick were cut from the rods and polished with an emery cloth until optically clear. Samples containing seeds were discarded.

The growth process was performed isothermally with the time being measured starting when the sample was inserted in the furnace or microwave cavity. Growth temperatures ranged from 500 to 600° C, inclusive. The samples then were ground into a fine powder with a mortar and pestle. Specimens for x-ray diffraction were prepared and analyzed in a Phillips ADP 3720 x-ray diffractometer. The relative fraction of crystallinity in each of the specimens was determined by comparing the intensities of all peaks observed to the peak intensities of the sample heat-treated in the microwave at 600° C for 10 minutes. All of the peaks encountered during x-ray diffraction analysis corresponded to the orthorombic phase of lithium disilicate. The effect of temperature on the crystallization of Li_2O-SiO_2 is listed in Table 2. There was considerable difference in the crystallization kinetics between the two processes. Heat treating the discs for 10 minutes using microwave energy was sufficient to fully crystallize the samples at temperature as low as 580° C. Table 3 shows the effect of time and temperature on the relative crystallinity of the samples heat-treated using microwave energy. It was determined that significant crystallization could be achieved at temperatures as low as 500° C using microwave energy. Figure 5 indicates the relative percent crystallinity as a function of time for samples heat-treated in the microwave. Figure 6 shows x-ray diffraction patterns of samples (MHH) heated at 540° C at different

times. This demonstrates the development of the crystalline phase with time for a given temperature.

Section III. Diffusion

A sodium alumino-silicate (NAS) Corning glass (code#0317) was chosen for this investigation. The glass was surface modified using a slurry ion-exchange. The interdiffusion of K^+ for Na^+ was carried out in the presence of a microwave electric field at 2.45 GHz. Similar chemical/heat treatments were carried out in a conventional furnace for the sake of comparison. Electron microprobe (EMP) was used to derive the concentration profile of potassium after ion-exchange. The diffusion coefficients were calculated for both heating methods.

The objectives of this study were 1) to evaluate the contribution of the migration loss mechanism to the overall measured dielectric loss, 2) to evaluate the effect of conduction losses on the K^+-Na^+ interdiffusion enhancements brought about by microwave energy, if any, and 3) to calculate the diffusion coefficient of K^+ in the case of microwave driven ion-exchange reactions.

In a previous study [10,22], microwave energy was used to interdiffuse $K^+ \ll Na^+$ in a series of NAS glasses. The existence of an interdiffusion enhancement brought about by microwave energy (the so called "Microwave Effect") was established previously for the NAS glass system. Furthermore, the microwave effect was found to depend on glass composition, and increased with increasing Al/Na values up to Al/Na=1.0. A correlation between the dielectric loss of the glass matrix and the microwave interdiffusion enhancement was established.

The microwave effect was pronounced for the Al/Na=1.0 glass composition. This composition has the highest dielectric loss, as measured by the frequency shift method, and the highest electrical conductivity, as predicted by the NAS structural glass model. However, no correlation was established between the dielectric loss and the electrical conductivity of the different glasses; nor was it established between the observed microwave effect and the conductivity related losses of the different glasses. It was only natural to ask whether the

conduction losses are responsible for the observed interdiffusion enhancements caused by microwave energy.

The Corning glass (code#0317) was chosen for this study because it is a versatile glass used in industry [23]. Furthermore, this glass composition is close to that of the Al/Na=1.0 glass composition studied previously. The dielectric behavior of the Corning glass was evaluated over a broad range of temperatures (25-1000° C) for different frequencies in the GHz range (0.39, 0.91, 1.42, 1.94, 2.46, and 2.98). The relative dielectric constant, the dielectric loss factor, the loss tangent, and the depth of penetration versus temperature are illustrated in Figure 7.

Resistivity as a function of temperature is illustrated in Figure 8. These measurements were obtained from Corning Inc. (Advanced Products Department, Corning, N.Y.). The conduction losses were calculated at 2.45 GHz (the microwave working frequency) calculated by subtracting the conduction losses from the measured losses. As illustrated in Figure 9, the conduction losses were negligible below 400° C and the measured losses were independent of conduction losses. At elevated temperatures (above 400° C), the conduction losses appeared to increase rapidly.

A study was conducted to evaluate the effect of conduction losses on the K^+-Na^+ interdiffusion enhancements brought about by microwave energy, if any. The K^+-Na^+ ion-exchange was carried out by the slurry method, in which the glass was coated with a slurry containing the desired ions (K^+ in this case). The Corning glass samples were heated using the MHH technique for 45 minutes. The heat treatment temperatures were chosen in light of the results illustrated in Figure 9. The chosen temperatures were 400° C, a temperature at which no conduction losses are exhibited, and 450° C, a temperature at which the conduction losses are pronounced. Electron microprobe (EMP) analysis was used to determine the potassium and sodium ion depth profiles for both the microwave and conventionally processed samples. Electron microprobe (EMP) analysis was used quantitatively to derive the concentration profile (in wt%) of both K^+ and Na^+. This was done by calibrating the EMP counts to those of the as received glass composition and those of selected mineral standards.

Larger K^+ diffusion depths of penetration were achieved in the glass samples ion-exchanged in the presence of a microwave electric field. Furthermore, the interdiffusion enhancements occurred for both temperatures--400 and 450°C. Therefore, the conduction losses may have contributed to the microwave effect, but they were not solely responsible for the observed results.

The diffusion coefficients for the microwave and conventionally processed samples were calculated according to equation (3):

$$D_{c1} = -1/(2t)\ (dx/dC)\ \delta_0^{C1}\ xdC \qquad (3)$$

Where D_{c1} is the interdiffusion coefficient at the concentration c_1, t is the diffusion time, x is the depth of penetration into the glass, and C is the concentration of potassium. This is a graphical method [24] by which the interdiffusion coefficient, in the case of a semi infinite body, can be obtained. The K^+ and Na^+ concentration profiles were converted from weight percent to mol percent prior to calculations. The initial K^+ concentration of the as-received Corning glass was not taken into account. The interdiffusion coefficient of glasses ion exchanged by microwave heating at 450° C was found to be $8.12x10^{-10}$ cm^2s^{-1}. The interdiffusion coefficient of glasses ion exchanged conventionally at 450° C was found to be $2.15x10^{-10}$ cm^2s^{-1}. Thus, under apparently similar processing conditions, the interdiffusion coefficient of $K^+ \ll Na^+$ in the presence of microwave energy was 3.78 times greater than that achieved by conventional heating.

Section IV. $BaO \cdot Al_2O_3 \cdot 2SiO_2$

Glass Preparation

Gels were prepared by the sol-gel process with two compositions, $BaO \cdot Al_2O_3 \cdot 2SiO_2$ and $(Sr_{0.15},Ba_{0.85})O \cdot Al_2O_3 \cdot 2SiO_2$. The precursor materials used were tetraethylorthosilicate (TEOS), aluminum-sec-butoxide (ASB), barium acetate and strontium acetate.

In the first step, a dilute solution of TEOS in ethanol was partially hydrolyzed by adding 1/4 of the theoretical water needed for full hydrolysis and a few drops of HCl. This solution was refluxed at 60° C for three hours. Step two was the slow addition of a dilute

solution of ASB in isopropanol to the cooled TEOS/ethanol mixture. This solution was allowed to react overnight. Step three consisted of dissolving barium acetate in 3.75 times the amount of water needed to fully hydrolyze the TEOS and enough acetic acid to lower the pH below 4. This solution was added slowly to the TEOS/ASB mixture with sufficient excess acetic acid to clear the sol. The resulting sol was stirred for 20 minutes before casting. Gelation normally occurred within 30 minutes of casting.

The second composition was identical to the first with the exception of the partial substitution of strontium acetate for barium acetate.

The gels were dried to a powder at several temperatures (50, 200 and 800° C). The dried gels were characterized using differential thermal analysis (DTA) to obtain information such as organic burnout and the glass transition temperature (Tg) needed for vitrification of the gels. X-ray diffraction analysis also was performed on the DTA samples to determine the crystalline phases present, if any. X-ray diffraction indicated that the gels were amorphous up to at least 900° C.

Seeding

Several seed materials with the potential to promote forming the monoclinic phase also were investigated. Monoclinic zirconia, copper oxide and strontium aluminosilicate (produced by the sol-gel process and crystallized at 1300° C for four hours) were used in amounts ranging from 0.1wt% to 10wt%. The temperatures investigated (1050 to 1300° C) included those below and above the zirconia monoclinic→ tetragonal phase transformation. The gel powders were cold pressed into discs at 4000 psi for the vitrification study.

Vitrification

Vitrification was carried out in a conventional furnace at temperatures extracted from the processing "window" provided by the DTA results in Figure 4. The temperatures used for vitrification were 800, 900, 950, 1020 and 1050° C. The glasses were screened using XRD to evaluate the extent of crystallization, if any, that occurred during heat treatments.

Archimedes density measurements were performed on the vitrified samples to

determine the bulk density of the glass before crystallization. This was done on samples of approximately three grams with water as the liquid medium.

Crystallization

In the next phase of the study, the glass samples were heat treated using conventional and MHH. Temperatures investigated ranged from 1050 to 1300° C. The time allowed for crystallization was 3 hours in the conventional furnace and ninety minutes at 1100° C in the microwave furnace.

Crystallized samples were analyzed using x-ray diffraction analysis and the bulk densities were determined by the Archimedes method.

RESULTS & DISCUSSION

$BaO \cdot Al_2O_3 \cdot 2SiO_2$

The DTA for a gel dried at 50° C is shown in Figure 10. The two peaks below 200° C were attributed to elimination of the alcohols and pore water of the gel. The exotherm at 400° C was attributed to burning out the remaining organic materials. The small endotherm slightly below 1200° C was confirmed by x-ray diffraction to be due to the crystallization of the hexagonal phase. Table 4 provides the x-ray diffraction results of the unseeded glasses after crystallization in both the conventional and microwave furnaces.

Differential thermal analysis also was performed on seeded samples. The substitution of strontium for barium in the gel crystallized only the hexagonal phase. Zirconia, when added as a seed in amounts of one and ten weight percent, crystallized as the hexagonal phase at both 1050° C and 1250° C. Monoclinic strontium aluminosilicate ($SrO \cdot Al_2O_3 \cdot 2SiO_2$) was used as a seed in two, five and ten weight percents additions. This resulted in the formation of the hexagonal phase. Results for the samples seeded with CuO were more promising. At 1050° C, a 10 wt% addition of CuO exhibited a small amount of monoclinic phase among the hexagonal phase. At 1300° C, a one percent addition of CuO also showed signs of the monoclinic phase. Figure 10(c) is the DTA for the sample with 10 wt% CuO added. The range from 900 to 1250° C is expanded in Figure 10 to elucidate the

crystalline peaks. X-ray diffraction performed on samples heated below 1100° C, between 1100 ° C and 1200 ° C, and above 1200 ° C provided confirmation of the phases described in the DTA plot. The sample exhibited peaks corresponding primarily to the monoclinic celsian phase with a small number of low intensity peaks corresponding to the hexagonal phase. Seeding with the crystalline phase formed upon heating at 1300° C with a one percent CuO addition did not enhance monoclinic crystallization in any sample.

Samples seeded with 1, 5 and 10 wt% $SrO \cdot Al_2O_3 \cdot 2SiO_2$ and CuO also were heat-treated using microwave energy. All of the samples seeded with $SrO \cdot Al_2O_3 \cdot 2SiO_2$ crystallized as the hexagonal phase. A one percent CuO addition also crystallized as the hexagonal phase. The x-ray diffraction pattern of the sample containing 5 wt% CuO exhibited peaks corresponding to both the monoclinic and hexagonal phases. Semi-quantitative analysis indicated and equal amount of both phases. Under the same conditions, a 10 wt% addition of CuO contained a 70/30 mix of the monoclinic and hexagonal phases. Table 5 shows the results of the effects of seeding on the phases crystallized.

The bulk density was measured for samples with various amounts of seed material heat-treated at 950° C for 20 hours and then at 1300° C for 4 hours.

CONCLUSIONS

The experimental evidence of the existence of the so called "microwave effect" was established in several systems. Dense, foam-free, optically transparent gel-derived silica monoliths were produced using microwave energy (1600W). A processing schedule using microwave energy for 14 hours yielded a dense silica glass with high transmission (>93%) and an UV cut-off similar to that of fully dense gel-derived silica glass processed conventionally under chlorination. The volumetric heating produced by microwave energy allowed high heating rates, fast dehydration and rapid densification. The dehydration process has not been completed under the processing conditions described in this study. More work is needed in order to improve on the dehydration process of samples irradiated with microwave energy.

Glass discs of lithium disilicate glass were nucleated in a conventional furnace and the growth stages were performed using both conventional heating and microwave energy. The growth stage of the heat treatment executed in the microwave produced samples that appeared uniform in color. X-ray diffraction analysis confirmed that the volume fraction of the crystal phase may be controlled by varying the processing parameters. It was also determined that significant crystallization can be achieved at temperatures as low as 500°C using microwave energy.

Dielectric measurements over a range of temperatures and frequencies were performed on an NAS glass series. The frequencies selected for this study were 400MHz, 912MHz, 1429MHz, 1948MHz, 2.45GHz and 2.98GHz. The dielectric measurements were performed from room temperature up to 1000° C. The dielectric loss factor (ϵ'') of the Corning glass increased with increasing temperatures and/or decreasing frequencies. The tan δ behavior as a function of temperature and frequency was similar to that of ϵ''. Electron microprobe was used to derive the concentration profiles of sodium and potassium after ion exchange in both a microwave and conventional ovens. Interdiffusion reactions carried out using the slurry technique (potassium for sodium) performed in the microwave oven at 400° C and/or 450° C for 45 minutes resulted in deeper potassium concentration profiles as compared to those performed in a conventional oven. The increase in potassium depth of penetration was attributed to an increase in diffusion brought about by the microwave electric field. The conduction independent losses were calculated at 2.45 GHz over a wide temperature range (25° C-500° C). The conduction losses may have contributed to the observed enhancements in the interdiffusion $K^+ \leftrightarrow Na^+$ brought about by microwave energy, but were not solely responsible for them. The microwave interdiffusion coefficients as calculated by a graphical method were about four times greater than the conventional interdiffusion coefficient.

Powders of the composition $BaO \cdot Al_2O_3 \cdot 2SiO_2$ were produced using the sol-gel process. Low temperature heat-treatments of the pressed powders did not increase the bulk density of the samples. During crystallization, only the sample with 10 wt% CuO added and heated in the microwave for 15 minutes exhibited noticeable densification. Crystallization of the monoclinic celsian phase was achieved with the addition of CuO as a seed material.

A 5 wt% addition of CuO produced a significant amount of the monoclinic phase. A completely monoclinic material was achieved with a 10 wt% addition of CuO. Relying on the limited results obtained, it appeared that the use of microwave energy for the crystallization process did not decrease either the temperature or the amount of seed material needed to produce the monoclinic phase when compared to the samples heat-treated in conventional furnace. Only in the case of the ten weight percent CuO addition sample heated to 1050° C using microwaves was the formation of the thermodynamically stable monoclinic phase at lower temperatures using microwave energy consistent with the results obtained for the lithium disilicate glasses.

FUTURE WORK

- Evaluate the dielectric properties of the gel-derived barium aluminosilicate glass over a range of temperatures and frequencies.
- Modify the chemistry in order to change the gel formation process to produce a gel that can be densified without external pressure during forming.
- Continue investigation of time, temperature and seeding on the crystallization of the celsian phase.
- Use a variable frequency microwave source to study the enhancement of crystallization as a function of microwave energy input and frequency (this can be performed using a variable frequency microwave furnace--VFMF)
- Prepare samples for high temperature mechanical testing.
- Determine the effect of CuO and other materials additions on the high temperature behavior of the matrix.
- Proceed with the addition of SiC as a second phase and perform a compatibility study.

The present work was presented at the American Ceramic Society Meeting and Exposition, Cincinnati, OH and at the 17th Annual Conference on Composites and Advanced

Ceramics, Cocoa beach, Fl. The basic science developed in this work has led to new initiatives in microwave processing.

With support of this project, Zak Fathi has graduated with a doctoral degree in April 1994. Mr Fathi's work was supported primarily by DARPA since 1989. Alex Cozzi has left the DARPA project to accept a graduate fellowship from the High Temperatures Materials Laboratory at Oak Ridge National Lab.

REFERENCES

1. W.J. Lackey, D.P. Stinton, G.A. Cerny, L.L. Fehrenbacher and A.C. Schaffhauser, "Ceramic Coatings for Heat Engine Materials - Status and Future Needs," Proc. Int. Symp. on Cer. Components for Heat Engines, Oct. 1983.

2. N.P. Bansal, J.A. Setlock and C.H. Drummond, III, "Celsian Glass-Ceramic Composites," Hi-Temp Review, NASA, cp-10039, pp. 62.1 - 62.12 1989).

3. D. Bahat, "Heterogenous Nucleation of Alkaline Earth Feldspar Glasses," J. Mat. Sci., **4**, pp. 847-854 (1969).

4. D. Bahat, "Kinetic Study of the Hexacelsian-Celsian Phase Transformation," J. Mat. Sci., **5**, pp. 805-810 (1970).

5. C.H. Drummond III, W.E. Lee, N.P. Bansal and M.J. Hyatt, "Crystallization of a Barium Aluminosilicate Glass," Ceram. Eng. Sci. Proc., **10**, [9-10], pp. 1485-1502 (1989).

6. W.K. Treadway and S.H. Risbud, "Gel Synthesis of Glass Powders in the $BaO \cdot Al_2O_3 \cdot 2SiO_2$ System," J. Non-Cryst. Solids, **100**, pp. 278-283 (1988).

7. V.S.R. Murthy, Li Jie and M.H. Lewis, "Interfacial Microstructure and Crystallization in SiC-Glass Ceramic Composites," Ceram. Eng. Sci. Proc., **10** [7-8], pp. 938-951 (1989).

8. M. Chen, W.E. Lee and P.F. James, "Preparation and Characterization of Alkoxide-Derived Celsian Glass Ceramic," to be published in JNCS.

9. N.P. Bansal and M.J. Hyatt, "Crystallization and Properties of Sr-Ba Aluminosilicate Glass-Ceramic Matrices," Ceram. Eng. Sci. Proc., **12,** [7-8], pp. 1222-1234 (1991).

10. Z. Fathi, I. Ahmad, J.H. Simmons, D.E. Clark and A.R. Lodding, "Surface Modification of Sodium Aluminosilicate Glasses Using Microwave Energy," Ceramic Transactions, Microwaves: Theory and Application in Materials Processing, Vol. 21, pp. 612-630, (D.E. Clark, F.D. Gac and W.H Sutton, eds.) The American Ceramic Society, Inc., Westerville, OH (1991).

11. A.D. Cozzi, Z. Fathi, R.L. Schulz and D.E. Clark, "Nucleation and Crystallization of Li_2O-$2SiO_2$ in a 2.45 GHz Microwave Field," presented at the 17th Annual Conference on Composites and Advanced Ceramics, January 10-15, 1993, Cocoa Beach, Florida.

12. A.D. Cozzi, Z Fathi and D.E. Clark, "Crystallization of Sol-Gel Derived Barium Aluminosilicate In a 2.45 GHz Microwave Field," presented at the American Ceramic Society Meeting and Exposition, Cincinnati, OH, April, 1993 (to be published).

13. L. L. Hench, S. H. Wang and J. L. Nogues, "Gel-Silica Optics," Multifunctional Materials 878, Robert L. Gunshor, ed., 76-85, SPIE, Bellingham, WA, (1988).

14. S. H. Wang, C. Campbell and L. L. Hench, "Optical Properties of Gel-Silica Glasses," in Ultrastructure Processing of Advanced Ceramics, 145-157, J. D. Mackenzie and D. R. Ulrich, eds., John Wiley & Sons, New York, NY, (1988).

15. C. J. Brinker and G. W. Scherer, "Sol-Gel Science: the Physics and Chemistry of Sol-Gel Processing," Academic Press, Boston, (1990).

16. S. H. Wang, "Sol-Gel Derived Silica Optics," Ph. D. Dissertation, University of Florida, (1988).

17. E. J. A. Pope, "Microwave Sintering of Sol-Gel Derived Silica Glass," Am. Ceram. Soc. Bull. 70, 11, 1777-1778, (1991).

18. J. P. Zhong, Z. Fathi, G. P. LaTorre, D. C. Folz and D. E. Clark, "Microwave Densification of Porous Silica Gel," Ceramic Transactions, D. E. Clark, W. R. Tinga, and J. R. Laia, Jr. eds., Vol. 36, 157-164, (1993).

19. F. G. Araujo, G. P. LaTorre, and L. L. Hench, "Structural Evolution of a New Type VI Sol-Gel Porous Silica Glass,"

20. S. Wallace, Porous Silica -Gel Monoliths: Structural Evolution and Interactions with Water, Ph. D. Dissertation, University of Florida, 1991.

21. L. L. Hench and J. K. West, "The Sol-Gel Process," Chem. Rev. 90, pp. 33-72 (1990).

22. Z. Fathi, D. C. Folz, R. Hutcheon, and D.E. Clark, "Surface Modification of Sodium Aluminosilicate Glasses Using Microwave Energy II," Ceramic Transactions, D. E. Clark, W. R. Tinga, J. R. Laia eds., Vol. 36, 333-340, (1993).

23. H. Miska, "Understanding the basics of chemically strengthened glass," Materials Engineering, June 1976.

24. I. Fainaro, M. Shalom, M. Ron, S. Lipson, "Interdiffusion of silver in the glasses and the related variations in the electronic polarizability," Physics and Chemistry of Glasses Vol. 25, No.1, February 1984.

Table 1. Processing Characteristics of Gel-Silica Glass

Samples	Conventional Fully dense	Microwave Processing		
		1600 W Input		800W Input
Processing Times	>3 Days	14 Hrs	7 Hrs	7 Hrs
Sintering Temperature (° C)	1150-1200	1100	1100	1200
Density (g/cc)	2.220	2.204	2.200	2.13
50%UV Cut-Off(Wavelength nm)	<185	<185	~185	210

Table 2. Effect of Temperature on the Relative Crystallization of Li_2O-$2SiO_2$

Heating method	Temperature (° C)	Time (minutes)	Percent crystallinity
microwave	600	10	100
conventional	600	10	6
microwave	580	10	100
conventional	580	10	0
microwave	560	10	56
conventional	560	10	0
microwave	540	10	19
conventional	540	10	0

Table 3. Effect of Time and Temperature on the Relative Crystallinity of Samples Heat-treated Using Microwave Energy.

Heating method	Temperature (° C)	Time (minutes)	Percent crystallinity
microwave	540	5	2
microwave	540	10	19
microwave	540	30	41
microwave	540	5	0
microwave	540	20	25
microwave	540	50	51

Table 4. X-ray Diffraction Results of Unseeded $BaO \cdot Al_2O_3 \cdot 2SiO_2$ After Crystallization Using Conventional and Microwave Energy.

Material	First		Second		Phases
	Temp	Time	Temp	Time	Detected
Conventional					
$BaO \cdot Al_2O_3 \cdot 2SiO_2$	800° C	20 hrs	none		none
$BaO \cdot Al_2O_3 \cdot 2SiO_2$	800° C	20 hrs	1300 ° C	4 hrs	hexagonal
$BaO \cdot Al_2O_3 \cdot 2SiO_2$	900° C	20 hrs	none		none
$BaO \cdot Al_2O_3 \cdot 2SiO_2$	900° C	20 hrs	1300 ° C	4 hrs	hexagonal
$BaO \cdot Al_2O_3 \cdot 2SiO_2$	1050° C	20 hrs	none		hexagonal
$BaO \cdot Al_2O_3 \cdot 2SiO_2$	1050° C	20 hrs	none		hexagonal
$BaO \cdot Al_2O_3 \cdot 2SiO_2$	1300° C	4 hrs	none		hexagonal
$BaO \cdot Al_2O_3 \cdot 2SiO_2$	1300° C	72 hrs	none		hexagonal
$BaO \cdot Al_2O_3 \cdot 2SiO_2$	1500° C	4 hrs	none		hexagonal
Microwave					
$BaO \cdot Al_2O_3 \cdot 2SiO_2$	900° C	3 hrs	none		none
$BaO \cdot Al_2O_3 \cdot 2SiO_2$	1100° C	1.5 hrs	none		hexagonal

Table 5. X-ray Diffraction Results of Seeding of $BaO \cdot Al_2O_3 \cdot 2SiO_2$ Glass Crystallized Using Conventional and Microwave Energy.

Seed Material wt% unless noted	Heat Treatment Temp	Time	Phases Detected
Conventional			
(1) 5 mol% Sr → Ba	1050° C	20 hrs	hexagonal
(2) 5 mol% Sr → Ba	1250° C	20 hrs	hexagonal
(3) 15 mol% Sr → Ba	1050° C	20 hrs	hexagonal
(4) 15 mol% Sr → Ba	1250° C	20 hrs	hexagonal
(5) 1% ZrO_2	1050° C	20 hrs	hexagonal
(6) 1% ZrO_2	1250° C	20 hrs	hexagonal
(7) 10% ZrO_2	1050° C	20 hrs	hexagonal
(8) 10% ZrO_2	1250° C	20 hrs	hexagonal
(9) 1% CuO	1050° C	20 hrs	hexagonal
(10) 1% CuO	1250° C	20 hrs	hex, mono
(11) 10% CuO	1050° C	20 hrs	hex, mono
(12) 10% CuO	1250° C	20 hrs	mono, tr. hex
(13) 0.1% CuO	1300° C	4 hrs	hexagonal
(14) 0.1% CuO + 0.5% (10)	1300° C	4 hrs	hexagonal
(15) 0.1% CuO + 1% (10)	1300° C	4 hrs	hexagonal
(16) 0.1% CuO + 5% (10)	1300° C	4 hrs	hexagonal
(17) 0.5% CuO	1300° C	4 hrs	hexagonal
(18) 0.5% CuO + 0.5% (10)	1300° C	4 hrs	hexagonal
(19) 0.5% CuO + 1% (10)	1300° C	4 hrs	hexagonal
(20) 0.5% CuO + 5% (10)	1300° C	4 hrs	hexagonal
(21) 1% CuO	1300° C	4 hrs	mono, hex
(22) 1% CuO + 0.5% (10)	1300° C	4 hrs	mono, hex
(23) 1% CuO + 1% (10)	1300° C	4 hrs	mono, hex
(24) 1% CuO + 5% (10)	1300° C	4 hrs	mono, hex

Table 5 continued.

Seed Material	Heat Treatment		Phases Detected
	Temp	Time	
Microwave			
1% CuO	1100° C	1.5 hrs	hexagonal
5% CuO	1100° C	1.5 hrs	50 hex/50 mono
10% CuO	1100° C	1.5 hrs	30 hex/ 70 mono
1% $SrO \cdot Al_2O_3 \cdot 2SiO_2$	1100° C	1.5 hrs	hexagonal
5% $SrO \cdot Al_2O_3 \cdot 2SiO_2$	1100° C	1.5 hrs	hexagonal
10% $SrO \cdot Al_2O_3 \cdot 2SiO_2$	1100° C	1.5 hrs	hexagonal

(a)

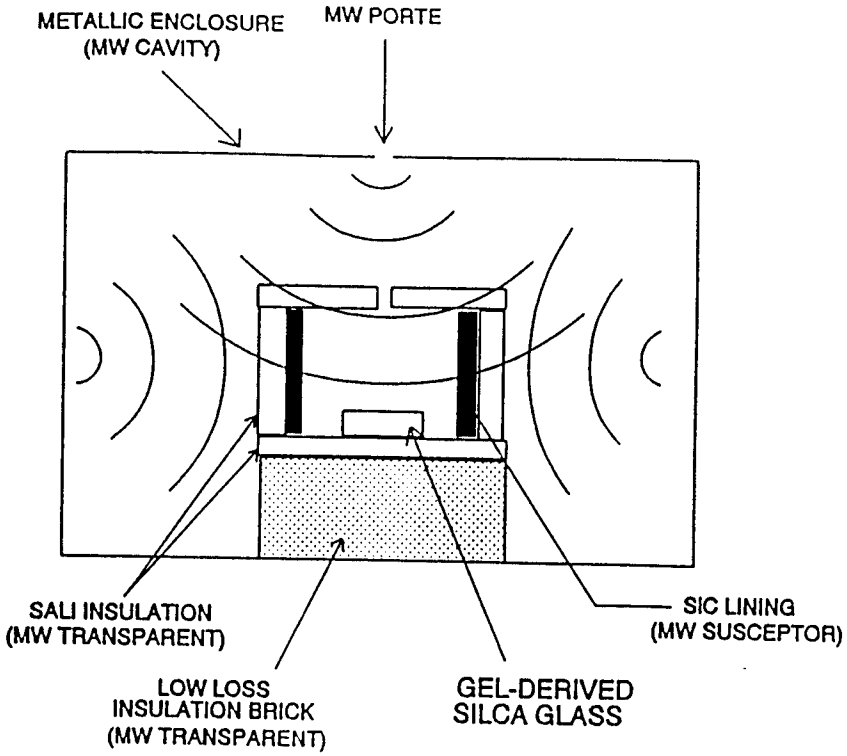

(b)

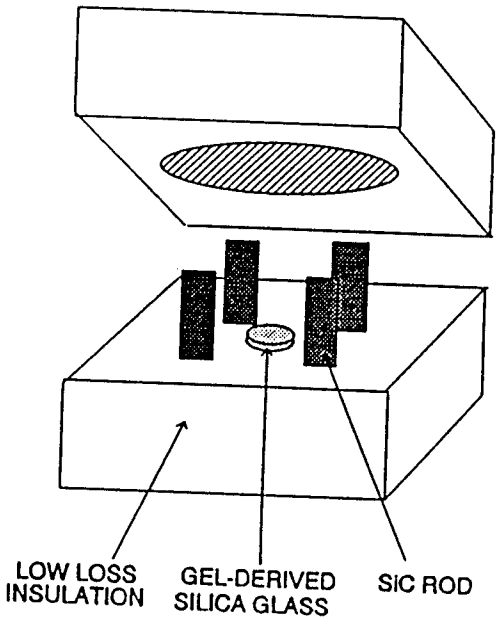

Figure 1. (a) The insulating/suscepting chamber used in this study, and (b) the picket fence configuration.

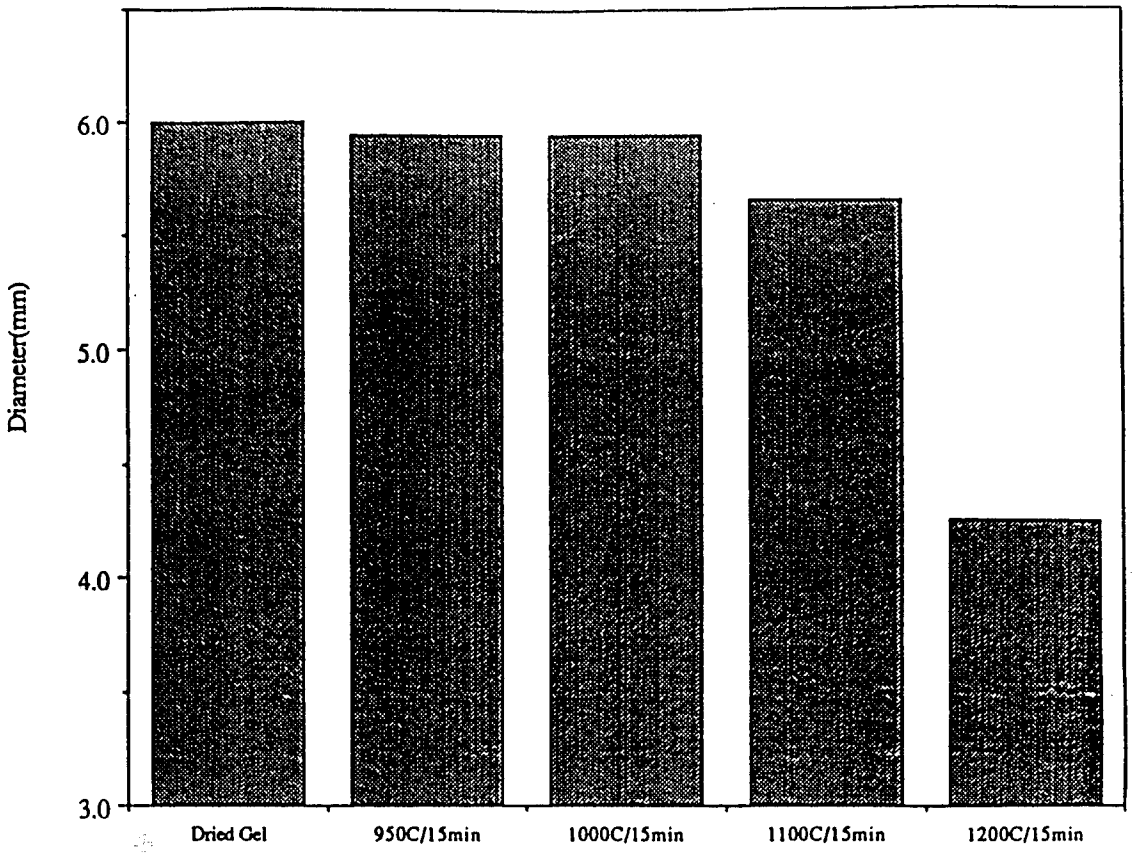

Figure 2. Diametral shrinkage following the various thermal treatments.

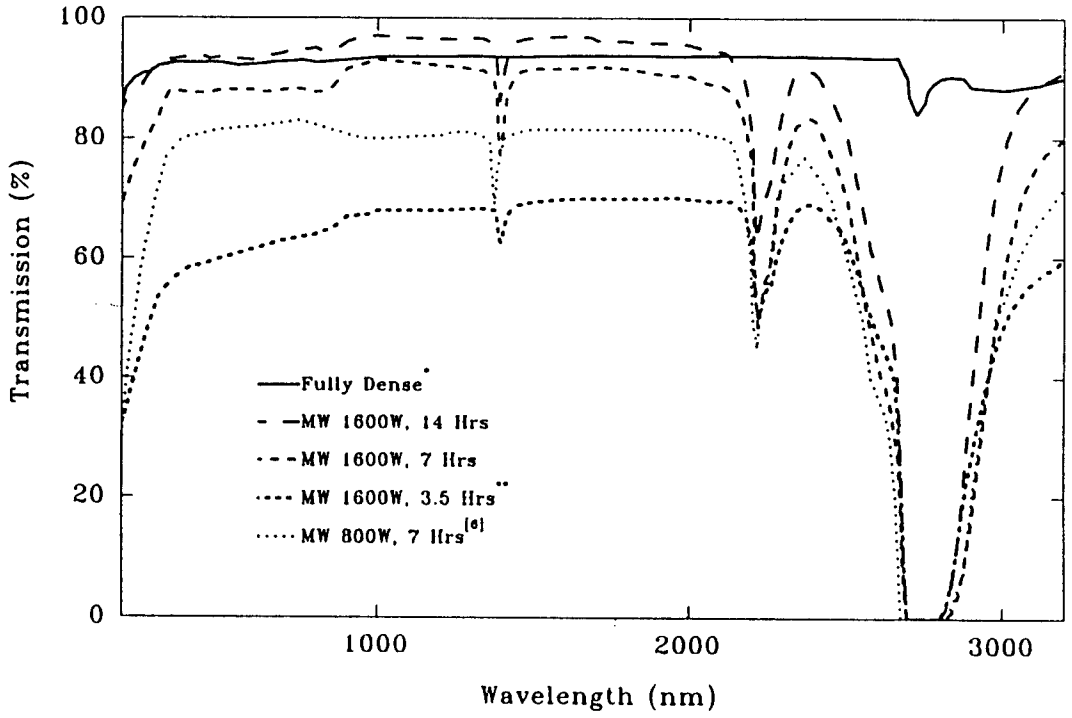

* From conventional processing under chlorination, GelTech, Inc., Alachua, FL 32615

** Using "picket fence" susceptor illustrated in Figure 1.b.

Figure 3. UV-VIS-NIR transmission spectra of typical microwave-processed, gel-derived silica glass samples

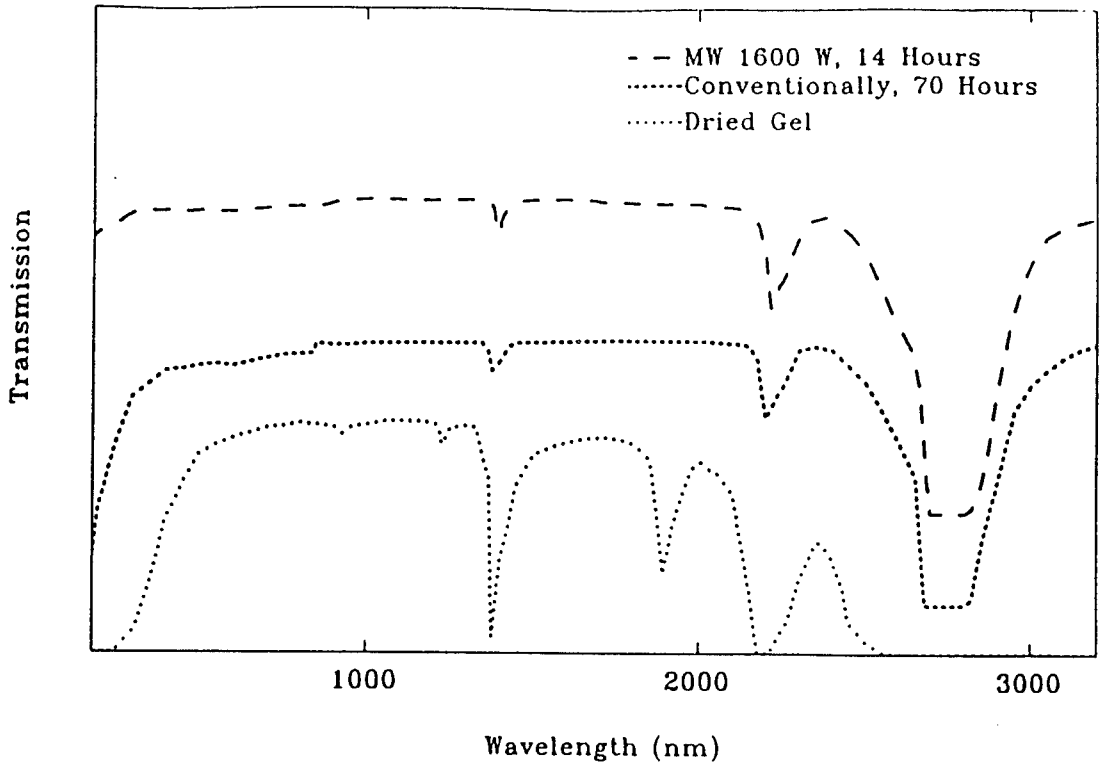

Figure 4. Comparison of samples processed in air at various temperatures in both microwave and conventional ovens.

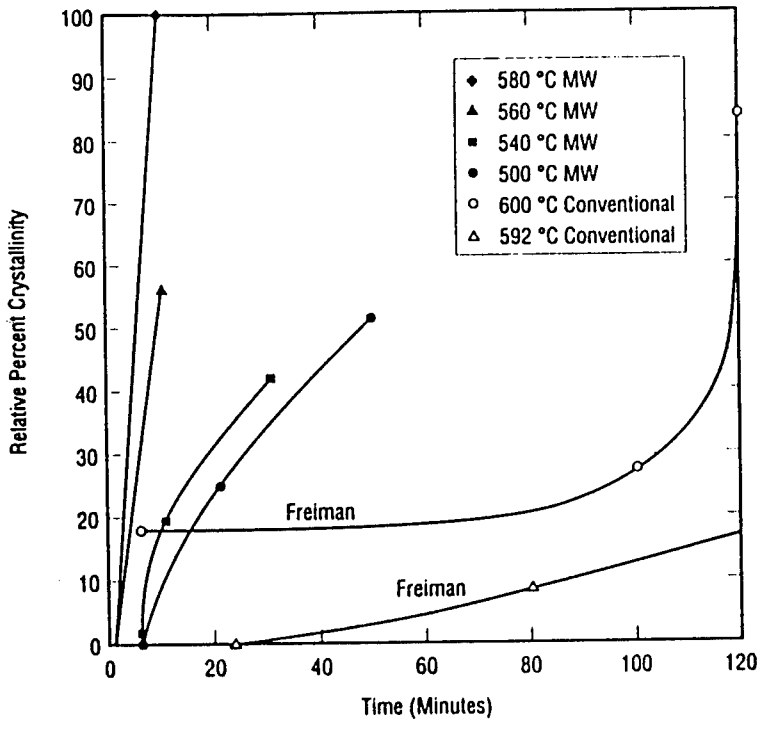

Figure 5. Relative percent crystallinity vs. time for Li_2O-$2SiO_2$ heated using microwave energy.

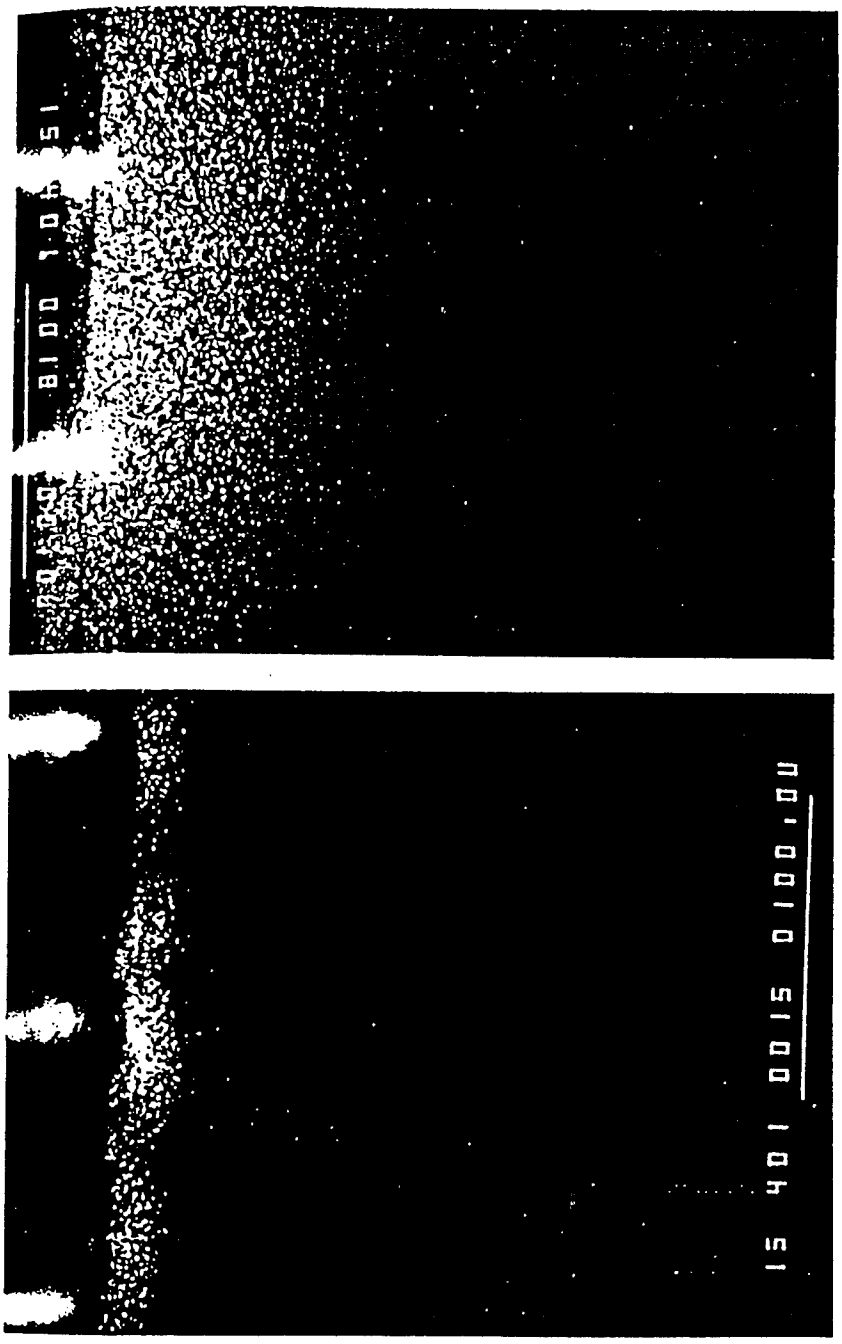

Figure 6. X-ray diffraction patterns for specimens heat treated at 450° C using microwaves.

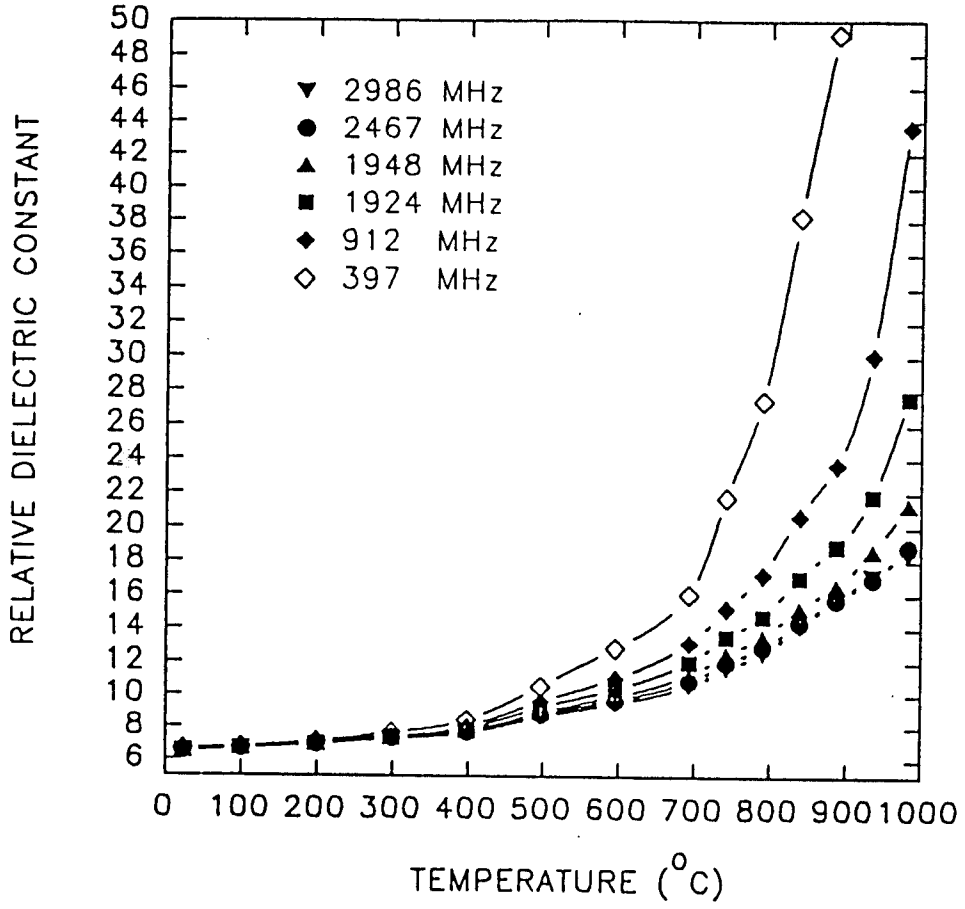

Figure 7(a). The relative dielectric constant, k′, of the Corning glass as a function of temperature for different frequencies.

Figure 7. The dielectric behavior of the Corning glass as a function of temperature for different frequencies: a) the relative dielectric constant vs. temperature, b) the dielectric loss factor vs. temperature, (c) the loss tangent vs. temperature, and (d) the microwave penetration depth vs. temperature.

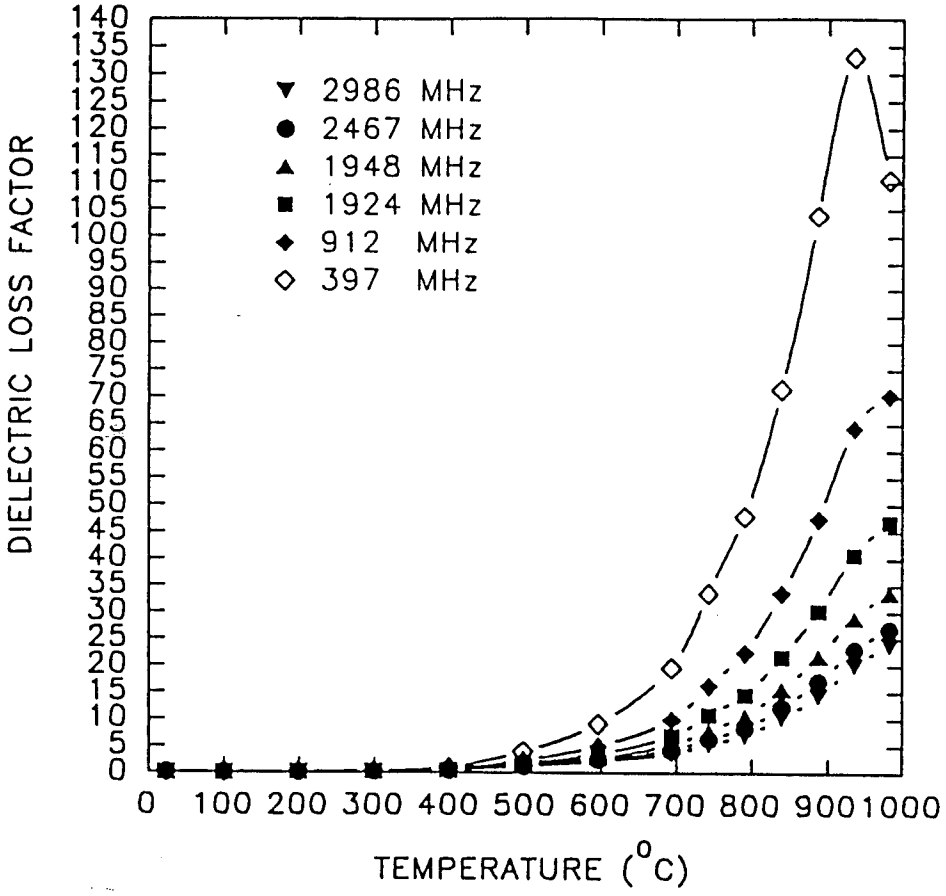

Figure 7(b). The dielectric loss factor, k", of the Corning glass as a function of temperature for different frequencies.

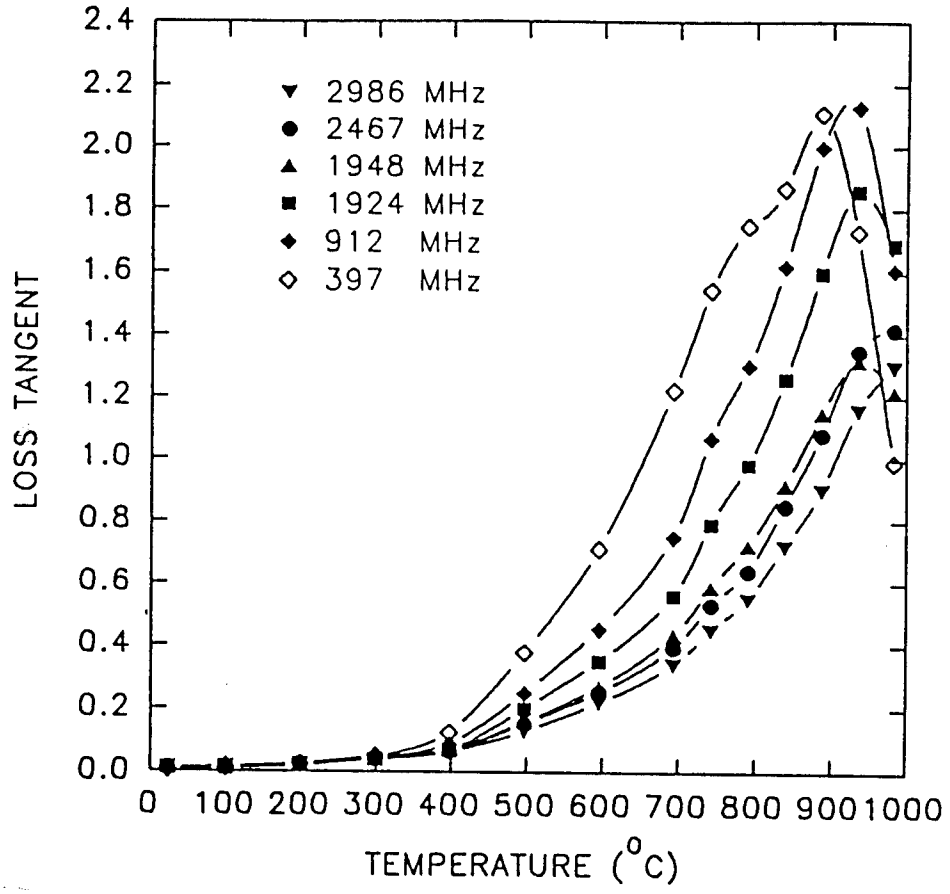

Figure 7(c) The loss tangent, tanδ, of the Corning glass as a function of temperature for different frequencies. Calculated from tanδ = k″/k′.

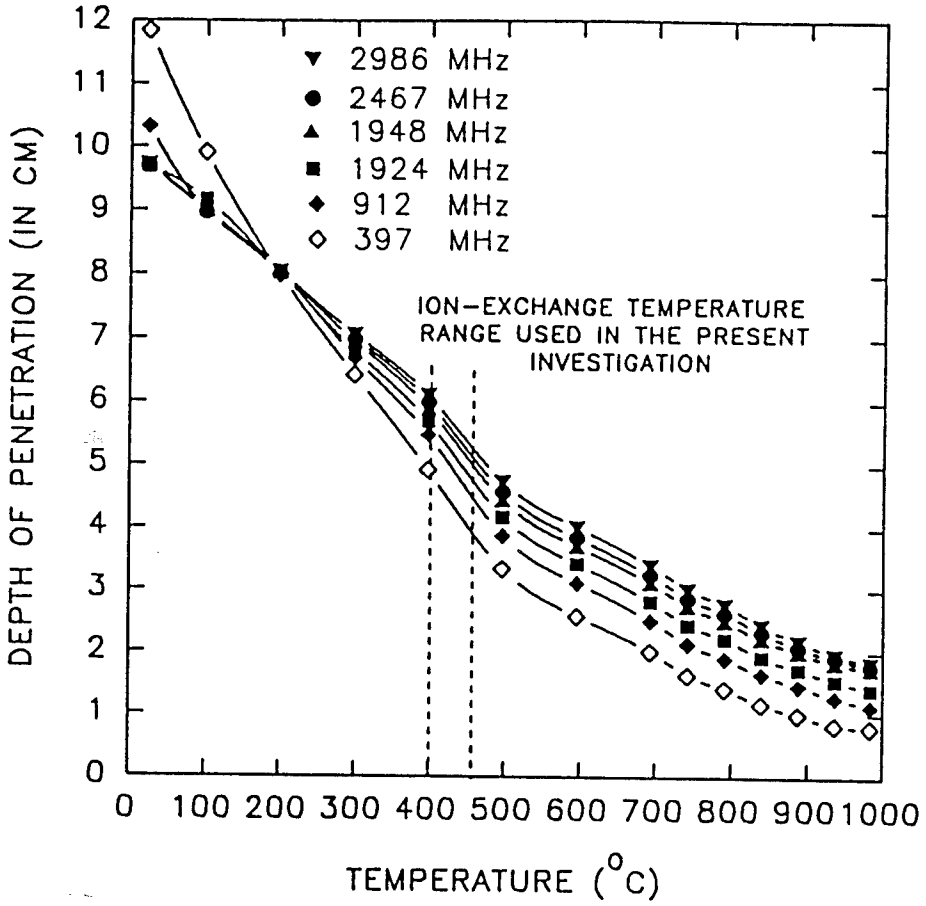

Figure 7(d). The penetration depth, Dp, of the Corning glass as a function of temperature for different frequencies.

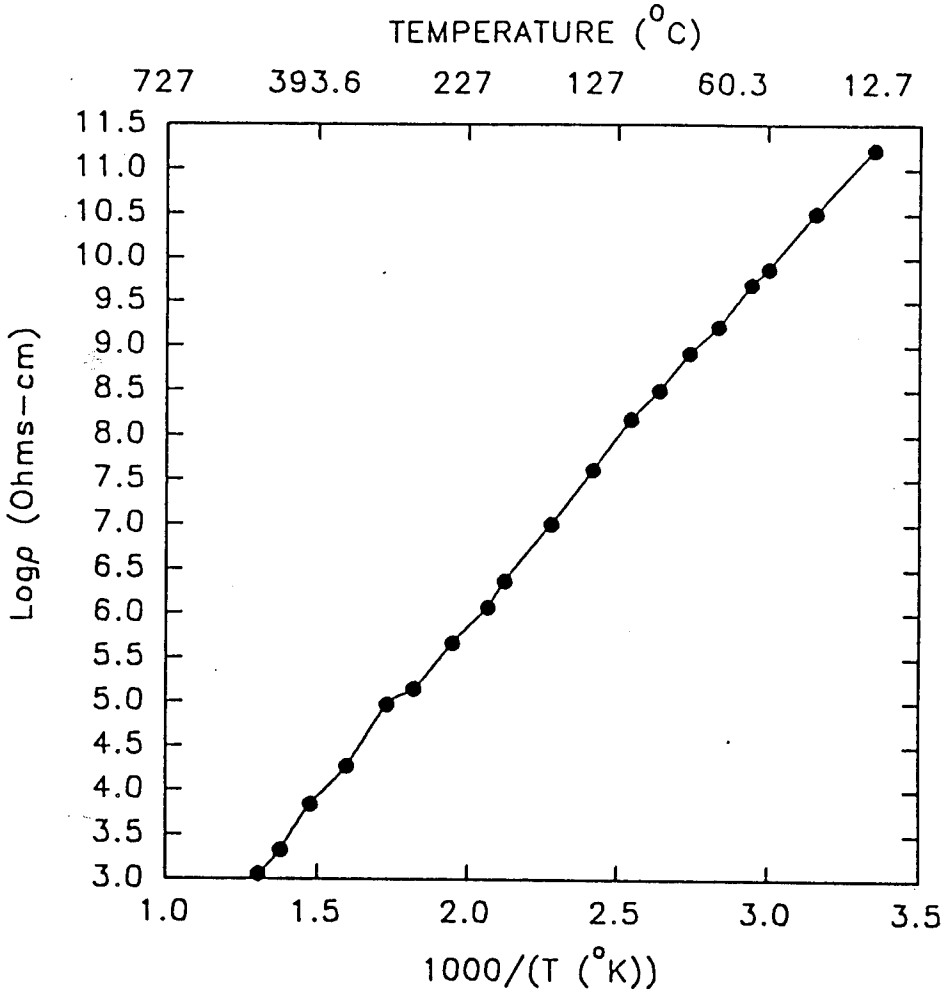

Figure 8. The Corning glass resistivity as a function of temperature.

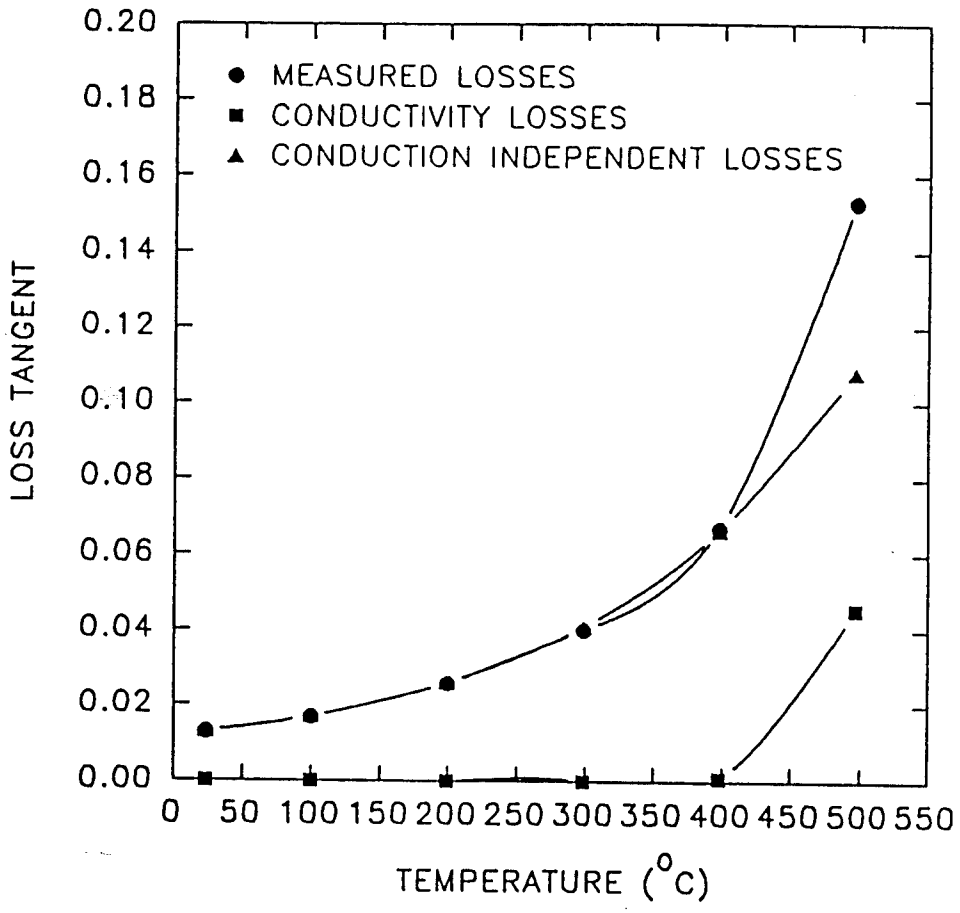

Figure 9. The measured losses, the calculated conduction losses, and the conduction independent losses as a function of temperature at 2.45 GHz.

(a)

(b)

(c)

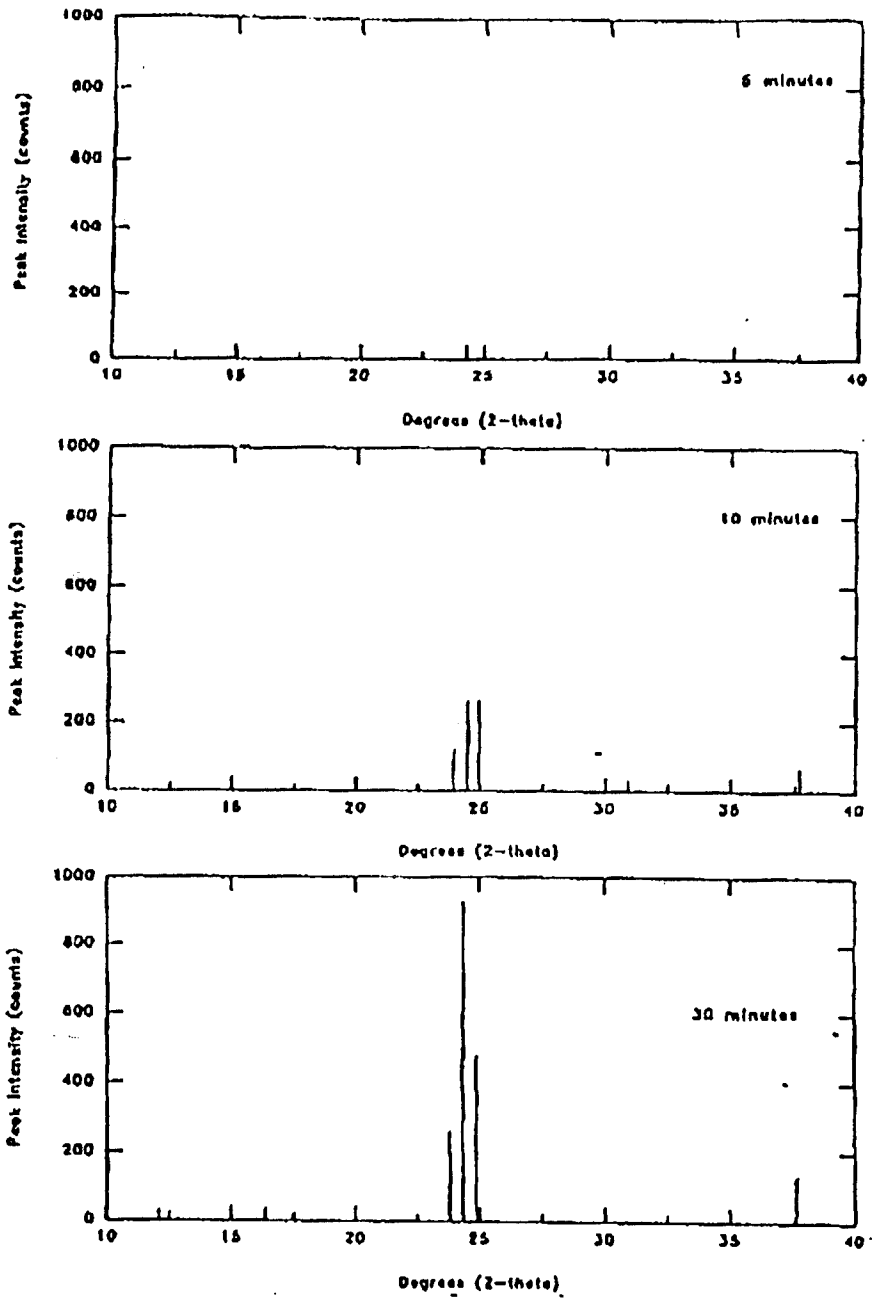

Figure 10. (a) DTA plot of the unseeded and seeded $BaO\text{-}Al_2O_3\text{-}2SiO_2$ glass-ceramics; (b) DTA plot of $BaO\text{-}Al_2O_3\text{-}2SiO_2$ gel derived at 50° C; and, (c) DTA plot of $BaO\text{-}Al_2O_3\text{-}2SiO_2$ with 10 wt% CuO added.

MICROWAVE PROCESSING AT THE UNIVERSITY OF FLORIDA

D.E. CLARK, D.C. FOLZ, R.L. SCHULZ, Z. FATHI, A.D. COZZI, A. BOONYAPIWAT, P. KOMARENKO, R. DiFIORE AND C.B. JONES
Dept. of Materials Science & Engineering, University of Florida, Gainesville, FL, 32611.

ABSTRACT

Microwave energy for processing materials is emerging as a vital manufacturing technology for the nineties and beyond. Research to date has shown significant advantages in several areas, including drying and sintering, joining, surface modification and waste remediation. Increased processing rates, improved physical and mechanical properties and, in some cases, reduced hazardous emissions have sparked the interest of many manufacturers in the ability to integrate microwave processing techniques into existing and future manufacturing operations. This presentation will provide an overview of the microwave processing research and development work in progress at the University of Florida.

INTRODUCTION

The use of microwave energy for materials processing, particularly at high temperatures, is considered by many to be an emerging technology. The advantages provided through the use of microwave energy has led researchers to evaluate its potential for both traditional and high-tech product production. Some of these advantages include rapid processing[1,2], ability to achieve equal or superior properties while still shortening the processing run[3,4,5], achievement of materials and/or properties difficult to achieve using conventional techniques[6,7], preferential heating of specific product components[8] and, in some cases, the ability to lower processing costs through reduction of throughput time as well as lower energy consumption costs[9,10,11].

At the University of Florida (UF), both graduate and undergraduate research projects have focussed on efficient and unique use of microwave energy for materials processing as well as on developing microwave technologies for industrial applications. Some of the more recent work performed in the Microwave Processing Research Facility at UF will be highlighted. For a more detailed discussion of each of these research areas, specific references to further reading are provided.

MICROWAVE ISSUES ADDRESSED

As research has progressed over the past ten years, many questions regarding the potential use of microwave energy for materials processing have arisen. At UF, researchers have teamed up with other groups in order to address issues, including (1) the existence of a *microwave effect*; (2) the ability to *control* the distribution of heat within the microwave cavity during processing; and (3) the application of microwave energy to selected processes operations to increase their efficiency, and enhance properties of the resultant products.

Results of studies on diffusion via ion exchange, sol-gel processing and waste remediation will be highlighted. Other focus areas include joining and repair processes, design of microwave susceptor materials and cavities and combustion synthesis. Much of

the UF research has been presented at previous symposia sponsored by the Materials Research Society, the National Institute of Ceramic Engineers (through the American Ceramic Society) and the International Microwave Power Institute, and references to the early work are included in this paper.

HIGHLIGHTS OF RECENT RESEARCH

Is there a microwave effect?

There are several thermal phenomena that are observed when materials are processed in a microwave field. These include: selective heating, volumetric heating and rapid heating. These phenomena can be understood in terms of the microwave energy absorption and conversion to heat within the material. Additionally, a non-thermal effect has been reported by several investigators. These thermal and non-thermal phenomena are collectively referred to as the *microwave effect*, since they are not observed during conventional processing.

Although there is much evidence to indicate that some type of non-thermal effect is created in the microwave field, no quantitative data has surfaced to prove conclusively that a novel mechanism(s) for microwave materials processing exists. Studies to evaluate the potential for using microwave energy for traditional and novel processing of a variety of materials have suggested the existence of a microwave effect leading to enhanced reaction rates, enhanced diffusion and improved properties. The team has worked with Atomic Energy of Canada (AECL) to correlate dielectric properties with heating trends and materials properties observed in processing experiments. In one study to correlate phase changes and dielectric properties in joint interlayer materials, the loss tangent ($\tan\delta$) for various interlayer compositions was related to differential scanning calorimetry (DSC) measurements. As shown in Figure 1, at temperatures where phase changes occurred in the various materials, an associated change in $\tan\delta$ was observed. As shown in the dielectric data, the composition containing 50 mol% NiO in an Al_2O_3 matrix exhibited a large increase in $\tan\delta$ at high temperatures. Since this material is an excellent absorber of microwaves at high temperatures, it is being used as an interlayer material for the joining study in progress.

In studies to evaluate microwave energy for the fabrication of ultra-high optical quality silica glass, densification of silica gel was performed at different temperatures and times. In conventional processing of silica gels, long times in a chlorine atmosphere are required to complete dehydration and achieve full densification[12]. After chlorination, a residual amount of chlorine remains in the gel-derived glass as structural impurities which can alter the refractive index and change the optical characteristics of the resultant glass. Because of its coupling to OH groups and Si-O-Si bridges, microwave energy offers the potential for efficient dehydration and densification without the necessity of a controlled atmosphere.

A series of samples were microwave heat-treated over a range of temperatures and times. As shown in Table 1[13], conventional processing times for fully densified gel-derived silica glasses typically require at least 3 days[14,15]. The microwave-processed samples prepared during this study took hours $\leq$ 14 hours. And, as indicated by UV-VIS-NIR transmission spectra (Figure 2)[12], the microwave-processed gel glasses heat treated in air approached the residual water content of the fully dense glasses produced under a chlorine atmosphere. Thus it may be possible to eventually produce fully dense gel glasses with microwave energy without depending on pressure control of the atmosphere.

a)

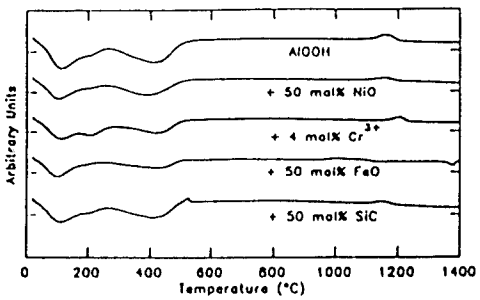

b)

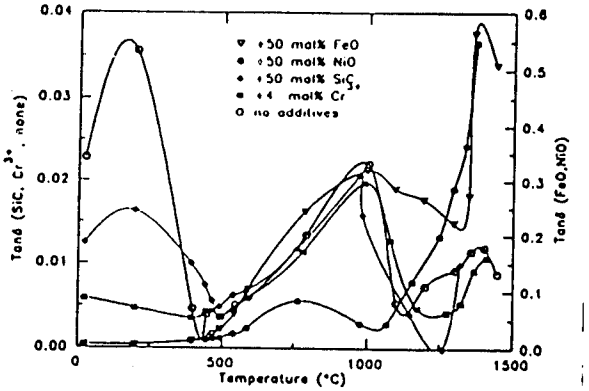

Figure 1. Correlations between phase changes and dielectric properties of potential joint interlayer materials. a) DSC of alumina gels with various additives; b) loss tangent as a function of temperature.

Table 1. Processing and Characteristics of Gel-Derived Silica Glasses.

Samples	Conventionally Fully Dense	Microwave Processing			
		1600 W Input			800W Input
Processing Time	>3 Days	14 Hrs	7 Hrs	3.5 Hrs*	7 Hrs
Sintering Temperature (°C)	1150-1200	1100	1100	1100	1200
Density (g/cc)	2.220	2.04	2.200	2.200	2.13
50%UV Cut-Off (nm)	<185	<185	~185	205	210

* Using "picket fence" susceptor

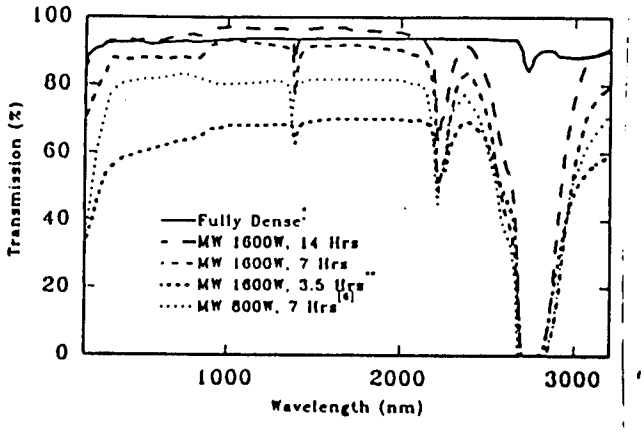

Figure 2. UV-VIS-NIR transmission spectra for microwave processed sol-gel-derived silica glass samples as compared to fully dense silica glass.

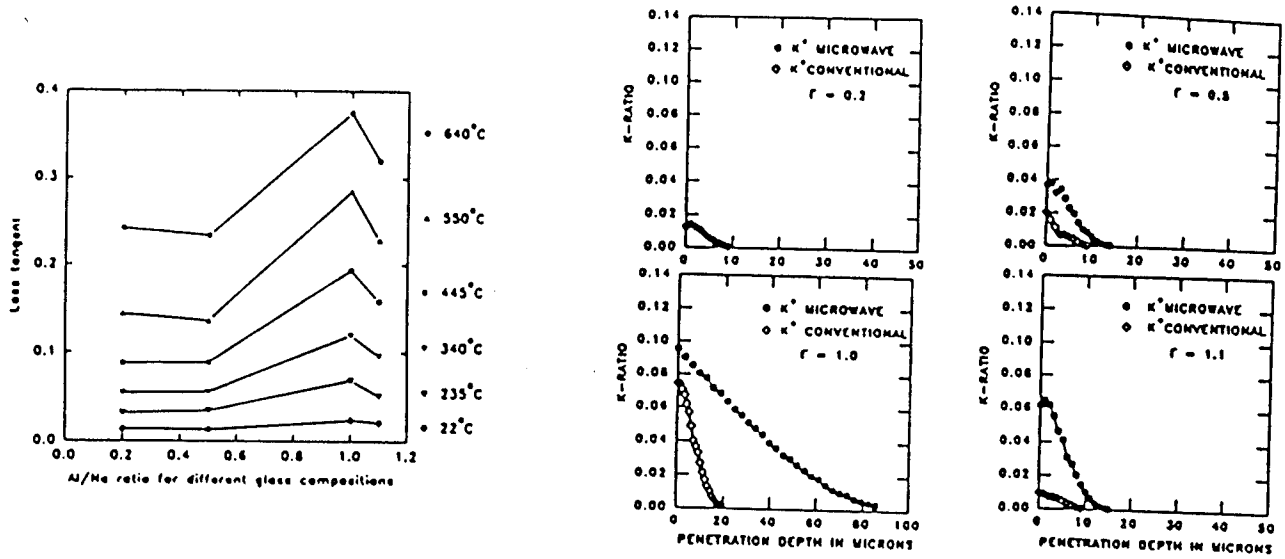

Figure 3. Dielectric properties and interdiffusion plots for varying Al/Na ratio glasses used for the ion exchange experiments.

The most focussed UF study to address the existence of a microwave effect examined diffusion of ionic species in glass via ion exchange[16,17,18,19,20,21]. In this study, K^+ from a molten salt is exchanged for Na^+ in the glass. Figure 3 relates the dielectric properties and interdiffusion of K^+/Na^+ for a range of sodium aluminosilicate (NAS) glass compositions. The structure of the glass can be altered by controlling the Al/Na ratio (K-ratio). The K-ratio is defined as the x-ray intensity counted for the K^+ versus those of a mineral standard (biotite for this study). The structure for a Al/Na ratio of 1.0 creates a higher potential for ionic movement. In this glass, Al^{+3} ions reduce the ability of Na^+ to bond with oxygen and Na^+ ions are more mobile.

The loss tangent ($\tan\delta$) versus Al/Na (Γ) ratio plot shows a peak for the 1.0 composition over a wide range of ion exchange temperatures. If there is a microwave effect, it may be more easily observed under conditions where maximum losses occur. Indeed, the four plots of potassium concentration (K-ratio) versus penetration depth for the Al/Na ratios of 0.2, 0.5, 1.0 and 1.1 exhibit the anticipated behavior. For the 0.2 composition, no difference is observed between the conventional and microwave-processed samples. However, the differences in penetration depths increases substantially for the 1.0 glass before decreasing once again in the 1.1 glass, corresponding to the drop in $\tan\delta$ for $\rangle$1.0 ratios. As seen in Figure 3, for the 0.2 and 0.5 glasses, the $\tan\delta$ values show no significant differences, while a definite increase in ion penetration depth is observed in the microwave-processed glass. If the observed diffusion enhancement was due only to thermal effects, the

tanδ value (a measure of the microwave energy absorbed and translated into heat in the material) for the 0.2 and 0.5 samples should have reflected this in an increased tanδ value. There has been some discussion among researchers as to the accuracy of temperature measurements within a microwave field. For this study, the authors believe that if the microwave sample temperatures were higher than measured by the monitoring system, all the glasses would have exhibited an increase in interdiffusion. However, this was not the case. In fact, the Γ = 0.2 glass composition was identical for both the microwave and conventional processes.

To further investigate the apparent microwave effect, diffusion studies using an ionic pair were performed. In this case, K^+ (80 mol%) and Ag^+ (20 mol%) were used in the form of a potassium nitrate (KNO_3) salt with 20 mole percent silver nitrate ($AgNO_3$) added. The NAS glass samples were exposed to the salt solution for 30 minutes at 400° C in both the microwave and conventional ovens.

As seen in Figure 4, both ionic species diffused into the NAS glass samples. The silver ions have a higher activity than the K^+ ions. When ion exchange processes are carried out in a molten salt containing both silver and potassium nitrates, the silver ions are found in greater numbers than the potassium ions at the surface of the modified glass. The Ag^+ ions diffused deeper into the samples than the K^+ ions under the influence of conventional and microwave heating. However, the depth of penetration of the Ag^+ ion was significantly increased in the microwave field over the depth achieved in the conventional environment.

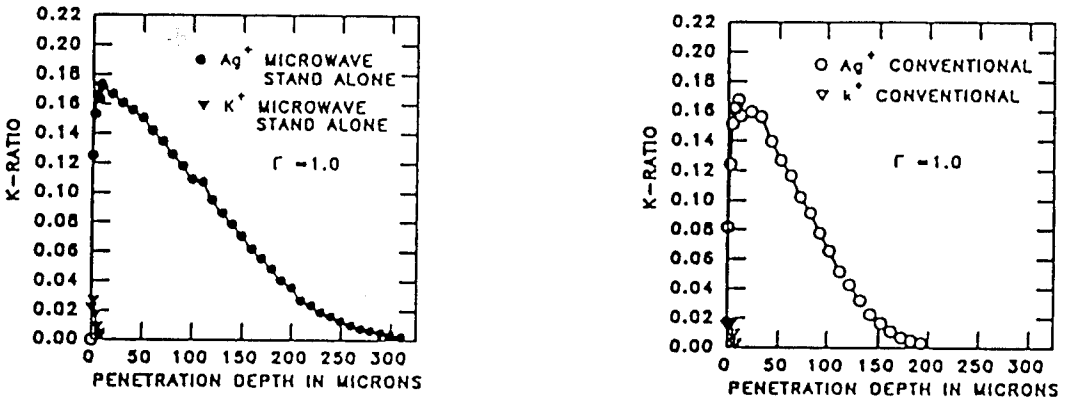

Figure 4. Microwave and conventional diffusion of ionic pairs into NAS glass samples with ratio of Al/Na of 1.0.

Although the ion exchange experiments performed at UF indicated the presence of a significant microwave effect in certain glasses, other studies have shown little or no difference between conventionally and microwave-processed samples.

Silica sol-gel was used to coat soda-lime-silicate glasses that had been flawed intentionally using the Vickers indentation technique[22,23]. Coated samples were heat treated using both microwave and conventional techniques. Figure 5 shows a Weibull plot of the fracture stress for both sets of heated samples (at least 15 samples for each process) as well as the fracture stress for an uncoated reference sample. The sol-gel-coated glasses shifted to higher fracture strengths; however, no significant differences were noted between the microwave and conventionally heated samples. At the operating frequency of 2.45 GHz, no pronounced microwave effect was observed.

Control of Heat Distribution

As presented by Johnson et al.[24], it is evident that the hybrid heating cavity used in the microwave oven can have a significant effect on the processing environment seen by the samples. Although some processing has been performed successfully using direct microwave irradiation, it is notable that many researchers in microwave materials processing are designing elaborate *cavities* for high-temperature processing and for increased thermal uniformity. These techniques range from re-designing the metal microwave cavity itself[25,26] to building *microwave susceptor cavities* to surround the materials during processing[2,3]. The susceptor cavities designed by various groups have taken on different geometries and used a variety of materials[27].

In contrast to the *picket fence* assembly used by researchers at Oak Ridge National Laboratory[4], the UF susceptor cavities are composite materials made up of silicon carbide granules embedded in an alumina matrix. The susceptor elevates the temperature inside

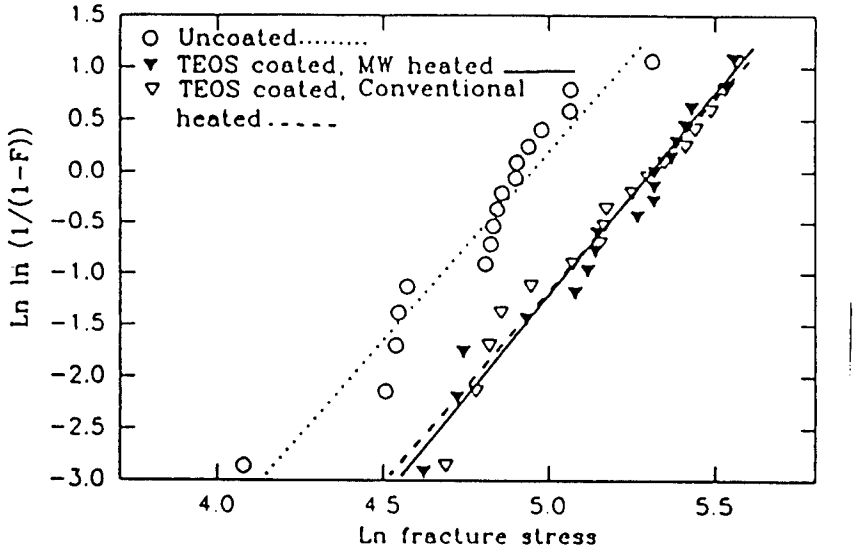

Figure 5. Weibull plot of soda-lime-silica glass showing effects on fracture stress of sol-gel-coated samples heated using conventional and microwave techniques.

the sample cavity rapidly and the insulating properties of the matrix helps in holding the temperature constant inside the cavity. The use of suscepting cavities for some processing experiments has led to a research project to evaluate the heating effects resulting from varying the amount of silicon carbide within the alumina matrix.

As illustrated in Figure 6, the study provided results to confirm that increases in suscepting mass can increase the peak temperature inside the hybrid cavity. The ramp rates were almost identical with those susceptor cavities with higher amounts of silicon carbide showing a slight increase in ramp rate for identical power applied.

For materials requiring higher peak temperatures or increased ramp rates over those observed in the SiC/Al_2O_3 system, NiO is being used as the suscepting agent in the composite cavities. This choice became evident during the interlayer studies (Figure 1). Temperatures as high as 1670° C have been achieved routinely in air using this susceptor system.

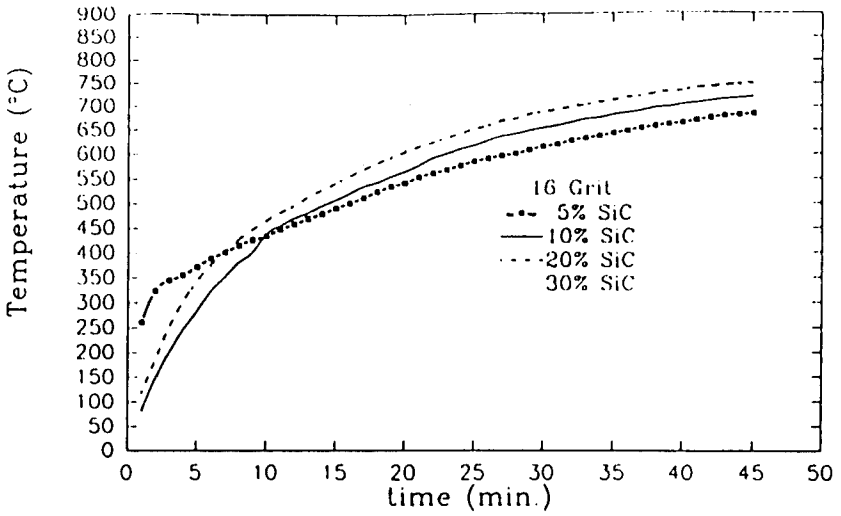

Figure 6. Time versus temperature curves for susceptor cavities with varying amounts of SiC.

There is an issue of whether or not hybrid heating results in microwave interaction with the material inside the susceptor cavity. The evidence that microwaves were penetrating through the salt solution and to the surface of the NAS samples is shown in Table 2. This is evident in the expression for the percentage of power absorbed (P_a) by each experimental component in the microwave cavity during processing. The hybrid heating cavity absorbed approximately 13% of the incident power (P_i) and the salt solution absorbed approximately 30%. This leaves 57% of the microwave power to impinge on the NAS glass samples. While all of the incident power (P_i) certainly was not absorbed by the glass, a significant amount of power was *available* for absorption. Although these investigations are in the early stages, this study has been helpful in identifying and producing microwave hybrid heating susceptors for other on-going studies.

Application of Microwave Energy to Selected Processes

While the research conducted at UF is not ready for immediate commercial use, processing techniques have been initiated that could be developed quickly for selected applications. Two of these applications will be highlighted in this paper: microwave combustion synthesis and microwave waste remediation.

Since 1990, the UF team has published/presented results of several studies in the area of microwave combustion synthesis[28,29,30]. These papers discussed the potential for using microwave ignition and combustion in the self-propagating high-temperature synthesis (SHS) process for producing composite powders and monoliths.

The latest work on microwave combustion synthesis at UF has focussed on producing high-purity Ti_3SiC_2 composite powders from Ti-Si-C starting powders[31]. As seen in Figure 7, the x-ray diffraction analysis of the phases resulting from microwave and conventional processing show a significant increase in production of the desired phase. Since this material is a *point compound*, the ability to form it easily is a significant step towards widespread commercial application of the composite powder.

Table 2. Power Absorption Characteristics for the Experimental Components Exposed to Microwave Energy at 2.45GHz.

Parameters*	SiC/Insulator	Insulator Alone	Slurry**	KNO_3	$AgNO_3$
α (1/m)	35.7	1	3.7	16	16
z (m)	$(1\text{-}1.5) \times 10^{-3}$	0.015	0.001	0.01	0.01
P_z/P_i	0.931	0.970	0.992	0.726	0.726
$(P_z-P_i)/P_i = \Delta P/P_i$	7-10%	3%	0.8%	27.4%	27.4%
P_a (for P_i = 800W)	≈50-80W	≈24W	≈6W	≈220W	≈220W
P_a for z = 0.5-1.0mm $\Delta P/P_i$ = 3.5-7% P_i = 1600W	≈50-110W	≈48W	≈12W	–	–

* α = attenuation factor
z = distance
P_z = Power as a function of distance

** slurry = potassium gel

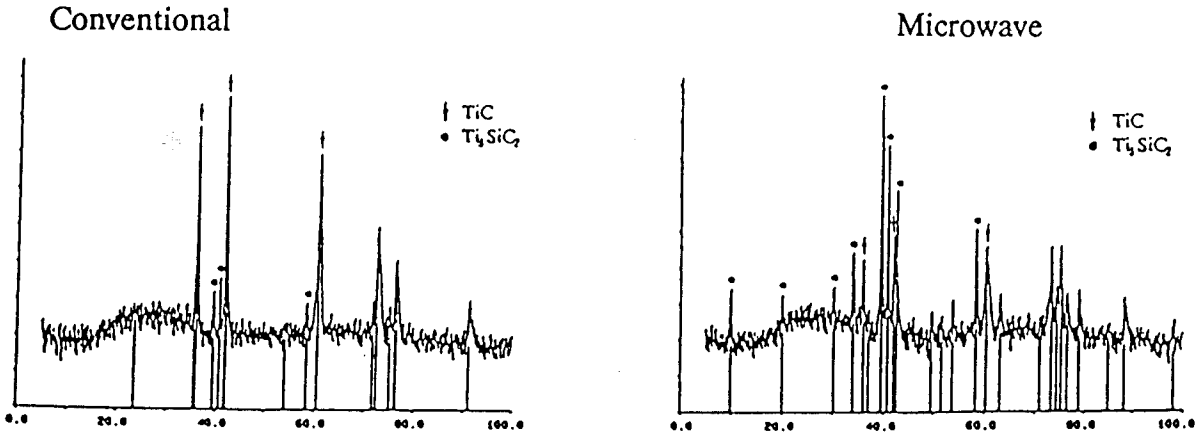

Figure 7. X-ray diffraction data illustrating the formation of Ti_3SiC_2 from Ti-Si-C powders using microwave and conventional ignition and combustion techniques.

There is much interest in forming this composite material as it is reported to have a high degree of fracture toughness and has good potential as a fiber coating in SiC/Ti fiber-reinforced composites. Microwave combustion and heating could be used to synthesize the Ti_3SiC_2 phase as a matrix material for tough ceramic composite structures. The microwave process has been shown to enhance the kinetics of formation of the required phase and could be developed into an efficient process.

The second area where microwave energy can assume a central role is that of waste remediation. Environmentally based technology/business ventures are already emerging. As more industrialized nations realize their responsibilities to maintaining health and quality of life for their citizens and for future generations, environmental regulations will be strengthened and their enforcement toughened. More cost-effective methods for waste handling must be integrated into all production processes.

Microwave remediation offers several advantages over conventional methods. Some of these include mobile and remote capabilities, potential for handling large working volumes, rapid processing, ability to reach extremely high processing temperatures, enhanced reaction rates and homogenization, reduced toxic emissions in some manufacturing operations, adaptability to feed materials of various compositions, size and shape, and potential energy/cost effectiveness.

Microwave processing has been used at UF and other research facilities to melt simulated nuclear waste glass in significantly reduced times as compared to glasses produced conventionally. The glasses processed in as little as 15 to 30 minutes were homogeneous[32,33]. Data from short term leaching experiments show that the chemical durability of the microwave processed samples is comparable to that of the conventionally processed glasses. While microwave processing appears to be a promising method for vitrification of high-level nuclear waste more studies must be conducted to fully assess its technical and economic merits.

Initial studies into microwave destruction and vitrification of electronic circuitry showed that a volume reduction of greater than 50 percent was possible, that important metals could be recovered easily and that vitrification could be achieved as part of a continuous waste processing operation[34]. Later studies showed that by using the inherent glass-forming properties of wastes and due to glass interactions with microwave energy, vitrification could be achieved in some wastes without the use of additives. Preliminary leaching studies on some types of circuitry vitrified using microwave energy show that current EPA standards for release of elements into the accessible environment have been met.

A new area of study in waste remediation at UF is the destruction of organic wastes. One organic compound of particular interest is sodium tetraphenyl borate (STPB). The STPB is used to precipitate out cesium in high-level radioactive waste. This technique greatly reduces the volume of high level waste that must be vitrified prior to permanent geologic disposal. However, the organic portion of the resulting compound, cesium tetraphenyl borate must be significantly reduced in order to be compatible with the glass matrix. Currently, an acid catalyzed hydrolysis reaction is used, however it creates several undesirable side effects. Preliminary experiments exposing the STPB to a microwave field have resulted in great reduction in weight (>80wt% difference) and volume. Sample residues have been submitted for high performance liquid chromatography (HPLC) characterization; however, results were not available as of this writing.

More information regarding the studies performed at UF on processing of both simulated nuclear waste glasses and electronic circuitry is discussed by Schulz et al. and is published in these proceedings.

SUMMARY

When initiated in 1988, the research on microwave processing of materials at the University of Florida was a small effort consisting of one graduate student and a home-model microwave oven. Since that time, microwave processing has become the main focus of the research team supporting between six and twelve graduate and undergraduate researchers. The *philosophy* of the team is that **microwave processing can be integrated into both traditional and novel manufacturing operations to produce materials with properties equal or superior to those that are processed conventionally.**

There is a microwave effect. In many cases this effect involves selective, volumetric and rapid heating. However, in certain instances, a non-thermal effect also may be operative. In either case, processing and product advantages may be realized.

Microwave energy has been used as an alternative to conventional heating methods in many types of important ceramic processes. Examples of these include: sintering, surface modification via ion exchange, combustion synthesis, sol-gel processing, repair, coatings, joining, drying, fabrication of superconductors and waste remediation. In nearly all cases, there appear to be advantages provided by microwave energy. However, much additional work is needed to determine if the advantages outweigh any disadvantages, particularly when the processes are scaled-up at the industrial level. Equally important, the economics must be carefully evaluated and demonstrated to be in favor of microwave energy before large scale commercialization will be implemented for any process.

ACKNOWLEDGEMENTS

The authors thank Westinghouse Savannah River Technology Center, the Office of Naval Research, and Advanced Research Projects Agency and the High Temperature Material Lab at Oak Ridge National Laboratory for partial financial support during these studies.

REFERENCES

1. Y.-L. Tian, in *Microwaves: Theory and Application in Materials Processing*, edited by D.E. Clark, F.D. Gac and W.H. Sutton (Ceramic Transactions **21**, Westerville, OH, 1991) pp. 283-300.

2. M.A. Janney, C.L. Calhoun and H.D. Kimrey, in *Microwaves: Theory and Application in Materials Processing*, edited by D.E. Clark, F.D. Gac and W.H. Sutton, (Ceramic Transactions **21** Westerville, OH, 1991) pp. 311-318.

3. A.S. De', I. Ahmad, E.D. Whitney and D.E. Clark, in *Microwaves: Theory and Application in Materials Processing*, edited by D.E. Clark, F.C. Gac and W.H. Sutton (Ceramic Transactions **21**, Westerville, OH, 1991) pp. 319-327.

4. A.S. De', I. Ahmad, E.D. Whitney and D.E. Clark, in *Microwave Processing of Materials II*, edited by W.B. Snyder, Jr., W.H. Sutton, M.F. Iskander and D.L. Johnson (Mat. Res. Soc. Proc. **189**, Pittsburgh, PA, 1990) pp. 283-288.

5. I. Ahmad, G.T. Chandler and D.E. Clark, in *Microwave Processing of Materials*, edited by W.H. Sutton, M.H. Brooks and I.R. Chabinsky (Mat. Res. Soc. Proc. **124**, Pittsburgh, PA, 1988) pp. 239-246.

6. C.E. Holcombe and N.L. Dykes, in *Microwaves: Theory and Application in Materials Processing*, edited by D.E. Clark, F.D. Gac and W.H. Sutton (Ceramic Transaction **21**, Westerville, OH, 1991) pp. 375-386.

7. L.T. Drzal, K.J. Hook and R.K. Agrawal, in *Microwave Processing of Materials II*, edited by W.B. Snyder, Jr., W.H. Sutton, M.F. Iskander and D.L. Johnson (Mat. Res. Soc. Proc. **189**, Pittsburgh, PA, 1990) pp. 449-454.

8. R. Silberglitt, D. Palaith, W.M. Black, H.S. Sa'adaldin, J.D. Katz and R.D. Blake, in *Microwaves: Theory and Application in Materials Processing*, edited by D.E. Clark, F.D. Gac and W.H. Sutton (Ceramic Transactions **21**, Westerville, OH, 1991) pp. 487-496.

9. R. Edgar, "The Economics of Microwave Processing in the Food Industry," *Food Technology*, 40[6], 106-12.

10. Goodson Lighting Limited, *Microwave Drying of Slip-Cast Ware*, a news brief in Am. Ceram. Soc. Bull. 72[4], April 1993, p. 75.

11. F.C.R. Wroe, in *Microwaves: Theory and Application in Materials Processing*, edited by D.E. Clark, F.D. Gac and W.H. Sutton (Ceramic Transactions **21**, Westerville, OH, 1991). pp. 449-458.

12. R. DiFiore, senior research project presented as fulfillment of graduation requirements at the University of Florida, Gainesville, FL, 1992, (unpublished).

13. J.P. Zhong, A. Fathi, G.P. LaTorre, D.C. Folz and D.E. Clark, presented at the Annual Meeting of the Engineering Ceramics Division of the American Ceramic Society, Cocoa Beach, FL, 1994 (to be published).

14. R.G. Araujo, G.P. LaTorre and L.L. Hench, (to be published in 1994).

15. S.H. Wang, *Structural Evolution of a New Type VI Sol-Gel Porous Silica Glass*, (a Ph.D. Dissertation, University of Florida, Gainesville, FL, 1988).

16. Z. Fathi, D.C. Folz, R.L. Schulz and D.E. Clark, presented at the Annual Meeting of the Engineering Ceramics Division of the American Ceramic Society, Cocoa Beach, FL, 1994 (to be published).

17. Z. Fathi, D.E. Clark and A.R. Lodding, in *Microwaves: Theory and Application in Materials Processing II*, edited by D.E. Clark, W.R. Tinga and J.R. Laia, Jr. (Ceramic Transactions **36**, Westerville, OH, 1993).

18. Z. Fathi, I. Ahmad and D.E. Clark, in *Ceramic Engineering and Science Proceedings*, edited by (Am. Ceram. Soc. Proc. Westerville, OH, 199) pp.

19. Z. Fathi, D.E. Clark and R.M. Hutcheon, in *Microwave Processing of Materials III*, edited by R.L. Beatty, W.H. Sutton and M.F. Iskander (Mater. Res. Soc. Proc. **269**, Pittsburgh, PA, 1992) pp. 347-352.

20. Z. Fathi, I. Ahmad, J.H. Simmons, D.E. Clark and A.R. Lodding, in *Microwaves: Theory and Application in Materials Processing*, edited by D.E. Clark, F.D. Gac and W.H. Sutton (Ceramic Transactions **21**, Westerville, OH, 1991) pp. 623-629.

21. Z. Fathi, *Surface Modification of Sodium Aluminosilicate Glasses Using Microwave Energy*, a Ph.D. Dissertation (University of Florida, Gainesville, FL, 1994).

22. A. Boonyapiwat, Z. Fathi and D.E. Clark, in *Microwaves: Theory and Application in Materials Processing II*, edited by D.E. Clark, W.R. Tinga and J.R. Laia, Jr (Ceramic

Transactions 36, Westerville, OH, 1993) pp. 341-350.

23. A. Boonyapiwat, J.J. Mecholsky, Jr. and D.E. Clark, presented at the Annual Meeting of the Engineering Ceramics Division of the American Ceramic Society, Cocoa Beach, FL, 1994 (to be published).

24. D.L. Johnson, D.J. Skamser and M.S. Spotz, in *Microwaves: Theory and Application in Materials Processing II*, edited by D.E. Clark, W.R. Tinga and J.R. Laia, Jr (Ceramic Transactions 36, Westerville, OH, 1993) pp. 133-146.

25. B.Q. Tian and W.R. Tinga, in *Microwaves: Theory and Application in Materials Processing*, edited by D.E. Clark, F.D. Gac and W.H. Sutton (Ceramic Transactions 21, Westerville, OH, 1991) pp. 647-654.

26. J. Asmussen, Jr., B. Manring, R. Frintz and M. Siegel, in *Microwaves: Theory and Application in Materials Processing*, edited by D.E. Clark, F.D. Gac and W.H. Sutton (Ceramic Transactions 21, Westerville, OH, 1991) pp. 655-666.

27. P. Komarenko and D.E. Clark, in *Microwaves: Theory and Application in Materials Processing II*, edited by D.E. Clark, W.R. Tinga and J.R. Laia, Jr (Ceramic Transactions 36, Westerville, OH, 1993) pp. 351-358.

28. D.E. Clark, I. Ahmad and R.C. Dalton, presented at the American Institute of Metallurgical Engineers Annual Meeting, Detroit, MI, 1990.

29. R.C. Dalton, I. Ahmad and D.E. Clark, in *Ceramic Engineering and Science Proceedings*, edited by L.J. Schioler (Am. Ceram. Soc. Proc. 11[7-8], Westerville, OH 1990) pp. 1729-1742.

30. I. Ahmad, R. Dalton and D.Clark, J. Microwave Power and Electromagnetic Energy 26[3], 128 (1991).

31. P. Komarenko and D.E. Clark, presented at the Annual Meeting of the Engineering Ceramics Division of the American Ceramic Society, Cocoa Beach, FL, 1994 (to be published).

32. C.M. Jantzen and J.R. Cadieux, in *Microwaves: Theory and Application in Materials Processing*, edited by D.E. Clark, F.D. Gac and W.H. Sutton (Ceramic Transactions 21, Westerville, OH, 1991) pp. 441-450.

33. R.L. Schulz, Z. Fathi, D.E. Clark and G.G. Wicks in, *Microwaves: Theory and Application in Materials Processing*, edited by D.E. Clark, F.D. Gac and W.H. Sutton (Ceramic Transactions 21, Westerville, OH, 1991) pp. 451-458.

34. R.L. Schulz, D.C. Folz, D.E. Clark and G.G. Wicks in *Microwaves: Theory and Applications in Materials Processing II*, edited by D.E. Clark, W.R. Tinga and J.R. Laia, Jr. (Ceramic Transactions 36, Westerville, OH, 1993) pp. 81-88.

EFFECT OF MICROWAVE HEATING ON THE MASS TRANSPORT IN CERAMICS

Iftikhar Ahmad
Technology Assessment & Transfer, Inc.
133 Defense Highway, Suite 212
Annapolis, MD 21401

David E. Clark
Department of Materials Science & Engineering
University of Florida
Gainesville, Florida 32611

ABSTRACT

The reaction and diffusion of zinc oxide in crystalline alumina has been investigated using conventional and microwave heating. Electron microscopy and secondary ion mass spectrometry analyses reveal that microwave heated specimens of both polycrsytalline and single crystal alumina show a larger reaction zone than conventionally heated specimens.

INTRODUCTION

Microwave energy is emerging as an attractive alternative method to materials synthesis and processing of ceramics and composites. In the past several years numerous applications have been reported and published in MRS and ACerS proceedings [1-4]. Reduction in processing time and temperature is commonly reported in several papers. These results lead to the speculation of enhanced diffusion rates induced by the microwave field. The speculation is based either on enhanced sintering [5] and reaction rates [6] or on direct observation of diffusivity during microwave heating [7]. This interesting phenomenon has attracted scientists to model this phenomenon [8,9].

The reaction between zinc oxide and aluminum oxide using microwave energy was reported earlier [6]. This paper presents the reaction and diffusion of zinc oxide in crystalline alumina.

MATERIALS AND METHODS

The diffusion studies were carried out using compacts of powdered zinc oxide and crystalline (polycrystalline and single crystal) alumina. Chemically pure (99.9%) laboratory grade zinc oxide having average particle size of 0.3μ was purchased from Aldrich Chemical Company. Polycrystalline alumina substrates (99% pure) were furnished by 3M company and single crystal alumina (HEMLUX & HEMCOR) were purchased from Crystal Systems Inc. These different grades were discs half an inch in diameter and 0.020 inch in thickness, cut on the (0001) orientation and polished on both sides. HEMLUX is the superior grade sapphire with minimal light scattering and/or lattice distortion. HEMCOR is a versatile economical grade with extensive light scattering and/or lattice distortion.

The polycrystalline or single crystal alumina specimens were sandwiched in pellets of 2 grams of zinc oxide pressed at 4000 psi. These were then placed in 10 gms of zinc oxide powder in a fused quartz crucible and placed in either the microwave oven or the conventional furnace for heating. The polycrystalline specimens were heated at 1000°C for one hour whereas the single crystal specimens were heated at 1100°C for three hours in either a conventional furnace or microwave oven.

A JEOL Superprobe 733 was used to observe the width of the reaction layer. Since the reaction width was small (a micron) the Superprobe was not used for quantitative microprobe analysis. However, it was used only for electron microscopy and x-ray mapping for the concentration of zinc in crystalline alumina.

Secondary ion mass spectrometry (SIMS) is among the major techniques of surface analysis of solids and is particularly noted for its outstanding sensitivity of chemical and isotopic detection. Quantitative or semi-quantitative analysis can be performed for small concentrations of most elements (including the lightest) in the periodic table. The high versatility of SIMS is mainly due to the combination of high sensitivity with good topographic resolution both laterally and in depth. The information at depths of the order of one atomic layer and very high sensitivity of elemental or isotopic detection, contributes to making SIMS a major technique of depth profiling [10]. Because of this

versatility, depth profiling of the single crystal alumina was performed by SIMS. These specimens were analyzed for depth profiles of zinc and aluminum in the alumina crystal.

RESULTS AND DISCUSSION

The polycrystalline alumina substrates, sandwiched between zinc oxide pellets, were heated in conventional furnace as well as in the microwave oven. After heating, the samples were prepared for examining the cross-section to determine the depth of penetration of zinc oxide in the polycrystalline alumina substrates. The extent of zinc diffusion into the polycrystalline alumina substrates was observed by backscattered electron micrographs (not shown) and the corresponding x-ray maps for zinc concentration. Figure 1 shows the x-ray maps for substrates heated by microwave energy and conventional means. Figure 1 (a), corresponding to microwave heated specimen shows a larger depth of penetration of zinc oxide into the polycrystalline alumina substrate as compared to Figure 1 (b) for conventional heating.

Although a distinct difference is observed in the extent of zinc oxide diffusion into the substrate, the surface roughness of the substrate and presence of grains boundaries, can possibly create some doubts about the diffusion paths and the width of the reaction layer or depth of penetration of zinc oxide. To eliminate the likelihood of any error, experiments were conducted with single crystal alumina.

Single crystals of alumina were used for similar experiment mentioned above. Single crystals in the form of small discs, sandwiched between pressed pellets of zinc oxide, were heated in a conventional furnace and the microwave oven. These samples were characterized by various techniques to observe any differences in the two heating methods. However, in this paper only x-ray mapping and SIMS depth profiling will be presented.

Similar to the electron micrographs (not shown) and the x-ray maps for zinc concentration in the polycrystalline substrates, the single crystal samples were prepared by polishing an edge of both the conventionally and microwave heated sample to a finish of 0.25 μ. Figure 2 shows the x-ray map for zinc concentration in the single crystal alumina, with the band in the microwave heated sample (Figure 2 a) being much wider than that for conventional heating (Figure 2 b). These results are very similar to those obtained with the polycrystalline alumina substrates.

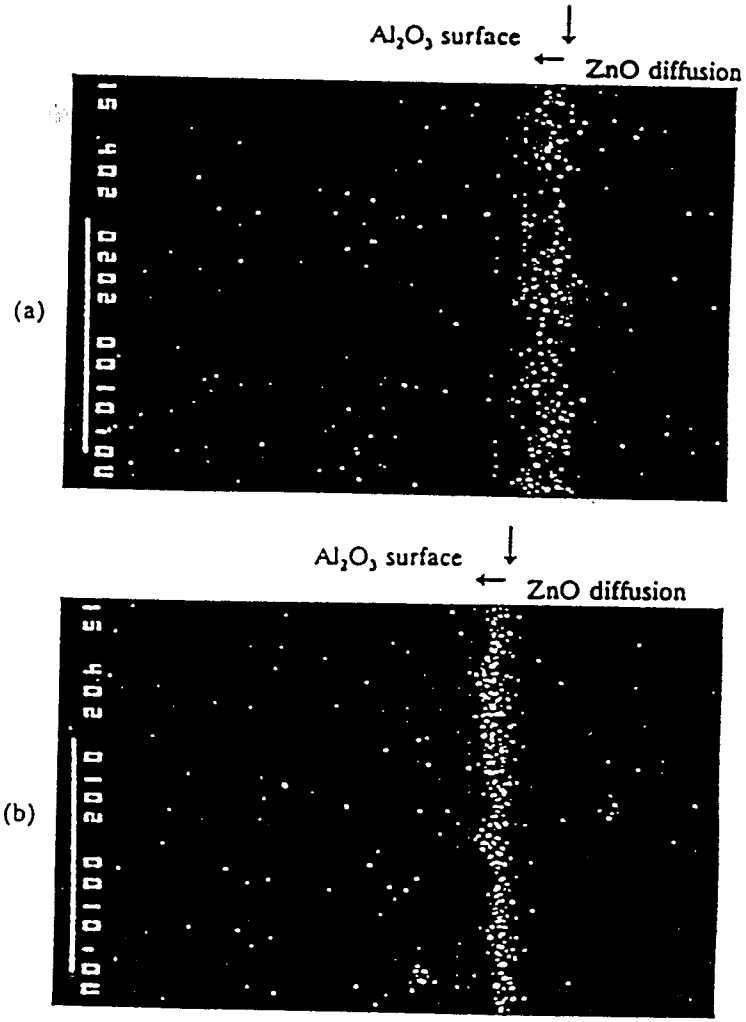

Figure 1. X-ray mapping of zinc concentration in polycrystalline alumina for (a) microwave heating (b) conventional heating.

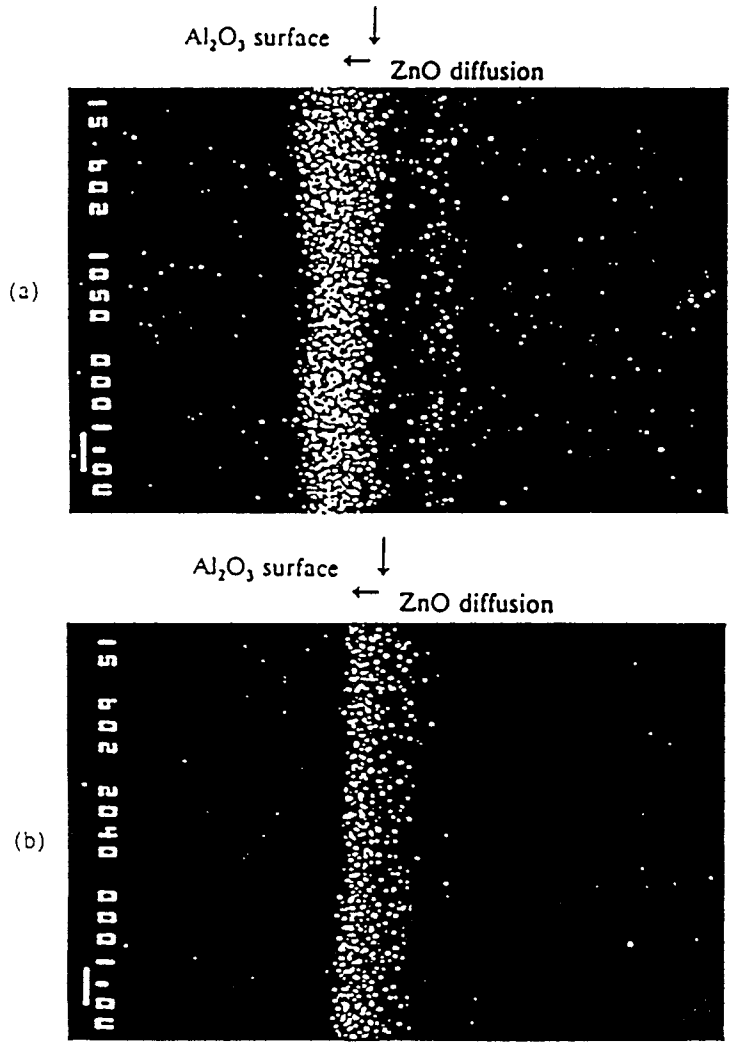

Figure 2. X-ray mapping of zinc concentration in single crystal alumina for (a) microwave heating (b) conventional heating.

The SIMS depth profile curves for aluminum and zinc isotopes in the single crystal alumina (HEMLUX) heated by microwave energy are shown in Figure 3. Figure 4 shows depth profiles of aluminum and zinc isotopes in the same crystal (HEMLUX) heated by conventional method. The curves for these samples are consistent with results from the x-ray maps for both the conventionally and microwave heated specimens. The penetration depth of zinc is greater than one micron for microwave heated specimens and somewhat greater than half a micron for the conventionally heated samples.

Another set of single crystal alumina (HEMCOR) was used similarly to make sure that the results were consistent. Figure 5 shows the profiles for single crystals microwave heated in zinc oxide, whereas Figure 6 shows the profiles for specimens heated in zinc oxide by conventional means, which show analogous results.

There is hardly any difference in the profiles for zinc concentration for HEMLUX (Figure 4) and HEMCOR (Figure 6) crystals heated conventionally. However, with microwave heating the economical grade crystal HEMCOR (Figure 5) shows more depth of penetration of zinc oxide than the superior grade crystal HEMLUX (Figure 3). Thus the presence of lattice distortions apparently results in higher diffusion and hence a larger reaction zone, when the specimen is heated by microwave energy, but seems to have no significant effect with conventional heating.

CONCLUSIONS

Microwave heating appears to enhance the reaction and diffusion of zinc oxide in both polycrsytalline and single crystal alumina substrates as compared to conventional heating. The presence of lattice distortions in single crystal alumina exhibited a larger reaction width with microwave energy, whereas no significant difference was observed with conventional heating.

ACKNOWLEDGEMENTS

The authors like to thank Dr. A. Loddings of the Chalmers University of Technology, Gothenburg, Sweden, for the SIMS analyses. The authors are also grateful to the Advanced Research Project Agency (ARPA) for the financial support which made this research possible.

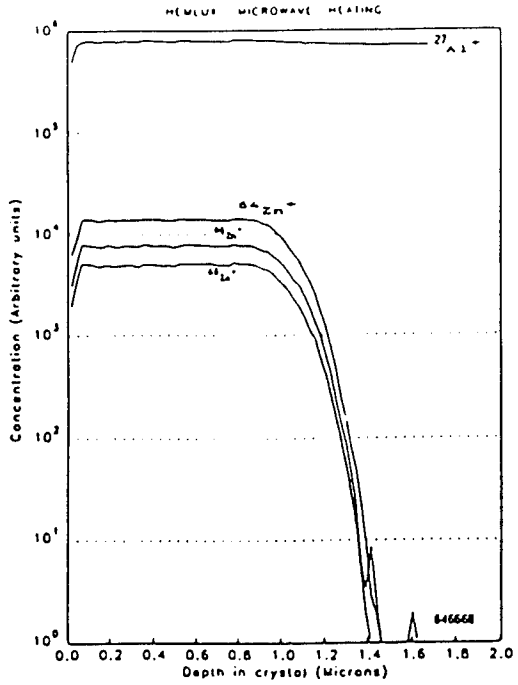

Figure 3. SIMS depth profile curves for Al and Zn in HEMLUX single crystal alumina with microwave heating.

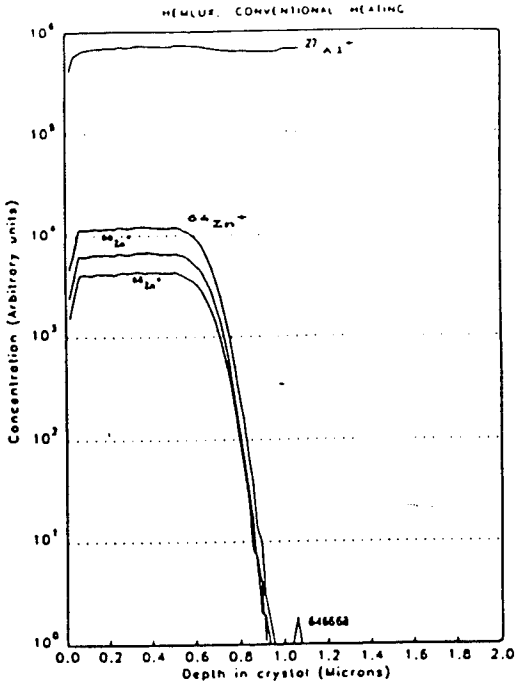

Figure 4. SIMS depth profile curves for Al and Zn in HEMLUX single cyrstal alumina with conventional heating.

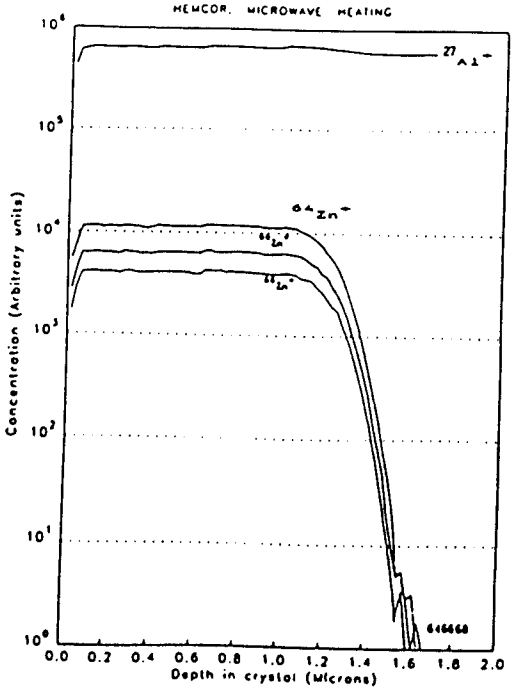

Figure 5. SIMS depth profile curves for Al and Zn in HEMCOR single crystal alumina with microwave heating.

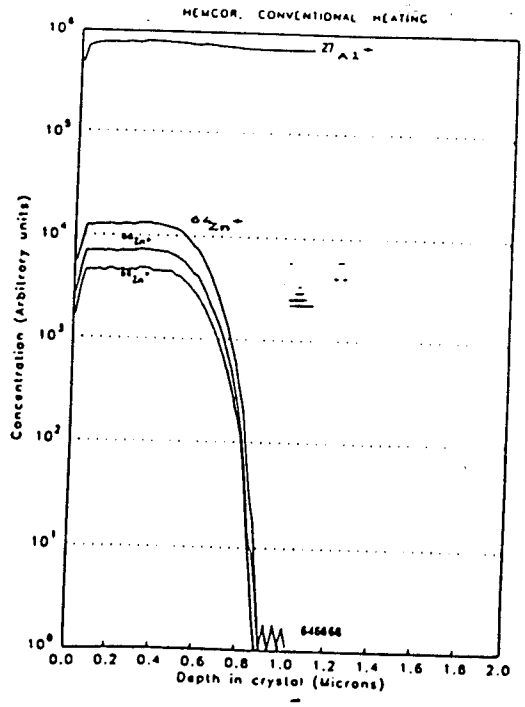

Figure 6. SIMS depth profile curves for Al and Zn in HEMCOR single cyrstal alumina with conventional heating.

REFERENCES

1. Sutton, W.H., Brooks, M.H. and Chabinsky, I.J., Microwave Processing of Materials I, Materials Research Society Symposium Proceedings, Vol. 124, (1988).
2. Snyder, W.B., Sutton, W.H., Iskander M.F. and Johnson, D.L., Microwave Processing of Materials II, Materials Research Society Symposium Proceedings, Vol. 189, (1991).
3. Clark, D.E., Gac, F.D. and Sutton, W.H., Microwaves: Theory and Application in Materials Processing, *Ceramic Transactions*, Vol. 21, (1991).
4. Beatty, R.L., Sutton W.H. and Iskander, M.F., Microwave Processing of Materials III, Materials Research Society Symposium Proceedings, Vol. 269, (1992).
5. Janney, M.A. and Kimrey, H.D. "Diffusion-Controlled Processes in Microwave-fired Oxide Ceramics," Microwave Processing of Materials II, Materials Research Society Symposium Proceedings, Vol. 189, pp. 215-227, (1991).
6. Ahmad, I. and Clark, D.E., "Effect of Microwave Heating on the Solid State Reactions of Ceramics," Microwaves: Theory and Application in Materials Processing, *Ceramic Transactions*, Vol. 21, pp. 605-612, (1991).
7. Fathi, Z., Ahmad I., Simmons, J.H., Clark D.E. and Lodding, A.R., "Surface Modification of Sodium Silicate Glasses," Microwaves: Theory and Application in Materials Processing, *Ceramic Transactions*, Vol. 21, pp. 623-629, (1991).
8. Booske, J.H., Cooper, R.F., McCaughan, L., Freeman S. and Meng, B., "Studies of Nonthermal Effects during Intense Microwave Heating of Crystalline Solids," Microwave Processing of Materials III, Materials Research Society Symposium Proceedings, Vol. 269, pp. 137-143, (1992).
9. Katz, J.D., Blake, R.D. and Kenkre, V.M., "Microwave Enhanced Diffusion?" Microwaves: Theory and Application in Materials Processing, *Ceramic Transactions*, Vol. 21, pp. 95-105, (1991).
10 Lodding, A.R., "Secondary Ion Mass Spectrometry," in Inorganic Mass Spectrometry, *Chemical Analysis Series*, Vol. 95, pp. 125-171, John Wiley and Sons, New York (1988).

CRYSTALLIZATION OF SOL-GEL DERIVED BARIUM ALUMINOSILICATE IN A 2.45GHz MICROWAVE FIELD

A.D. Cozzi, Z. Fathi and D.E. Clark, Department of Materials Science & Engineering
University of Florida, Gainesville, FL 32611-2066

ABSTRACT

An investigation into the crystallization kinetics of celsian from $BaO{\cdot}Al_2O_3{\cdot}2SiO_2$ glass was done. Celsian, in the monoclinic phase, is desirable as a composite matrix material because of its high potential use temperature (>1500°C) and its low coefficient of thermal expansion (2.2 x 10^{-6}/°C). The glass, of composition $BaO{\cdot}Al_2O_3{\cdot}2SiO_2$, to be used for crystallization was prepared by the sol-gel process. A second composition of $(Sr_{0.15}Ba_{0.85})O{\cdot}Al_2O_3{\cdot}2SiO_2$ was also produced by sol-gel to evaluate the effect of strontium substitution on the formation of the monoclinic celsian phase. Copper oxide was investigated as a seed material to promote formation of the monoclinic phase. Stabilization of the gel was done in a conventional furnace while densification and crystallization were performed both in a Raytheon QMP 2101B-6 microwave at 2.45 GHz and in a conventional furnace.

INTRODUCTION

Barium aluminosilicate glass-ceramics are being investigated as matrix materials in high-temperature ceramic composites for structural applications. The potential maximum use temperature in air is > 1500°C, higher than the lithium aluminosilicates and the calcium aluminosilicates and comparable to the upper use temperature of mullite which is in the range of 1600°C* as determined from the phase diagram. Another appealing characteristic is its resistance to thermal shock due to its low coefficient of thermal expansion (α = 2.2 x10^{-6}/°C from RT to 1000°C). Other advantages include good resistance to oxidation and formability (net shaping) prior to crystallization.

The monoclinic celsian phase is stable at temperatures < 1500°C and is the desired crystalline phase. However, hexacelsian, the high-temperature, hexagonal phase, is often the primary phase that nucleates, even at low temperatures. The hexagonal phase is undesirable because of its higher coefficient of thermal expansion (α = 8 x 10^{-6}/°C) and because the hexagonal phase transforms at 300°C to the orthorhombic phase, accompanied by a 3% volume change. Bahat examined the heterogeneous nucleation of $BaO{\cdot}Al_2O_3{\cdot}2SiO_2$ with several common nucleating agents[1]. He reported that hexacelsian was still the primary phase to crystallize. Bahat continued work in the celsian system with a kinetic study of the hexacelsian-celsian phase transformation [2]. He found that the complete transformation to celsian often took days. However, seeding the hexacelsian with 5% celsian reduced the transformation time to celsian to a few hours.

"Ceraming", the process by which glasses are transformed into glass-ceramics, can be achieved by two means. Figure 1 is a flow diagram of the glass-ceramic process by both the traditional and the sol-gel routes. The traditional process consists of the conventional melting of the raw materials followed by a rapid cooling to the glassy state, bypassing the formation of any crystalline phases. The glass is then subjected to a controlled heat-treatment to bring about the nucleation and then the crystallization of the desired phase or phases. The traditional method with hot pressing or hot isostatic pressing for the nucleation, crystallization and densification in the production of celsian [3,4] requires melting of $BaO{\cdot}Al_2O_3{\cdot}2SiO_2$ glass at temperatures in excess of 2100°C. Thus, sophisticated furnaces are necessary. The major problems associated with this technique are: (a) contamination from the molybdenum electrode in amounts up to one weight percent, (b) uncontrolled heterogeneous nucleation influenced by the impurities and the walls of the container; and (c) the hexagonal phase, although thermodynamically unstable, is the first phase to crystallize.

Other research groups have pursued a low-temperature sol-gel method for the formation of the parent glass [5-7]. Although the parent glass is readily synthesized by the sol-gel process, little progress has been made towards the crystallization of the monoclinic phase. In the traditional processing method a substitution of strontium for barium produced the first direct crystallization of the celsian phase [8].

The use of microwave energy to process ceramic materials is still in the early stages of development. One of the objectives of this study addresses the use of microwave energy to study the densification, nucleation and crystallization of $BaO{\cdot}Al_2O_3{\cdot}2SiO_2$ glass. The kinetics of bulk crystallization involve a combination of nucleation and growth, both of which require energy to

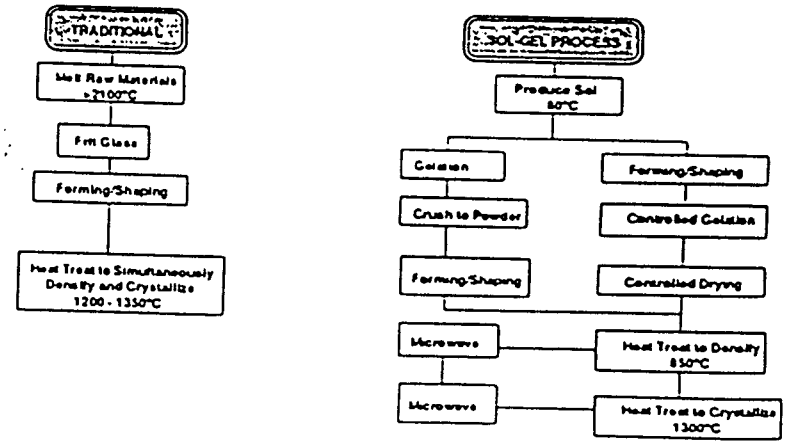

Figure 1. Flow diagram of the glass-ceramic process by conventional and sol-gel methods.

*Mullite melts at 1820 °C but small deviations from stoichiometry drastically lower its liquidus temperature

be added to the system. While producing thermal energy, microwave radiation also bathes the material in an electromagnetic field. Therefore, microwave processing may produce novel crystallization kinetics. It has been reported that microwaves interact with glass modifiers and enhance their diffusion in glass[9]. Since crystallization is a diffusion controlled process, any enhancement in the diffusion would result in increased crystallization kinetics. The same authors have shown that crystallization in lithium disilicates can be carried out at lower temperatures and shorter times in a microwave field [10].

EXPERIMENTAL PROCEDURE

Gel Preparation

The base gel was prepared by the sol-gel process described by the researchers in reference 7. The precursor materials used to prepare the gel were tetraethylorthosilicate* (TEOS), aluminum-sec-butoxide** and barium metal***. A solid state reaction was used to prepare the seed material, $(Sr_{0.75}Ba_{0.75})O{\cdot}Al_2O_3{\cdot}2SiO_2$, by heating a mixture of the precursors, barium carbonate****, strontium acetate*****, silica****** and alumina******* to 1500 °C for four hours. The other seed material, copper oxide******** (CuO), was obtained directly from the vendor.

The base gel was dried to a powder at several temperatures (50, 200, and 800°C). The dried gels were characterized using differential thermal analysis (DTA) to obtain information regarding organic burnout and T_g, which are needed for the densification of the gels. X-ray diffraction analysis was also performed on the DTA samples to determine any crystalline phases present. X-ray diffraction indicated that the gels were amorphous up to at least 900°C.

Powders of the monoclinic phases of copper oxide and strontium-barium aluminosilicate (produced by the sol-gel process and crystallized at 1300°C for four hours) were used in amounts varying from 1 wt% to 10 wt%. The powders were added to the dried gel and cold pressed at 4000 psi into discs.

*Tetraethylorthosilicate Fisher Chemical #O-4617

**Aluminum Sec-Butoxide (95%) Alpha Chemicals #11140

***Barium metal (99.5%) Aesar #10103

****Barium Carbonate (99.9%) Johnson Matthey #14341

*****Strontium Acetate Johnson Matthey #12203

******Silica Fisher Chemical #S150-3

*******Aluminum Oxide Fisher Chemical #A-591

********Copper oxide (CuO), Fisher Chemical #C-472L

Densification and Crystallization

Densification was carried out in a conventional furnace at temperatures determined from the processing "window" provided by the DTA results from the ten weight percent copper oxide powder in figure 2. The specimen containing 10 wt% CuO exhibited the lowest crystallization temperature, 950 °C. The temperatures investigated for densification ranged from 800 °C to 1050 °C. The densification temperatures for other specimens ranged from 800 to 1050°C. These glasses were screened using XRD to evaluate the extent of crystallization, if any, that occurred during the heat treatments.

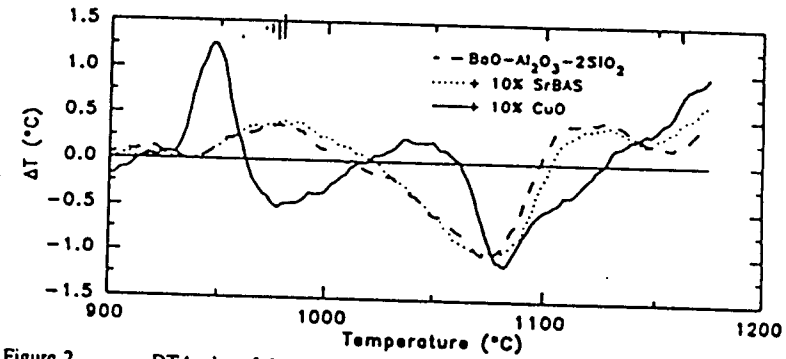

Figure 2. DTA plot of the unseeded and seeded $BaO{\cdot}Al_2O_3{\cdot}2SiO_2$ glass-ceramics.

In the next phase of the study, the glass samples were heat treated using conventional and microwave energy. Temperatures investigated ranged from 1050 to 1300°C. The time allowed for crystallization was three hours in the conventional furnace and 15 or 90 minutes at 1050°C or 1300 °C in the microwave furnace.

Crystallized samples were analyzed using x-ray diffraction analysis and the bulk densities were determined by the Archimedes method.

RESULTS & DISCUSSION

The DTA for a gel dried at 50°C is shown in figure 3. The two peaks below 400°C are most likely to be the elimination of the alcohols and the pore water of the gel. The exotherm a 400°C can be attributed to the burning out of the remaining organic materials. The smal endotherm slightly below 1200°C was confirmed by x-ray diffraction to be due to the crystallization of the hexagonal phase. Table I is the x-ray diffraction results of crystallization in both the conventional and microwave furnaces of unseeded glasses.

Conventional Heat-Treatment

Differential thermal analysis also was performed on various seeded samples. The substitution of fifteen mol percent strontium for barium in the gel crystallized only the hexagonal phase. Monoclinic strontium aluminosilicate ($SrO{\cdot}Al_2O_3{\cdot}2SiO_2$) and monoclinic

Table II. X-Ray Diffraction Results of Seeding $BaO{\cdot}Al_2O_3{\cdot}2SiO_2$ Glass Crystallized Using Conventional and Microwave Energy.

Seed Material wt. %	Heat Treatment Temp	Time	Phases Detected
Conventional			
1% CuO	1050 °C	20 hrs	hexagonal
1% CuO	1250 °C	20 hrs	hex/ mono
1% CuO	1300 °C	4 hrs	mono/ hex
5% CuO	1300 °C	3 hrs	monoclinic
10% CuO	1050 °C	20 hrs	hex/ mono
10% CuO	1300 °C	3 hrs	monoclinic
Microwave			
1% CuO	1100 °C	90 min	hexagonal
5% CuO	1050 °C	15 min	hexagonal
5% CuO	1300 °C	15 min	80% mono/ 20% hex
10% CuO	1100 °C	90 min	70% mono/ 30% hex
10% CuO	1050 °C	15 min	25% mono/ 75% hex
10% CuO	1300 °C	15 min	monoclinic
5% $SrO{\cdot}Al_2O_3{\cdot}2SiO_2$	1100 °C	90 min	hexagonal
10% $SrO{\cdot}Al_2O_3{\cdot}2SiO_2$	1100 °C	90 min	hexagonal

ACKNOWLEDGEMENTS

The authors would like to thank DARPA and the High Temperature Materials Laboratory at Oak Ridge National Laboratories for funding during this research.

REFERENCES

1. D. Bahat, "Heterogeneous Nucleation of Alkaline Earth Feldspar Glasses," J. Mat. Sci., 4, pp. 847-854 (1969).
2. D. Bahat, "Kinetic Study of the Hexacelsian-Celsian Phase Transformation," J. Mat. Sci., 5, pp. 805-810 (1970).
3. N.P.Bansal, J.A. Setlock and C.H. Drummond, III, "Celsian Glass-Ceramic Composites," Hi-Temp. Review, NASA, cp-10039, pp. 62-1 - 62-12 (1989).
4. C.H. Drummond, III, W.E. Lee, N.P. Bansal and M.J. Hyatt, "Crystallization of Barium Aluminosilicate Glass," Ceram. Eng. Sci. Proc., 10, [9-10], pp. 1485-1502 (1989).
5. W.K. Treadway and S.H. Risbud, "Gel Synthesis of Glass Powders in the $BaO{\cdot}Al_2O_3{\cdot}2SiO_2$ System," J. Non-Cryst. Solids, 100, pp. 278-283 (1988).
6. V.S.R. Murthy, Li Jie and M.H. Lewis, "Interfacial Microstructure and Crystallization in SiC-Glass Ceramic Composites," Ceram. Eng. Sci. Proc. 10 [7-8], pp. 938-951 (1989).
7. M. Chen, W.E. Lee and P.F. James, "Preparation and Characterization of Alkoxide-Derived Celsian Glass Ceramic, to be published in JNCS.
8. N.P. Bansal and M.J. Hyatt, "Crystallization and Properties of Sr-Ba Aluminosilicate Glass-Ceramic Matrices," Ceram. Eng. Sci. Proc., 12, [7-8], pp. 1222-1234 (1991).
9. Z. Fathi, I. Ahmad, J.H. Simmons, D.E. Clark and A.R. Lodding, "Surface Modification of Sodium Aluminosilicate Glasses Using Microwave Energy," Ceramic Transactions, Microwaves: Theory and Applications in Materials Processing, Vol. 21, pp.612-630, (D.E. Clark, F.D. Gac and W.H. Sutton, eds.) The American Ceramic Society, Inc., Westerville, OH (1991).
10. A.D. Cozzi, Z. Fathi, R.L. Schulz and D.E. Clark, "Nucleation and Crystallization of $Li_2O{\cdot}2SiO_2$ in a 2.45GHz Microwave Field," to be published in Ceram. Eng. Sci. Proc.

SURFACE MODIFICATION OF SODIUM ALUMINOSILICATE GLASSES USING MICROWAVE ENERGY II

Z. Fathi, D.C. Folz and D. E. Clark, Materials Science and Engineering, University of Florida, Gainesville, FL, 32611.

R. Hutcheon, AECL Research, Physics Division, Chalk River Lab, Chalk River, Ontario, Canada KOJ1JO.

ABSTRACT

A series of sodium aluminosilicate (NAS) glasses were produced. The glasses of interest were evaluated in terms of mechanical (using microhardness) and dielectric properties. Electron microprobe (EMP) was used to evaluate the effect of microwave heating on the extent and rate of ion exchange of silver and potassium ions for sodium ions (Ag^+ & $K^+ \leftrightarrow Na^+$) in comparison to conventional heating.

INTRODUCTION

In a previous study, microwave energy was used to interdiffuse potassium for sodium ions ($K^+ \leftrightarrow Na^+$) in a series of sodium aluminosilicate glasses (NAS)[1]. Sodium aluminosilicate glasses exhibited structural changes when Γ, the ratio of Al/Na, was varied. The extent to which microwave energy affected the $K^+ \leftrightarrow Na^+$ interdiffusion was found to be dependent on glass composition.

In this investigation, the effect of microwave radiation on ion exchange reactions of the ion pair, silver and potassium, for sodium (Ag^+ & $K^+ \leftrightarrow Na^+$) was examined. The penetration depths for the Ag^+ and K^+ ions were determined.

Silver has a considerable effect on the refractive index of a variety of glasses. Ion exchange of silver for alkali ions, in a variety of alkali silicate glasses, has been investigated extensively[2,3]. Various commercial products such as optical waveguides, can be produced by such a process. Thus the study of new methods for ion-exchanging silver for different alkali ions is of practical importance.

EXPERIMENTAL/RESULTS

The selected compositions in the sodium aluminosilicate system are shown in Table 1. The glasses produced had a constant concentration of alkali ions (15 mol% of NaO_2). The molar ratio of Al to Na (Γ) was varied (0.2, 0.5, 1.0 and 1.1).

Table 1. Compositions of the glasses investigated.

Components	Γ=0.2	Γ=0.5	Γ=1.0	Γ=1.1
Na_2O	15.0	15.0	15.0	15.0
Al_2O_3	3.0	7.5	15.0	16.5
SiO_2	82.0	77.5	70.0	68.5

The glasses were prepared by milling a mixture of high purity silica, sodium carbonate and high purity alumina for 24 hours. Powders for the glass compositions having Γ equal to 1.0 and 1.1 were sintered at 1500°C for 15 hours and subsequently quenched and crushed to form glass frits. The glass frits were then melted inside an alumina crucible at 1600°C for 12 hours. The glass compositions having Γ= 0.2 and 0.5 were melted at 1500°C for 24 hours. The alumina/melt was annealed at 700°C for few hours and allowed to furnace cool.

Glass density measurements were carried out using pycnometry at ambient temperature. Microhardness measurements also were performed on annealed glasses of the NAS glass series. Table 2 summarizes the characterization results.

The glasses of different compositions were cut, polished and cleaned prior to ion exchange. The glass faces to be ion exchanged were polished to a 1µm surface finish using diamond paste. Ion exchange was carried out using potassium nitrate salts containing 20 mol% of silver nitrate. Ion exchange reactions were performed isothermally at 400°C for 30 minutes using microwave and conventional techniques. The glass samples were washed and sonicated, first in water, then in acetone. The glass samples were cross sectioned and prepared for characterization.

The microwave ion exchange reactions were carried out in a modified industrial microwave oven with an operating frequency of 2.45 GHz. The glass samples were placed in pyrex test tubes containing the salts of interest and the test tubes were microwave hybrid heated (combination of radiant and microwave heating) or stand-alone microwave heated (no susceptor used with the sample) [4]. The temperature of the salts were monitored using an Inconel shielded, K-type

Electron microprobe (EMP)

Wavelength dispersive spectroscopy was performed on a JEOL 733 electron microprobe analyzer to determine the penetration depths involved in the ion exchange reactions. Interdiffusion of silver for potassium was performed on the NAS glass series using conventional heating. Figure 4 illustrates the results of silver for sodium ion exchange. The penetration depth of silver ions is shown to increase with increasing values of the structural factor(Γ). This is in agreement with the NAS glass model which predicts decreasing activation energy for diffusion as the structural factor is increased to higher values. The greatest penetration depth achieved by silver ions was found to be in the NAS glass composition having Γ=1.0.

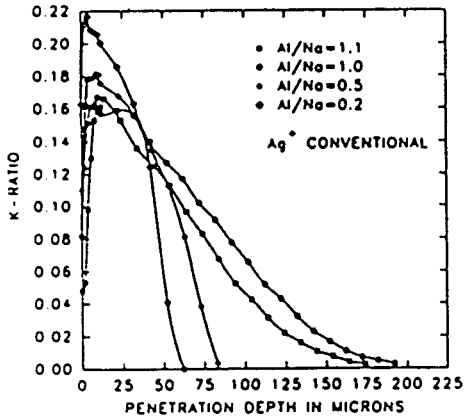

Figure 4. Penetration depth of Ag^+ into the NAS glass series

In order to study the effects of microwave energy on ion exchange, several interdiffusion reactions were performed in the presence of the microwave field. The ion pair exchange reactions ($Na^+ \leftrightarrow Ag^+, K^+$) run on the Γ=1.0 and 1.1 are shown in Figures 5a and 5b. Note that there was no significant difference between the samples prepared conventionally and those prepared by microwave hybrid heating. The absorption of microwaves by the salt and the silicon carbide lining was believed to be strong enough to shield the glass samples from the microwaves. The glass samples, Γ=0.5 and 1.0, that were ion exchanged directly without the use of a microwave susceptor show far-reaching penetrations achieved by the silver ion (Figures 6a and 6c).

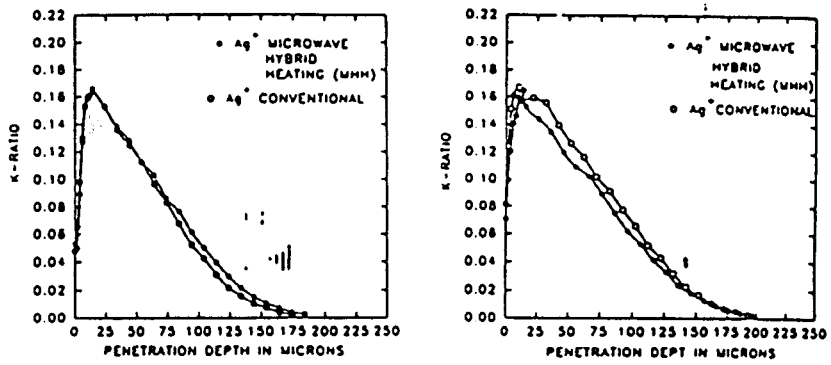

(a) Γ=1.0

(b) Γ=1.1

Figure 5. Penetration depth (in μm) of silver into glass compositions processed by microwave hybrid heating.

The glass samples, Γ=0.5 and 1.0, that were ion exchanged directly without the use of a microwave susceptor show far-reaching penetrations achieved by the silver ion (Figures 6a and 6c).

The silver ion has a smaller radius, higher polarizability and greater mobility as compared to the potassium ion; that accounts for the deep penetration achieved. Even though silver ions achieved greater penetration in the presence of microwaves when compared to conventional heating, no significant increase in penetration depth was apparent for potassium ions (Figures 6.b and 6.d)

If conventional thermal transport mechanisms were solely responsible for interdiffusion observed in these systems, similar variations in the penetration depth versus temperature would have been observed for both Ag^+ and K^+. However, since a significant increase in penetration depth versus temperature was noted only for the Ag^+ ions, a microwave heating mechanism is believed to have contributed toward the diffusion effects observed. In this case, the Ag^+ was more responsive to the electromagnetic field than K^+.

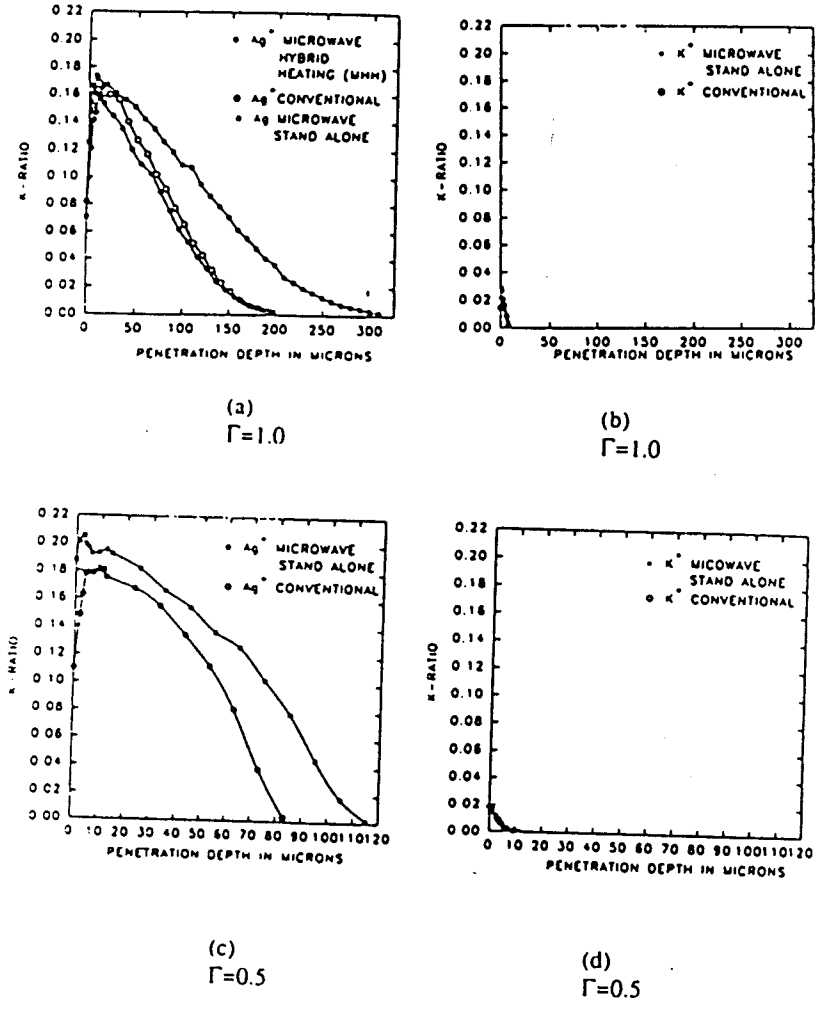

Figure 6. Penetration depths (in μm) of silver and potassium ions into glass samples processed using microwave energy (stand alone) and conventional heating.

SUMMARY

Dielectric measurements were performed on a series of NAS glasses having Γ=0.2, 0.5, 1.0 and 1.1. The dielectric constant, the dielectric loss factor and the loss tangent were evaluated as functions of temperature for each of the glass compositions. Microwave depth of penetration inside the different glasses also was quantified. The Γ=1.0 glass composition exhibited the greatest losses at the working frequency(2.45GHz). Surface modification of NAS glasses using microwave energy was demonstrated successfully. Ion exchange of Ag^+ and K^+ for Na^+ was performed on the NAS glass series. The extent to which microwaves affected the ion exchange reactions depended on the glass compositions and on the type of heating (hybrid or stand alone) used to carry out the reactions. Far reaching penetration depths of Ag^+ were achieved in the glasses while no significant interdiffusion increase was observed for K^+ under the experimental conditions described above.

ACKNOWLEDGEMENT:

The authors gratefully acknowledge support from the Defense Advanced Research Project Agency (Contract #4910 4509 409-12).

Special acknowledgement for J.P. Zhong, G. P. LaTorre and R.L. Shulz for help throughout this study and W.A. Acree for the electron micoroprobe analysis.

REFERENCES

1. Fathi, Z., Ahmad, I., Simmons, J.H, Lodding, A.R., Clark, D.E., Ceramic Transactions, Vol. 21, 623-629, (1991).
2. Chludzinski, P., Ramaswamy, R.V., Anderson, T.J., Physics and Chemistry of Glasses, Vol. 28., No. 5., October., 1987.
3. Fainaro, I., Ish Shalom, M., Ron, M., Lipson, S., Physics and Chemistry of Glasses, Vol. 25., No. 1., February., 1984.
4. De, A., Ahmad, I., Whitney, E.D., Clark, D.E., Ceramic Transactions, Vol. 21, 319-328, (1991).
5. Hutcheon, R.M., De Jong, M.S., Adams, F.P., Lucuta, F.P., McGregor, J.E., Bahen, L., Mat. Res. Soc. Symp. Proc., Vol. 269, 5412-551, (1992).

REPAIR OF GLASS BY SOL-GEL COATING USING EITHER CONVENTIONAL OR MICROWAVE HEATING

A. Boonyapiwat, Z. Fathi, D. C. Folz, and D. E. Clark,
Department of Materials Science and Engineering,
University of Florida, Gainesville, FL.

ABSTRACT

A method of repairing glass is discussed. Microindentation was used to deliberately weaken the glass. Some samples were dip coated with silica sol. Effects of dipping the glass in copper nitrate solution also were studied. Heat treatments were conducted in either a conventional furnace or a microwave oven. Four-point bend testing was used to evaluate the merit of each process. Microwave hybrid heating had the same effect on the repair of uncoated glass as conventional heating. Coating the glass with sol resulted in higher strength of glass than heat treatment alone. Treating the glass with copper nitrate without heat treating had no effect on strength. Microwave hybrid heating appears to yield higher reliability in sol-gel coated samples than conventional processing.

INTRODUCTION

The practical strength or fracture stress of brittle materials is much lower than their theoretical strength. Griffith [1] showed that microcracks or surface flaws may act as stress concentrators and lead to premature failure of the material. According to the fracture mechanics approach, fracture stress depends on the size and the shape of the existing crack. When a ceramic or a glass article is subjected to a load, sharp cracks act as effective stress concentrators, thus reducing practical strength of the piece. There are several methods that can be used to minimize the effects of these cracks; crack tip blunting (solution treatments) [2], crack length shortening (thermal treatments) [3], residual stress control (thermal treatments with and without solution treatments) [4-6], and crack bridging (solution/heat treatment combination) [4-8]. Any of these methods may be used to repair glass that has been damaged during its manufacture or use.

Effects of thermal treatment alone on the enhancement of fracture stress have been studied extensively [3]. Strength enhancement was attributed to the decrease in crack dimensions. Heat treatments at high temperatures and long soak times were required to allow the glasses to flow and fill cracks.

Sol-gel coatings have been explored as a means for increasing fracture stress of glasses [4-8]. The observed strengthening of the glass was attributed to a decrease in flaw size resulting from filling the cracks with gel. Adequate heat treatments of the sol-gel coated glasses resulted in densification of the gel. Dense gels, chemically tailored to have lower thermal expansion coefficients than the original glasses, induce compressive stresses at the crack site that result in additional strength increases [4,5].

Microwave energy has been used successfully to process a variety of materials [9-14]. This technique offers some advantages over conventional heating. Shorter processing times and enhanced materials properties have been reported. The overall objective of this work was to study the effect of microwave heating in combination with sol-gel and other solution treatments on glass repair.

EXPERIMENTAL PROCEDURE

Soda-lime silica glass microscope slides* were used in this study. Differential scanning calorimetry (DSC)** was used to determine the glass transition temperature. The hardness of the glasses was measured by both Knoop [15] and Vickers indentation***. A load of 100 grams and a dwell time of 15 seconds were used in Vickers indentation.

Glass slides were cut along their longitudinal sides to dimensions of 75×12.5×0.9mm to accommodate the MTS bending fixture****. Longitudinal edges were chamfered by polishing with 240-grit silicon carbide papers. Diamond paste (6μ) was used for final edges polishing.

A schematic diagram of the procedure used for indenting, repairing and testing specimens is presented in Figure 1. Specimens first were deliberately damaged by indenting them (Vickers indentation) at the center (load=1 kg, t=15 sec). The indent diagonals were aligned perpendicular and parallel to the longitudinal edges of the glass slides. Three types of damage can occur during indentation: plastic deformation, residual stress, and cracking. Radial and lateral crack propagation continues for the first 30 hours following the indentation [16,17]. Also, due to partial relaxation of residual stresses, the fracture strength increases during this period. To increase the accuracy of data collected on fracture samples, the indented samples were stored in a desiccator for a minimum of 48 hours prior to fracturing.

Silica sols suitable for coating were prepared using Chu's procedure [18]. The sols contained 10 wt% SiO_2 and had a H_2O/TEOS molar ratio=2 and a pH=1. These sols were aged for 7 months before they were used for coating the specimens. Dip coating at a drawing rate of 6 cm/min was employed.

Conventional heating of coated and uncoated specimens was conducted in a box furnace using heating rates of 2°C/min and 10°C/min. Various soaking temperatures and times were used.

Microwave hybrid heating [9] using a SiC susceptor was carried out in an industrial model microwave oven (2.45 GHz)#. A type-K shielded thermocouple was positioned close to the samples. Heating rate was controlled by adjusting microwave power duty cycles to achieve a rate similar to that used in conventional techniques.

Stand-alone microwave heating (no susceptor) was performed by assigning a fixed duty cycle and varying heating time.

Five to six specimens from each test condition underwent 4-point bending using an Instron testing machine##. The bend fixture employed in this work was an MTS fixture (40mm O.D. span and 20mm I.D. span). A cross head speed of 0.5mm/min, equivalent to a specimen stress rate of

---

* Fisher Scientific, Pittsburgh, PA Cat. # 12-550A.
** E. I. du Pont de Nemourous & co, Willmington, DE Model # 910.
*** LECO Corporation, St. Joseph, MI Model # M-400.
**** MTS System Corp., Minneapolis, MI Model # 642.05a-02.
\# Raytheon, Waltham, MA Model # Qmp 2101 b-6.2
\#\# Instron Corp., Canton MA Model # 1122.

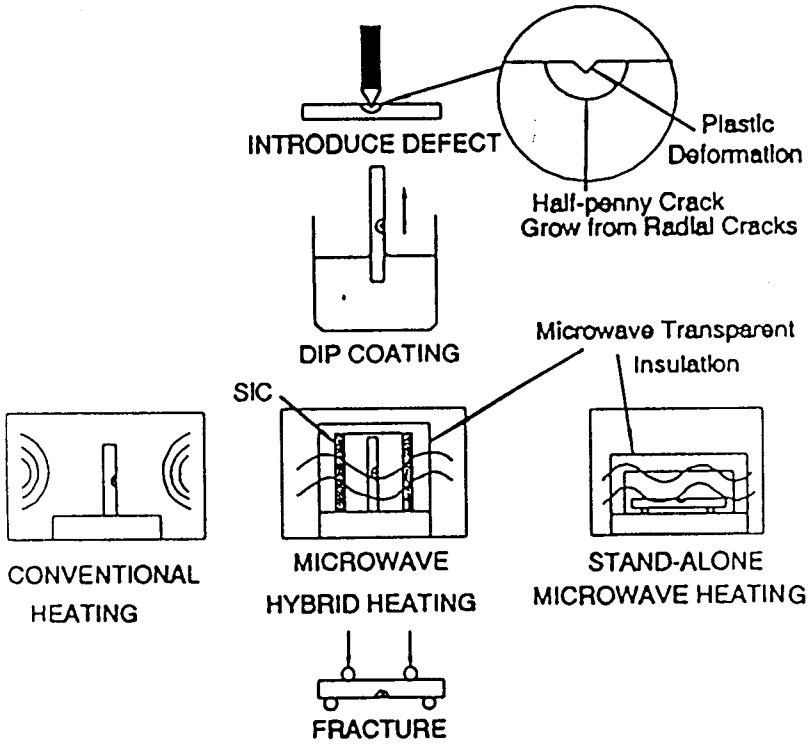

Figure 1. Schematic diagram of glass repair.

about 2 MPa/sec, was used. Plastic tape was applied on the compression side of the specimen to collect the broken pieces for subsequent fracture surface analysis. Fracture surfaces were observed using light microscopy and scanning electron microscopy (SEM).

RESULTS AND DISCUSSIONS

Properties of glass used in these experiments are presented in Table 1. The composition of the glass obtained from the glass supplier is presented in Table 2.

The results of bend testing of glasses heat treated at various temperatures are presented in Figure 2. The strength of the indented glass increased when samples were heat treated. The strength increased with increasing heat treatment up to temperatures ranging from 500 to 550°C. It is interesting to note that the best result, in terms of the scatter in strength, was obtained at 500°C. This temperature of approximately 500°C (T_g-530°C) was selected to perform subsequent heat treatments of the coated specimens.

Table 1. Properties of Glass.

T_g	530°C
Hk	464 Kg/mm²
Hv	495 Kg/mm²

Table 2. Composition of Glass.

Component	wt%
SiO_2	72.10
Fe_2O_3	0.045
Al_2O_3	1.80
CaO	7.30
MgO	3.80
K_2O	0.15
Na_2O	14.0
SO_3	0.30

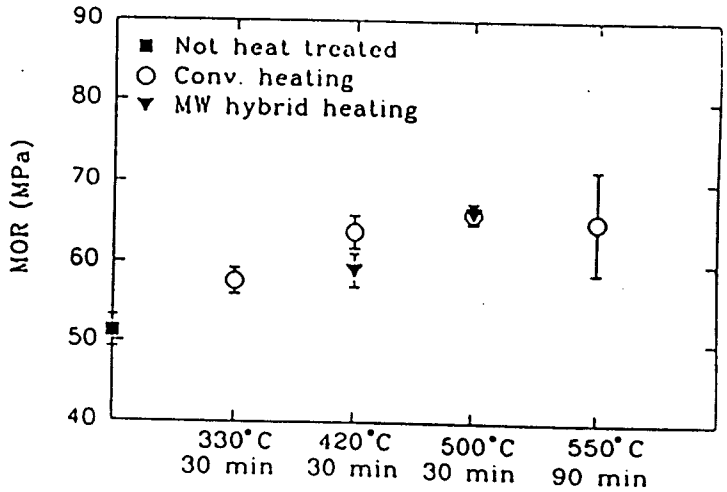

Figure 2. Strength of indented glasses heat treated at various temperatures.

The increase in strength of glass subjected to heat treatment is most likely due to relaxation of residual stress from indentation [16,19,20]. Microwave hybrid heating gave the same result in strength improvement as conventional heating when heat treated at 500°C. However it is still unclear why lower strengths were obtained with microwave hybrid heating at 420°C.

Fracture surfaces of glasses as-indented were compared to glasses that were indented and heat treated (Figure 3). By comparing Figure 3a and 3b, it can be noted that crack healing occurred below the plastic deformation zone.

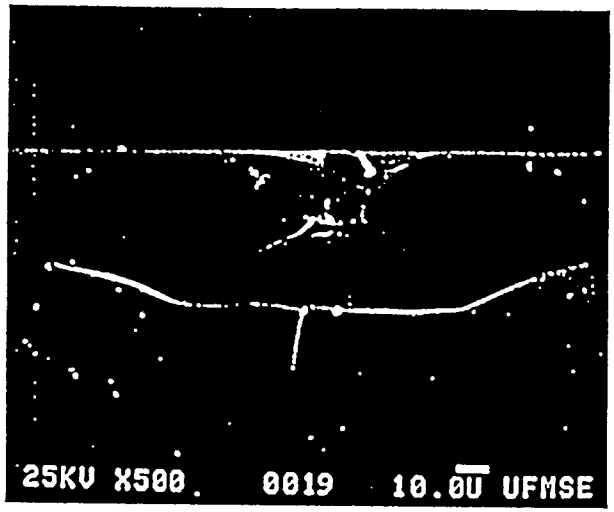

(a) As-indented.

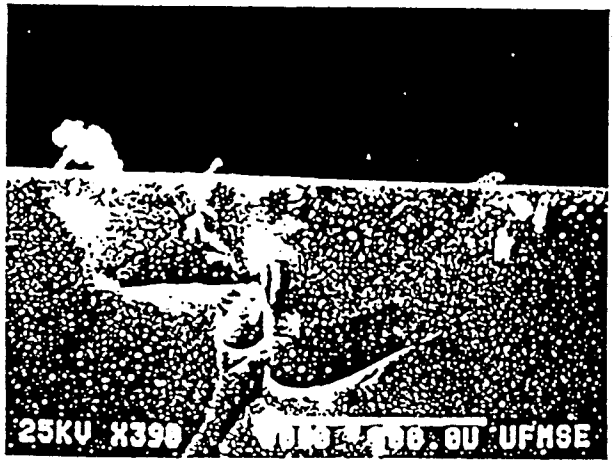

(b) Heat treated at 550°C for 100 minutes.

Figure 3. Fracture surfaces of indented glasses from SEM.

Effects of soaking time on the strength are presented in Figure 4. It evident that soaking times greater than 10 min had no effect on strength for either conventional or microwave hybrid heated samples. Also, the effect of heating rate was negligible (Figure 5).

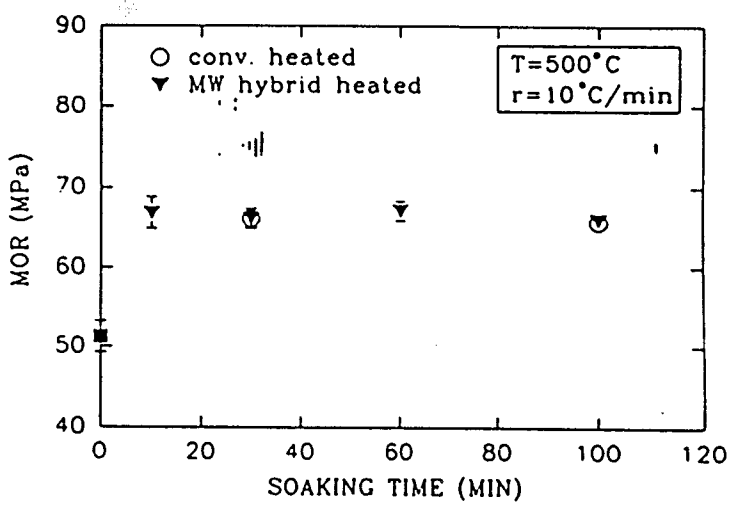

Figure 4. Effects of soaking time.

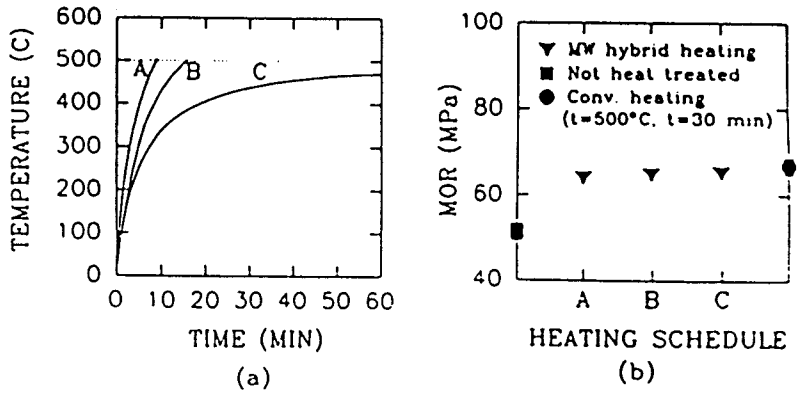

Figure 5. Microwave fast heating by hybrid heating method. (a) Heating schedule. (b) Fracture strength.

The effects of sol-gel coating on the strength of the glass are presented in Figure 6. The coated samples had slightly higher strengths than uncoated samples. This increase in strength was not from gel densification, as this gel began to densify only above 600°C [8]. As in samples subjected to corrosive liquid [21], the strength data in coated samples was scattered and inconclusive. However, microwave hybrid heating seemed to provide more strength and reliability than conventional heating in coated samples aged for 2 days.

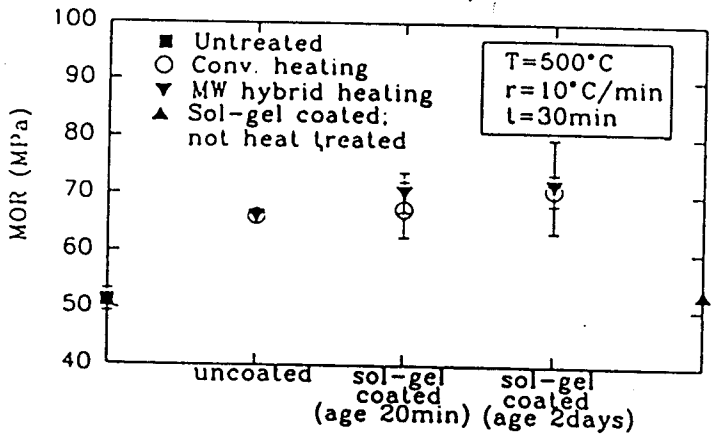

Figure 6. Effects of sol-gel coating on fracture strength of indented glasses.

Dipping in copper nitrate solution increased the strength of the glass only after heat treatment, as shown in Figure 7. Microwave hybrid heating had the same effect as conventional heating on fracture strength of glass dipped in copper nitrate solution.

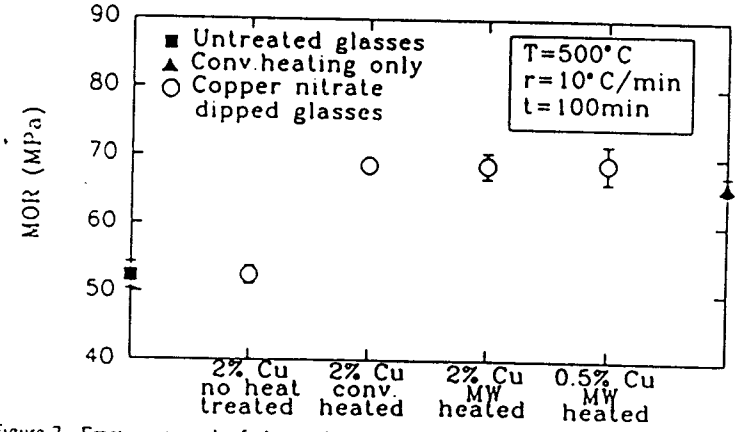

Figure 7. Fracture strength of glasses dip in copper nitrate solution.

Strengths of stand-alone microwave heated glass are presented in Figure 8. The strengths were increased slightly over unheat-treated glass and lower than glass heat treated by conventional processing at 330°C. With the used of better insulation materials during heating, this method could provide improved results.

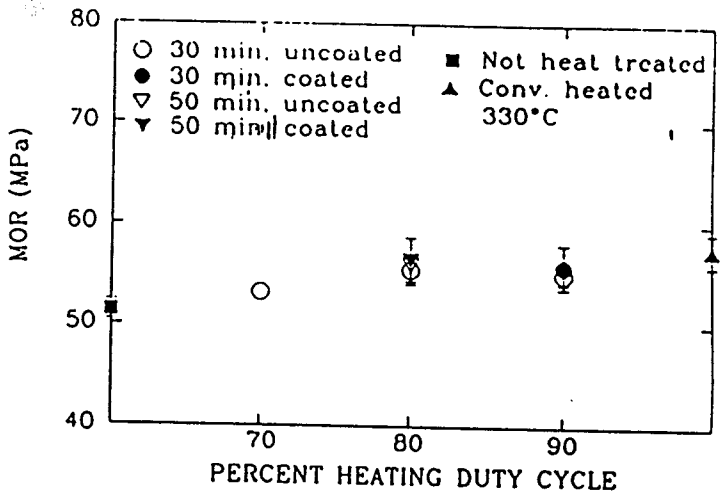

Figure 8. Fracture strength of glasses heated by stand-alone microwave.

CONCLUSION

Microwave hybrid heating had the same effect as conventional heating on the repair of uncoated glass. Coating the glass before heat treatment increased slightly the fracture strength, but the reliability of the glass did not improve. Microwave heating of sol-gel coated glass seemed to give better results than conventional heating since it rendered less scatter of data. Microwave hybrid heating had the same effect as conventional heating on fracture strength of glass dipped in copper nitrate solution. This glass can be heated using stand-alone microwave techniques; however, improvement in the experimental set up will be is required for significant property improvements.

ACKNOWLEDGEMENTS

The authors wish to express their gratitude to Dr. F. Ebrahimi for donating equipment use and time, G. P. LaTorre for his invaluable assistance on operating mechanical test equipment. A special thank is extended to Drs. J. J. Mecholsky, J. P. Zhong and E. H. Moore for their assistance on this project. Also, DAPRA is acknowledged for partial financial support during this project.

REFERENCES

1 A. A. Griffith, Philos. Trans. Soc. Lond. Ser. A221 (4) 163 (1920).
2 D. H. Roach and A. R. Cooper, Strength of Inorganic Glass (C. L. Kurkjian eds),185-195 (1985).
3 P. Hrma, W. T. Han, and A. R. Cooper, J. Non-Cryst. Solids, 102, 88-94 (1988).
4 M. Chen, P. F. James, F. R. Jones, D. A. Dalton, B. H. Howard, and S. Bedford, J. Non-Cryst. Solids, 139, 185-197 (1992).
5 P. F. James, M. Chen, F. R. Jones, J. Non-Cryst. Solids, 155, 99-109 (1993).
6 B. D. Fabes, W. F. Doyle, B. J. J. Zelinski, L. A. Silverman, and D. R. Uhlmann, J. Non-Cryst. Solids, 82, 349-355 (1986).
7 A. Madalena, M. Guglielmi, A. Raccanelli, and P. Colombo, J. Non-Cryst. Solids, 100, 461-465 (1988).
8 B. D. Fabes and D. R. Uhlmann, J. Am. Ceram. Soc., 73 [4] 978-988 (1990).
9 T. T. Meek, C. E. Holcombe, and N. Dyke, J. Mat. Sci. Lett. 6, 1060-1062 (1987).
10 A. S. De, I. Ahmad, E. D. Whitney, and D. E. Clark, Microwaves: Theory and Application in Materials Processing, Ceramic Transactions, Vol. 21, 329-339 (1992).
11 Y. Fang, D. K. Agrawal, D. M. Roy, and R. Roy, Microwave: Theory and Application in Materials Processing, Ceramic Transactions, Vol. 21, 349-356 (1992).
12 R. Roy, S. Komarneni, and L. Y. Yang, J. Am. Ceram. Soc., 68 [7] 392-395 (1985).
13 S. Surapanani, M. E. Mullins, and B. C. Cornilsen, Mat. Res. Symp. Proc. Vol. 189, 309-325, (1991).
14 S. Al-Assafi, I. Ahmad, Z. Fathi, and D. E. Clark, Microwave: Theory and Application in Materials Processing, Ceramic Transactions Vol. 21, 515-522 (1992).
15 ASTM Designation C730-85, Annual Book of ASTM Standards pp. 225-229 in Vol. 15.02. American Society for Testing and Materials, Philadelphia, PA (1985).
16 B. R. Lawn, K. Jakus, A. C. Gonzalez, J. Am. Ceram. Soc., 68 [1] 25-34 (1985).
17 S. R. Choi and J. A. Salem, Mat. Sci. Eng., A149, 259-264 (1992).
18 P. Chu, Master Degree Thesis, University of Florida (1988).
19 D. H. Roach and A. R. Cooper, J. Am. Ceram. Soc., 68 [11] 632-636 (1985).
20 W. T. Han, P. Hrma, and A. R. Cooper, Phy Chem. Glasses, 30 [1] 30-33 (1989).
21 E. K. Pavelchek and R. H. Doremus, J. Non-Cryst. Solids, 20, 303-308 (1976).

NUCLEATION AND CRYSTALLIZATION OF $Li_2O \cdot 2SiO_2$ IN A 2.45 GHz MICROWAVE FIELD

A.D. Cozzi, Z. Fathi, R.L. Schulz and D.E. Clark, Dept. of Materials Science and Engineering, University of Florida, Gainesville, FL 32611-2066

ABSTRACT

Rods of lithium aluminosilicate were nucleated at 450 ° C for 3 hours in a conventional furnace. The bars were then cut into discs and crystals were grown over a range of temperatures using both microwave and conventional heating. X-ray diffraction analysis was performed on the samples to determine the crystalline phases present. Peak intensities were compared to determine the relative percent crystallinity due to differing heat-treatments. The effect of the heat-treatment parameters using both microwave and conventional heating on the extent of crystallization is discussed.

INTRODUCTION

The interest in glass-ceramics stems from the potential to tailor their mechanical properties through various heat treatments.[1] Ceraming is the process by which glass-ceramics are formed through the controlled nucleation and growth of crystals from the glass. Microwave processing is a new ceraming technique that may provide significant improvements in product uniformity through the volumetric heating that has been observed in many ceramic systems.[2]

Phases in the lithium silicate system possess desirable properties which make it the basis of many glass-ceramic compositions. The ease of fabrication and its well-documented crystallization behavior[3,4] make it a model system for study. Other researchers have established the feasibility of heating glass-ceramics using microwaves.[5] Previous work on microwave/glass interaction has demonstrated deviations from expected results in diffusion and overall reaction kinetics.[6]

The main objective of this work is to determine the feasability of carrying out the growth stage of the ceraming process using microwaves. Other goals include comparing the effects of conventional heating and hybrid heating on the growth behavior of lithium disilicate crystals.

EXPERIMENTAL

Glass samples were prepared from TiO_2 free SiO_2* and reagent grade Li_2CO_3.** A batch of SiO_2 + 33.3 mol% Li_2O was melted at 1350 ° C for 72 hours in a covered platinum crucible. The melt was stirred several times with a platinum rod to homogenize the glass. By using a 1:2 molar ratio of Li_2O:SiO_2 in the melt, $Li_2O \cdot 2SiO_2$ crystallizes from the glass to a glass-ceramic of the same stoichiometry.

The glass was cast as rods 75 mm long and 13 mm in diameter and annealed at 300 ° C for 12 hours. Nucleation was performed at 450 ° C for 4 hours on all of the rods simultaneously to ensure consistency among the rods. All of the rods were clear with some containing seeds. Discs 4 mm thick were cut from the rods and polished with emery cloth*** until optically clear. Samples containing seeds were discarded.

The growth process was performed isothermally with the time being measured from when the sample was inserted in the furnace or microwave cavity. Samples heat-treated using microwaves were processed inside a microwave transparent cavity lined with a suscepting material. This process is referred to as microwave hybrid heating. The specimens are exposed to convection, infrared and microwave radiation. These processing procedures were described previously.[7] Growth temperatures ranged from 500 ° C to 600 ° C inclusive. In the microwave processed samples, two shielded thermocouples**** were used in close proximity to the sample to ensure temperature uniformity. Samples in which the temperatures differed by more than ±5 ° C were discarded.

The discs were then ground to a fine powder with a mortar and pestle. Specimens for x-ray diffraction were prepared and analyzed in a Phillips ADP

---

* Magnetic separated glass sand, Wedron Silica Co.

** Li_2CO_3 L-119 Fisher Scientific Co.

*** Grit 0000 emery paper, Buehler LTD.

**** Inconel overbraided thermocouple, Omega Engineering, Inc.

3720 x-ray diffractometer. The relative crystalline fraction of each specimen was determined by comparing the intensities of all of the peaks observed to the peak intensities of the sample heat-treated in the microwave at 600 °C for 10 minutes.

RESULTS AND DISCUSSION

All of the peaks encountered during x-ray diffraction analysis corresponded to the orthorhombic phase of lithium disilicate* The effects of temperature on the crystallization of $Li_2O \cdot 2SiO_2$ are listed in table 1. Growth

Table 1. Effect of Temperature on the Relative Crystallization of $Li_2O \cdot 2SiO_2$.

Heating method	Temperature (°C)	Time (minutes)	Percent crystallinity
microwave	600	10	100
conventional	600	10	6
microwave	580	10	100
conventional	580	10	0
microwave	560	10	56
conventional	560	10	0
microwave	540	10	19
conventional	540	10	0

at a temperature of 580 °C for 10 minutes in the microwave cavity was taken as fully crystallized as there was no increase in peak intensity detected for samples heat-treated at higher temperatures and similar times. As expected, the relative percent crystallinity increased with increasing temperature in both the microwave and conventionally heat-treated samples. However, there was considerable difference in the crystallization kinetics between the two processes. Heat treating the discs for only 10 minutes using microwave energy was sufficient to fully crystallize the samples at temperatures as low as

*JCPDS card 17-447 $Li_2O \cdot 2SiO_2$

580 °C. For a heat-treatment at 600 °C for 10 minutes in a conventional furnace, only six percent crystallinity was detected. Although this is only a semi-quantitative analysis, differences noted by visual inspection support the result of more extensive crystallization in the microwave cavity.

Table 2 is the effect of time and temperature on the relative crystallinity of the samples heat-treated using microwave energy. Again, as

Table 2. Effect of Time and Temperature on the Relative Crystallinity of Samples Heat-treated Using Microwave Energy.

Heating method	Temperature (°C)	Time (minutes)	Percent crystallinity
microwave	540	5	2
microwave	540	10	19
microwave	540	30	41
microwave	500	5	0
microwave	500	20	25
microwave	500	50	51

expected, longer heat treatment times increased the crystallinity of the samples. Figure 1 is the relative percent crystallinity as a function of time for samples heat-treated in the microwave. For the higher temperatures, the slope is steep. This indicates rapid growth of the nuclei. At lower temperatures, the slope is less steep and tapers off with time. At even lower temperatures, the curve flattens out and becomes almost linear. Also observed is an incubation time for samples processed below 560 °C. Little or no crystallization was detected in specimens heat-treated for only five minutes. Figure 2 are x-ray diffraction patterns for samples heated at 540 °C at different times using microwaves. As the time of the heat-treatment increases, the intensity of the peaks increase and more peaks appear. This demonstrates the development of the crystalline phase with time for a given temperature.

CONCLUSIONS

Glass discs of $Li_2O \cdot 2SiO_2$ were nucleated in a conventional furnace and the growth stages were performed using both conventional heating and

REFERENCES

1 A. A. Griffith, Philos. Trans. Soc. Lond. Ser. A221 (4) 163 (1920).
2 D. H. Roach and A. R. Cooper, Strength of Inorganic Glass (C. L. Kurkjian eds),185-195 (1985).
3 P. Hrma, W. T. Han, and A. R. Cooper, J. Non-Cryst. Solids, 102, 88-94 (1988).
4 M. Chen, P. F. James, F. R. Jones, D. A. Dalton, B. H. Howard, and S. Bedford, J. Non-Cryst. Solids, 139, 185-197 (1992).
5 P. F. James, M. Chen, F. R. Jones, J. Non-Cryst. Solids, 155, 99-109 (1993).
6 B. D. Fabes, W. F. Doyle, B. J. J. Zelinski, L. A. Silverman, and D. R. Uhlmann, J. Non-Cryst. Solids, 82, 349-355 (1986).
7 A. Madalena, M. Guglielmi, A. Raccanelli, and P. Colombo, J. Non-Cryst. Solids, 100, 461-465 (1988).
8 B. D. Fabes and D. R. Uhlmann, J. Am. Ceram. Soc., 73 [4] 978-988 (1990).
9 T. T. Meek, C. E. Holcombe, and N. Dyke, J. Mat. Sci. Lett. 6, 1060-1062 (1987).
10 A. S. De, I. Ahmad, E. D. Whitney, and D. E. Clark, Microwaves: Theory and Application in Materials Processing, Ceramic Transactions, Vol. 21, 329-339 (1992).
11 Y. Fang, D. K. Agrawal, D. M. Roy, and R. Roy, Microwave: Theory and Application in Materials Processing, Ceramic Transactions, Vol. 21, 349-356 (1992).
12 R. Roy, S. Komarneni, and L. Y. Yang, J. Am. Ceram. Soc., 68 [7] 392-395 (1985).
13 S. Surapanani, M. E. Mullins, and B. C. Cornilsen, Mat. Res. Symp. Proc. Vol. 189, 309-325, (1991).
14 S. Al-Assafi, I. Ahmad, Z. Fathi, and D. E. Clark, Microwave: Theory and Application in Materials Processing, Ceramic Transactions Vol. 21, 515-522 (1992).
15 ASTM Designation C730-85, Annual Book of ASTM Standards pp. 225-229 in Vol. 15.02, American Society for Testing and Materials, Philadelphia, PA (1985).
16 B. R. Lawn, K. Jakus, A. C. Gonzalez, J. Am. Ceram. Soc., 68 [1] 25-34 (1985).
17 S. R. Choi and J. A. Salem, Mat. Sci. Eng., A149, 259-264 (1992).
18 P. Chu, Master Degree Thesis, University of Florida (1988).
19 D. H. Roach and A. R. Cooper, J. Am. Ceram. Soc., 68 [11] 632-636 (1985).
20 W. T. Han, P. Hrma, and A. R. Cooper, Phy Chem. Glasses, 30 [1] 30-33 (1989).
21 E. K. Pavelchek and R. H. Doremus, J. Non-Cryst. Solids, 20, 303-308 (1976).

microwave energy. The growth stage of the heat-treatment executed in the microwave produced samples that appeared uniform in color. X-ray diffraction analysis confirmed that the volume fraction of the crystal phase may be controlled by varying the processing parameters. It was also determined that significant crystallization can be achieved at temperatures as low as 500 • C using microwave energy.

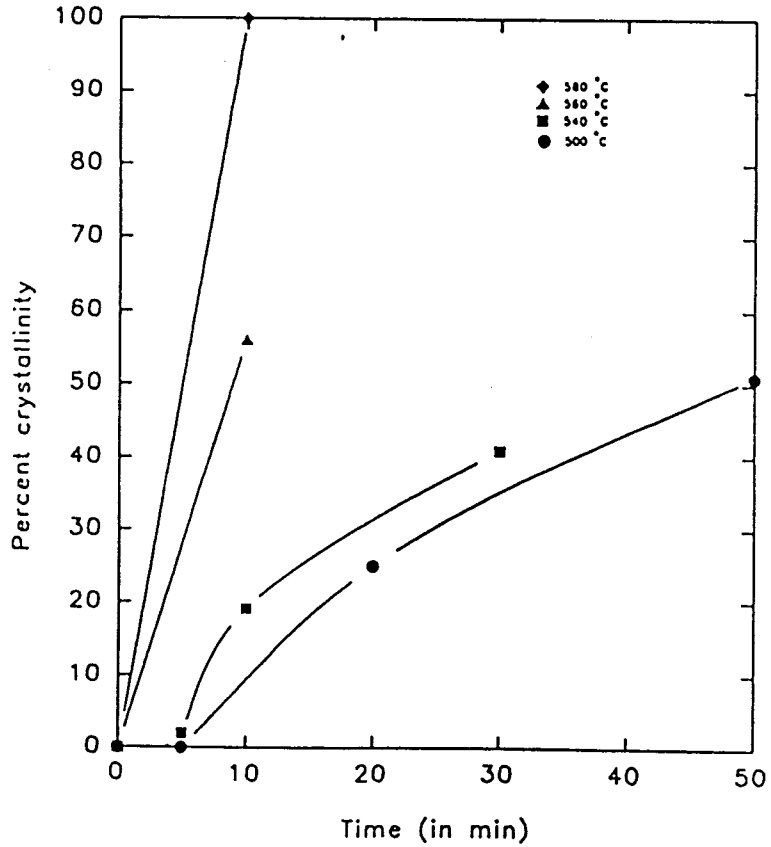

Figure 1. Relative percent crystallinity vs. time for $Li_2O \cdot 2SiO_2$ heated using microwave energy.

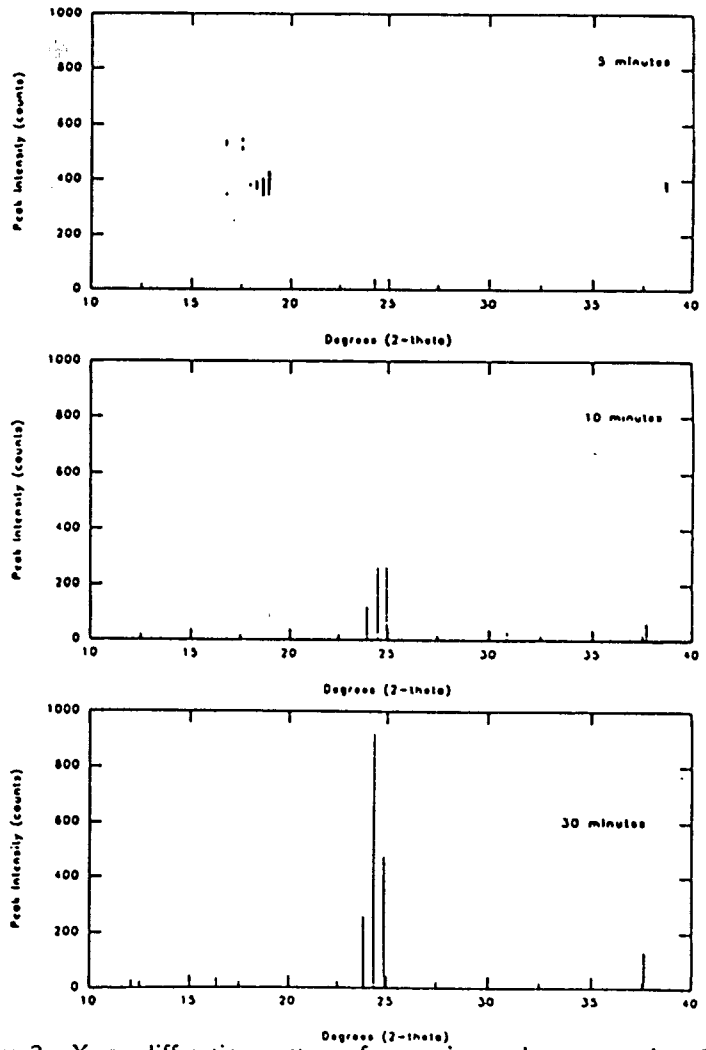

Figure 2. X-ray diffraction patterns for specimens heat-treated at 540 • C using microwaves.

ACKNOWLEDGMENTS

The authors would like to thank DARPA for funding this work under contract # N00014-91-J-4075. We would also like to thank Diane Folz for assistance and support during this project.

REFERENCES

1. S.W. Freiman and L.L. Hench, "Effect of Crystallization on the Mechanical properties of Li_2O-SiO_2 Glass-Ceramics," J. Amer. Cer. Soc., Vol. 55 No. 2, pp. 86-89 (1972).

2. W.H. Sutton, "Microwave Processing of Ceramic Materials," Bull. Amer. Ceram. Soc., Vol. 68 No. 2, pp. 376-386 (1989).

3. F.P. Glaser, "Crystallization of Lithium Disilicate from Li_2O-SiO_2 Glasses," Phys. and Chem. of Gl., Vol. 8 No. 6, pp. 224-232 (1967).

4. S.W. Freiman and L.L. Hench, "Kinetics of Crystallization in Li_2O-$2SiO_2$ Glasses," J. Amer. Cer. Soc., Vol. 51 No. 7, pp.382-387 (1968).

5. J.F. MacDowell, "Microwave Heating of Nepheline Glass-Ceramics," Bull. Amer. Cer. Soc., Vol. 63 No. 2, pp. 282-286 (1984).

6. Z. Fathi, I. Ahmad, J.H. Simmons, D.E. Clark and A.R. Lodding, "Surface Modification of Sodium Aluminosilicate Glasses Using Microwave Energy," Ceramic Transactions, Microwaves: Theory and Application in Materials Processing., Vol. 21, pp. 623-630, (D.E. Clark, F.D. Gac and W.H. Sutton, eds.) The American Ceramic Society Inc., Westerville, OH (1991).

7. A. De, I. Ahmad, E.D. Whitney and D.E. Clark, "Microwave (Hybrid) Heating of Alumina at 2.45 GHz: I. Microstructural Uniformity and Homogeneity," Ceramic Transactions, Microwaves: Theory and Application in Materials Processing., Vol. 21, pp. 319-328, (D.E. Clark, F.D. Gac and W.H. Sutton, eds.) The American Ceramic Society Inc., Westerville, OH (1991).

SURFACE MODIFICATION OF SINGLE CRYSTAL ALUMINA USING MICROWAVE ENERGY

Z. Fathi and D.E. Clark, Dept. of Materials Science and Engineering, University of Florida, Gainesville, Fl 32611-2066

I. Ahmad, Technology Assessment and Transfer, Inc., Annapolis, MD 21401.

ABSTRACT

Single crystal alumina samples were surface modified using both microwave energy and conventional heating. Surface modification as used in this paper means the alteration of the surface by diffusing in either Zn or Cr ions. Scanning electron microscopy (SEM), x-ray mapping and secondary ion mass spectroscopy (SIMS) were used to assess the penetration depth of the diffusing ionic species.

INTRODUCTION

One of the key objectives of materials research is to promote efficient processing methods. Microwave energy is a unique energy source and may be seen as an alternative processing method by which shorter processing times are often achieved. A better understanding of microwave/materials interaction and microwave equipment design is the key factor in promoting this technology to an industrial scale. With the exception of food processing and few other applications, microwave processing of materials is still at an early stage (laboratory scale).

In the last few years there has been increasing evidence of unusual effects brought about by the use of microwave energy. Reduction of activation energies for diffusion, enhanced ionic interdiffusion, enhanced sintering and grain growth have been observed during microwave heating[1-2]. These "microwave effects" have sparked extensive research aimed at developing a better understanding of microwave/materials interaction. Although substantial progress has been made in this area, no general theory has been developed that encompasses all the observed effects. More study is needed in the areas of computational techniques, modeling, quantifying microwave/materials interactions and dielectric measurements of materials at microwave frequencies.

The present study was undertaken to better understand the previously observed phenomenon of increased ionic diffusion in a microwave field. The single crystal alumina system was the system of choice for this type of diffusion study. The absence of interfaces and grain boundaries limits the diffusion mechanisms to lattice diffusion and thus facilitates discussion of the results. A comparison of the penetration depths of zinc and chromium ions accomplished by microwave processing and those achieved by conventional means will be discussed.

EXPERIMENTAL

The single crystals of alumina (Hemex and Hemlux) were purchased from Crystal Systems, Inc. Both grades were cut on the (0001) orientation and were polished on both sides. Hemex is the superior grade sapphire with the least light scattering. Hemlux is a high grade sapphire with minimal light scattering and/or lattice distortion.

A. Al_2O_3-ZnO system

When Al_2O_3 and ZnO react at moderately high temperatures (800° C or higher), a single phase compound ($ZnAl_2O_4$) is formed. The formation of this spinel is as follows:

$$ZnO + Al_2O_3 \rightarrow ZnAl_2O_4 \qquad (1)$$

The rate of formation of $ZnAl_2O_4$ was found to be diffusion controlled[3]. Furthermore, the reaction could be seen primarily as a one way transfer of zinc oxide to alumina especially in the temperature range of interest in this study (1100° C).

Hemlux crystals were sandwiched between pressed pellets of zinc oxide. The assembly was then heated in a conventional furnace and a microwave applicator at 1100° C for 180 minutes. The ZnO/Al_2O_3 samples were microwave hybrid heated. This is performed by inserting the ZnO/Al_2O_3 assembly inside a microwave-transparent microwave chamber that is lined with a suscepting coating (β-SiC). This heating method is referred to as hybrid heating because the ZnO/Al_2O_3 assembly is exposed to both microwave radiation and IR radiation generated by the walls of the lined

insulation.

After the heat treatments, cross sections of the samples were prepared for analysis. Scanning electron microscopy (SEM) micrographs and their corresponding x-ray maps for zinc concentration were helpful in visualizing the extent of zinc diffusion into the single crystal alumina samples. Figure 1 shows the backscattered electron image for the reaction layer or the depth of penetration of zinc in the single crystal alumina. The x-ray maps of zinc in the single crystal alumina show a significant difference with the zinc diffusion band in the microwave heated sample being much wider than that of conventionally heated sample.

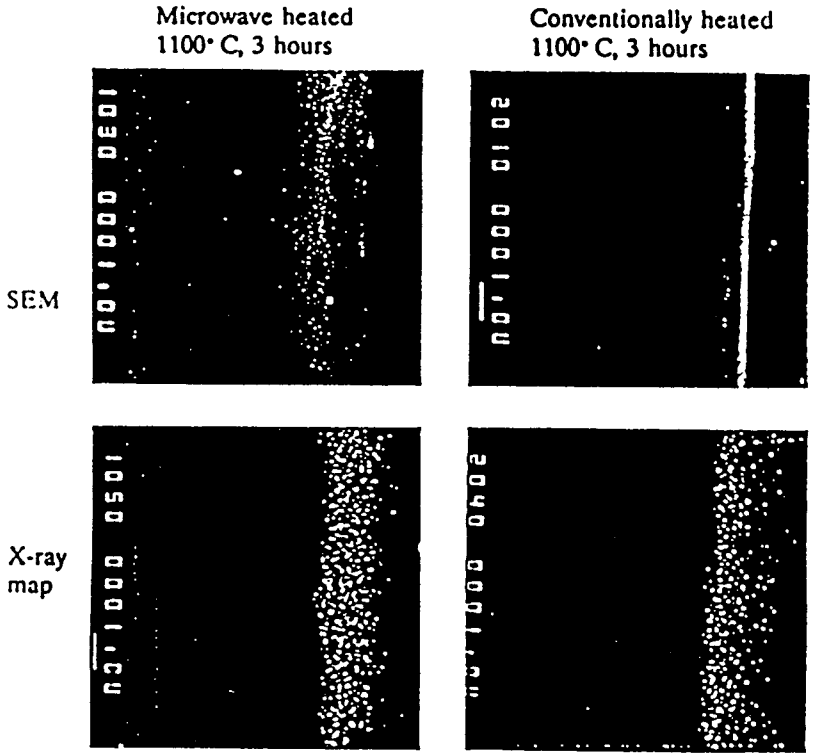

Figure 1. SEM micrographs and corresponding x-ray maps of the single crystal alumina heated in zinc oxide for 180 minutes at 1100° C

Depth profile curves for aluminum and zinc isotopes in the single crystal alumina (Hemlux) were obtained using secondary ion mass spectroscopy (SIMS). The results are shown in Figure 2a and 2b for both the microwave hybrid-heated and conventionally processed samples. The penetration depth of zinc is greater than one micrometer for microwave heated specimens and greater than half a micrometer for conventionally processed samples. There is a flat region on the profiles of zinc isotopes until the concentration falls abruptly. This suggests that the stoichiometric zinc aluminate spinel layer is formed as a result of the reaction.

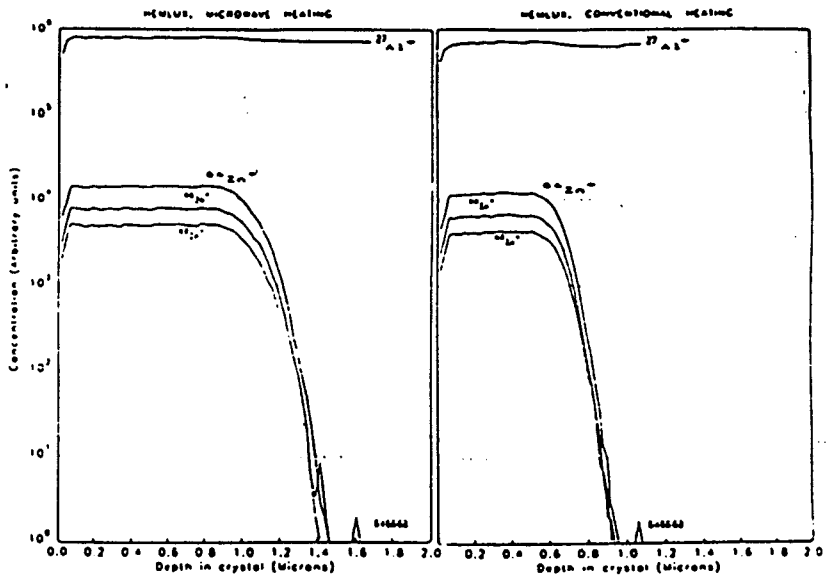

Figure 2. Depth profiles curves for aluminum and zinc isotopes in single crystal alumina (HEMLUX) heated for 180 minutes at 1100° C by a) microwave energy and b) conventional energy

The larger depth of penetration for zinc indicates an enhancement of the overall reaction kinetics in the microwave field. Since the reaction between ZnO and Al_2O_3 is diffusion controlled, one might speculate that the increase in zinc penetration depth is directly related to a zinc diffusion enhancement when heated with microwave energy.

B. Al_2O_3-Cr_2O_3 system

This system exhibits complete solid-state solubility with chromium ions substituting for aluminum ions on the octahedral interstitial sites. The two different grades of single crystal alumina (Hemlux and Hemex) were embedded in Cr_2O_3 powder and heat-treated in a conventional furnace at 1650° C for 35 minutes. This step was taken to deposit a layer of Cr_2O_3 on the sample surfaces before any subsequent heat treatment. A portion of each of the single crystal alumina disks was cross-sectioned and x-ray mapped (see Figure 3a and 3b).

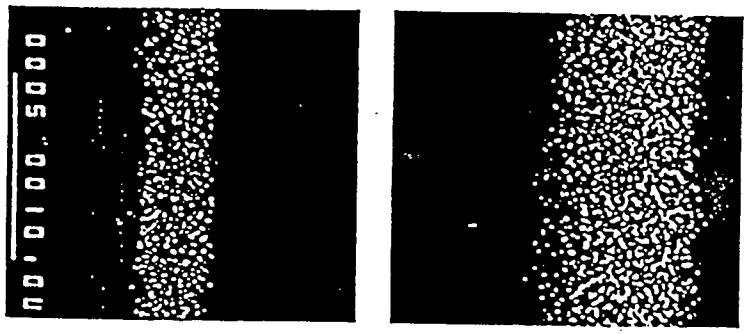

(a) (b)

Figure 3. X-ray maps of single crystal alumina heated at 1650° C for 30 minutes a) HEMLUX grade and b) HEMEX grade.

Each grade of single crystal alumina was then cut in half and prepared for more heat treatment. The microwave hybrid heated specimens were inserted in the microwave chamber and heated at 1200° C for 1 hour. The temperature was monitored using an Inconel shielded K-type thermocouple. The accuracy of the temperature reading was estimated at ±6° C. The conventionally heated samples were similarly processed at 1200° C for 60 minutes. The specimens were then cross-sectioned and polished to a 0.25 μm surface finish. The back scattered electron image in Figure 4a and 4b contrasts the chromia-alumina reaction layer for the Hemlux grade heat treated with microwave energy and conventional methods. There are artifacts associated with the SEM data caused by rounded sample edges. As indicated by the arrows, a careful examination of Figures 4a and 4b and their corresponding x-ray maps in Figures 4c and 4d indicate that the reaction band width is very similar in both cases.

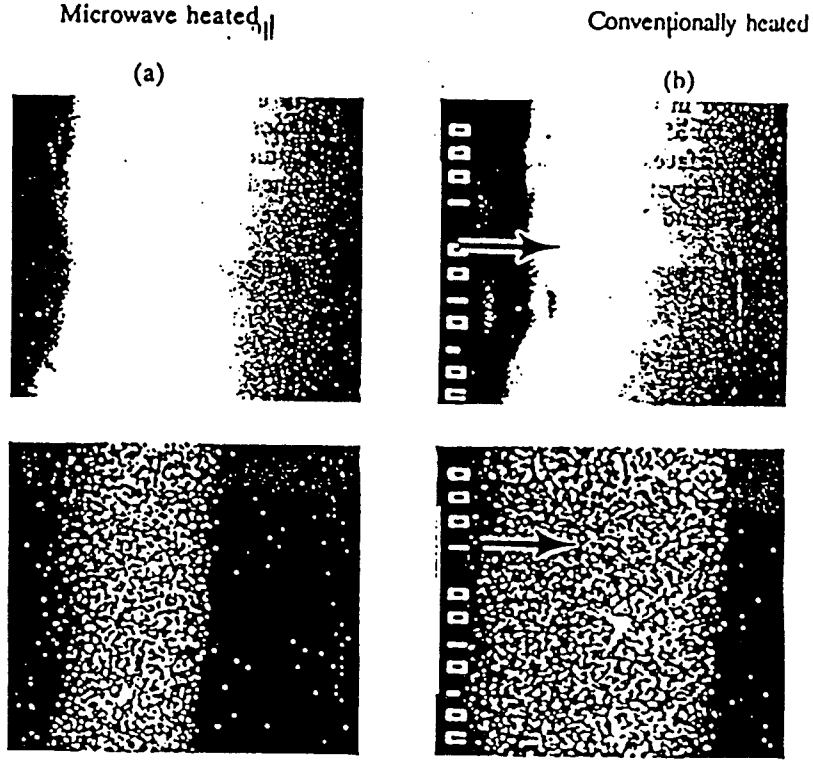

Figure 4. SEM micrographs and corresponding x-ray maps of the single crystal alumina (HEMLUX) heated in chromium oxide for 60 minutes at 1200° C.

Similarly, Figure 5a, 5b, 5c and 5d show the backscattered electron images and x-ray maps for the Hemex single crystal alumina heat treated in both

microwave and conventional ovens. No noticeable change in the band width was apparent for either grade of single crystal alumina.

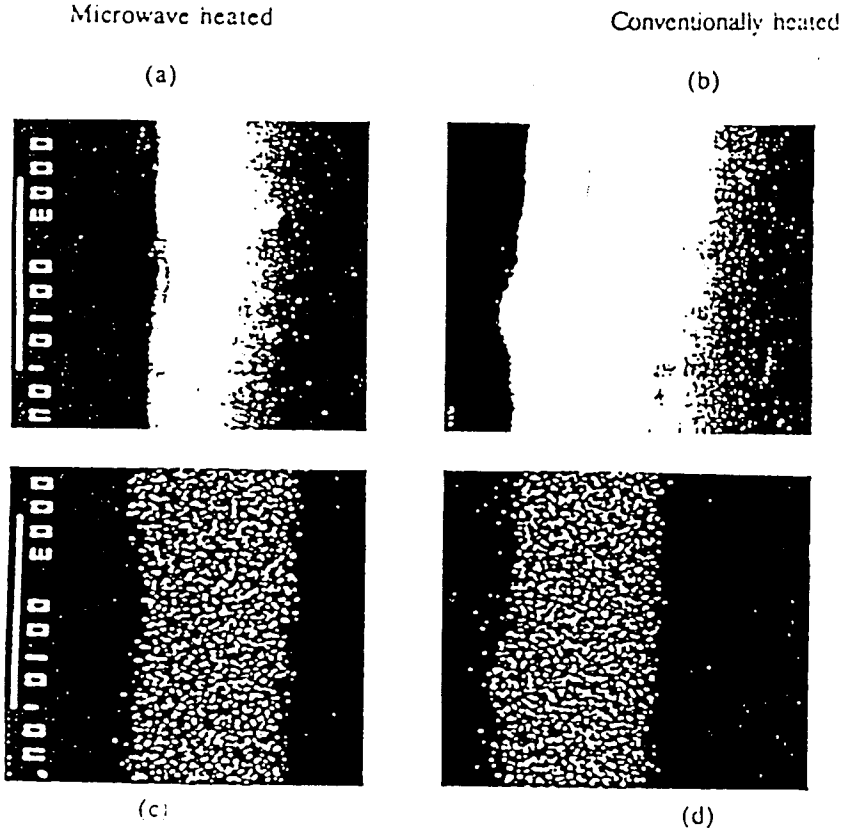

Figure 5. SEM micrographs and corresponding x-ray maps of the single crystal alumina (HEMEX) heated in chromium oxide for 60 minutes at 1200° C

Monitoring temperatures inside a microwave applicator is often a point of controversy[4]. The fact that chromium diffusion was not enhanced under the processing conditions might be a positive result on its own. If there was a systematic error in monitoring temperatures, such as reading lower temperatures than the true temperature of the ceramic article, there should have been a greater reaction band displayed by chromium ions.

CONCLUSION

More work needs to be done in order to understand how microwave radiation affects material transport and reactions. Microwave energy appears to provide a means by which deeper penetration of zinc ions into single crystal alumina can be achieved. However, it is premature to give definite reasons for this apparent enhancement of Zinc diffusion. No significant diffusion enhancement was observed for chromium under the processing conditions undertaken in this study.

ACKNOWLEDGEMENTS

The authors would like to thank DARPA for funding this work under contract # N00014-91-J-4075. We would like to thank Diane Folz for assistance and support during this project. Special acknowledgement for W.A Acree in the Major Analytical Instrumentation Center (MAIC) at the University of Florida for the SEM micrographs and x-ray maps.

REFERENCES

1. J.D. Katz, R.D. Blake and V.M. Kenkre, "Microwave enhanced diffusion?", Ceramic Transactions, Microwaves: Theory and Application in Materials Processing., Vol.21, pp.95-105,(D.E. Clark, F.D. Gac and W.H. Sutton, eds.) The American Ceramic Society Inc., Westerville, OH (1991).
2. Z. Fathi, I Ahmad, J.H Simmons, D.E. Clark and A.R. Lodding,"Surface Modification of Sodium Aluminosilicate Glasses Using Microwave Energy",Ceramic Transactions, Microwaves: Theory and Application in Materials Processing., Vol.21, pp.623-630,(D.E Clark, F.D. Gac and W.H. Sutton, eds.) The American Ceramic Society Inc., Westerville, OH (1991).
3. I. Ahmad and D.E Clark, "Effect of Microwave Heating on Solid State Reactions of Ceramics",Ceramic Transactions, Microwaves: Theory and Application in Materials Processing., Vol.21, pp.605-612,(D.E. Clark F.D. Gac and W.H. Sutton, eds.) The American Ceramic Society Inc., Westerville, OH (1991).
4. J.D. Katz, "Microwave sintering of ceramics", Annu. Rev. Mater. Sci. 22 153-70 (1992).